1-1-2003

Development of statistical models to simulate and optimize self-consolidating concrete mixes incorporating high volumes of fly ash

Rajeshkumar Patel
Ryerson University

In compliance with the
Canadian Privacy Legislation
some supporting forms
may have been removed from
this dissertation.

While these forms may be included
in the document page count,
their removal does not represent
any loss of content from the dissertation.

Development of statistical models to simulate and optimize self-consolidating concrete mixes incorporating high volumes of fly ash

By

Rajeshkumar Patel

B.E. Civil, S.P. University, India, January, 1986

A thesis presented to Ryerson University
In the partial fulfillment for the degree of

Master of Applied Science
in
Civil Engineering

Toronto, Ontario, Canada, 2003

Your file Votre référence
ISBN: 0-612-87165-7
Our file Notre référence
ISBN: 0-612-87165-7

Author's Declaration

I hereby declare that I am the sole author of this thesis.

I authorize Ryerson University to lend this thesis to other institutes or individuals for the purpose of scholarly research.

Author's signature _____ Date July 03, 2003

I further authorize Ryerson University to reproduce this thesis by photocopying or by other means, in total or in part, at a request of other institutions or individuals for the purpose of scholarly research.

Author's signature _____ Date July 03, 2003

Borrowers

Borrowers undertake to give proper credit for any use made of the thesis. Ryerson University requires the signatures of all persons using or photocopying this thesis. Please sign below and give address and date.

Name	Signature of Borrower	Address	Date

Development of statistical models to simulate and optimize self-consolidating concrete mixes incorporating high volumes of fly ash

By

Rajeshkumar Patel

Master of Applied Science in Civil Engineering
Department of Civil Engineering
Ryerson University, Toronto
June 2003

Abstract

Self-consolidating concrete (SCC), a latest version of high performance concrete, has created tremendous interest today as it can be easily placed in congested reinforced concrete structures with difficult casting conditions. It also reduces the construction time and cost of the labor. Normally SCC is being developed using a superplasticizer to generate desired flow and a viscosity modifying admixture (VMA) to prevent segregation in the concrete. In this research project, instead of VMA, high volumes of fly ash were used along with superplasticizer to develop SCC. The minimum use of superplasticizer and optimum use of fly ash were desired to achieve required properties of SCC. The fly ash is expected to be useful not only in generating the flow but as segregation resistance as well. The aim of the present research project was to develop SCC for sustainable construction by optimizing the use of high volumes of fly ash with some proposed statistical models.

The rheological study for paste and mortar was carried out first, and Bingham model parameters such as plastic viscosity and yield stress were correlated with the marsh cone flow of paste and fresh concrete properties such as slump flow and filling capacity. The limits for plastic viscosity, yield stress, and specific marsh cone flow of paste and mortar were identified for concrete mixes to be qualified for SCC. Four independent variables such as total binder content (limit 350 to 450 kg/m3), percentage of fly ash replacing cement (limit 30 to 60 %), % of superplasticizer (limit 0.1 to 0.6 %), and W/B (limit 0.33 to 0.45) were considered for design of experiment and for development of statistical models for SCC. Statistically balanced twenry-one concrete mixes were chosen and fresh concrete tests such as slump and slump flow, V-funnel flow, filling capacity, L-box, bleeding, air content, segregation, and initial and final setting time tests were performed. Seven harden concrete tests (for mechanical characteristics and durability) such as compressive strength (1, 7, 28-day), freezing and thawing cycles resistance, surface scaling resistance, rapid chloride permeability, modulus of elasticity, flexural strength, and drying shrinkage were performed to evaluate the performance of SCC. Five statistical models for important properties of SCC such as slump flow, 1-day strength, 28-day strength, rapid chloride permeability, and material cost were developed.

The limits of rheological parameters of pastes and mortars can be useful to predict the flow behavior of SCC and the proposed models can be useful to design and optimize SCC mixes incorporating high volumes of fly ash.

Acknowledgements

I would like to thank my supervisor, Professor Mohamed Lachemi for providing me support, freedom, excellent guidance and advice for this research project. I would also like to thank Professor Medhat Shehata and Dr. K.M.A Hossain for their guidance and support for the research project. I acknowledge the support of Dr. N. Bouzoubaa of CANMET for this project. I am also very grateful to Dan Pennef for providing me excellent help in the concrete laboratory. I want to give special recognition to Chandi Ganguly for morale and academic support. I am also acknowledging support of my friends, Govind Meti, Bill Lambros, Fernando Igreda, Paresh Patel and Praful Patel.

There are not enough words to express my gratitude to my mother, my wife and my kids for sacrificing their family life to enable me to complete this research project successfully. Finally, I would like to express my deep feeling of joy to almighty God because researchers gets path and direction with miracles when there are faith, patience, and fortitude.

Table of contents

List of Tables

List of Figures

List of Abbreviations and Symbols

CCD	Central Composite Design
E_c	Modulus of elasticity
FA	Fly ash
f'_c	Compressive strength
FM	Fineness modulus
k	Numbers of factors
MSA	Maximum size of aggregate
n_c	Central point portion
n_f	Fraction factorial portion
RCP	Rapid chloride permeability
RDME	Relative dynamic modulus of elasticity
SP	Superplasticizer
S_{sp}	Specific marsh cone flow time, Seconds
V_{fa}	Volumetric fraction of aggregates
VMA	Viscosity modifying admixture
W/B	Water to binder ratio
X_1	Total binder content, kg/m^3
X_2	Percentage of fly ash partially replacing cement by mass
X_3	Percentage of solid content of superplasticizer with respect to total binder Content
X_4	Water to binder ratio
Y_1	Slump flow of concrete, mm
Y_2	1-day compressive strength of concrete, MPa
Y_3	28-day compressive strength of concrete, MPa
Y_4	Chloride ions charged passed (Rapid chloride permeability), Coulombs
Y_5	Material cost of concrete, CAN $

Chapter 1 Introduction

1.1 Background

Self-consolidating concrete (SCC) is a new generation of high performance concrete (HPC) that can be placed and compacted under its own weight with little or no vibration effort. It should be at the same time cohesive enough to be handled without segregation or bleeding. It should also fulfill the fresh concrete properties and long-term performance for both durability and strength. SCC is generally used to facilitate and ensure proper filling of restricted areas and good structural performance of heavily reinforced structural members [1].

Over the years, many technological developments have provided incremental advances in the design and placement of concrete structures. Concrete placement in congested reinforced concrete structures, narrow and slim sections, and under water construction is difficult. Inadequate homogeneity of the cast concrete due to poor compaction or segregation can dramatically lower the performance of mature concrete [2]. SCC can contribute to solve these problems. SCC was originally developed at the University of Tokyo, Japan in the late 1980s and now it is becoming more popular in rest of the world. It is considered to be one of the most significant advances in concrete technology for the past decade [3].

The main advantages of SCC are [1-3]:

- Facilitating constructibility and ensuring good structural performance;

- Improving the filling capacity in thin wall elements or highly congested structural members;
- Reducing the construction time and labor cost due to ease of placement characteristics;
- Eliminating the need for vibration;
- Reducing work hardship, and decreasing the number of heavy handling equipments;
- Reducing the noise pollution;
- Higher durability due to high performance characteristics.

The basic requirement of SCC is to have high degree of flowability with no segregation and better cohesiveness. High flowability can easily be achieved by adding superplasticizer to the concrete. Superplasticizer is not the only solution to maintain concrete cohesiveness during handling operations but special attention has to be paid to proportioning the mixture. To avoid segregation on superplasticizer addition, an easy way is to increase the sand content by 4 to 5 % at the cost of coarse aggregate content [1]. Reduction in coarse aggregate content requires more cement, which leads to higher temperature rise, higher shrinkage, and an increased cost. An alternative approach is to incorporate a viscosity-modifying admixture to enhance the segregate resistance. Most of the chemical admixtures are expensive, and their use may increase the material cost. Increased material cost of SCC may offset the saving in labor cost. But the use of supplementary cementing materials such as fly ash can have the following beneficial effects [1, 4]:

- Better slump flow without segregation and better cohesiveness;
- Lower cost as they replace cement, which is relatively costly;
- Lower heat of hydration;
- Lower permeability

1.2 Objectives and scope

The objectives of this research project are to study rheological properties of paste and mortar, to study fresh and harden properties of SCC, and to develop statistical models to design and optimize SCC mixes incorporating high volumes of fly ash. Mixture proportioning of SCC is found to be relatively difficult compared with normal concrete, as excellent deformability and good stability of concrete are desired in the case of SCC. Many trial mixes are needed to generate optimum flow without segregation and bleeding of concrete. In order to minimize cost, time and energy associated with trial mixtures, efforts have been made to establish correlation between rheological parameters of paste and mortar and fresh properties of SCC. The correlation could be proved helpful to predict the flow behavior of SCC from rheological parameters of corresponding paste and mortar. The influence of the fly ash on various fresh and harden properties of SCC is studied. Statistical models are developed for important properties of SCC such as slump flow, 1-day compressive strength, 28-day compressive strength, rapid chloride permeability, and material cost. With the help of these models, SCC mixes can be developed with minimum cost, time and effort. Desired properties of SCC can be achieved at an optimum cost with the proposed models.

The basic interest of the study was to use high volumes of fly ash in SCC in order to contribute in sustainable development by the following means:

- Reducing the use of Portland cement by using high volumes of fly ash as cement replacement;
- Consuming environmentally hazardous industrial wastes like fly ash;
- Consuming less amount of natural aggregates;
- Increasing the durability of concrete structure;
- Better operational performance.

Under the experimental test program, 21 mixes for paste, mortar, and concrete were designed by following the Box- Wilson central composite design (CCD) method. The four independent variables such as total binder content (limit 350 to 450 kg/m^3), percentage of fly ash replacing cement (limit 30 to 60 % by mass), % of superplasticizer (limit 0.1 to 0.6 % by mass), and W/B (limit 0.33 to 0.45) were varied within the prescribe limits. The amounts of coarse and fine aggregates were kept constant in all the mixes. No air-entraining admixture was used to produce SCC mixes. All the mixes were evaluated by performing several fresh and harden concrete tests.

In Chapter 2, rheology of concrete, fresh properties of SCC, tests on fresh properties of SCC, statistical models for proportioning and optimizing SCC mixes, and influence of fly ash on fresh and harden properties of SCC are discussed. In Chapter 3, the methodology of experimental program along with tests on rheology of paste/ mortar and fresh and harden properties are discussed.

The results of the rheological study of paste and mortar, and fresh and harden properties of SCC are presented and discussed in Chapter 4. The correlation between rheological parameters of paste / mortar and fresh properties of SCC is discussed in connection with prediction of flow behavior of SCC. Developed statistical models are discussed in Chapter 5. The response surface diagrams for each model are presented. The influence of fly ash on various model responses such as slump flow, 1-day strength, 28-day strength, rapid chloride permeability, and material cost are described. The conclusions of the research and recommendations for further studies are presented in Chapter 6.

Chapter 2 Literature Review

2.1 Introduction

Self-consolidating concrete (SCC) is a relatively new concept in concrete technology and generated great interest worldwide due to certain cost-effective advantages over normal concrete. Different approaches have been used to develop SCC by many researchers. One method to derive SCC is to divide concrete into two constituents; coarse aggregates and mortar. The rheology of mortar is then adjusted to achieve SCC with the incorporation of superplasticizer (SP) and viscosity modifying admixture (VMA) [5]. Another method is to optimize particle size distribution of binding materials (by increasing significantly the quantity of fine materials such as fly ash or limestone filler in concrete) [1, 5]. Even though the later approach needs some quantity of SP, it can be proved to be more cost-effective.

Rheology of paste, mortar, and SCC is important to characterize the flow behavior of SCC. Some of the researchers have developed few tests to assess the deformability of SCC in restricted areas. In this chapter, the rheology, fresh properties, and test procedures for fresh properties of SCC are discussed. The properties of FA, and its influence on various properties of SCC are also discussed.

2.2 Rheology of concrete

Concrete is a composite material, with aggregate, cement, and water as the main components. It is a concentrated suspension of solid particles (aggregates), in a viscous

liquid (paste). Paste is not a homogeneous fluid and is composed of particles of cement and cementing materials grains in water [6].

Normally there are two types of flow behavior: Newtonian fluid and non-Newtonian fluid. In the Newtonian fluid, the shear stress is proportional to the shear rate (shear strain rate) and at a given temperature, the viscosity remains constant at any shear rate. While in the non-Newtonian fluid, when the shear rate is varied, the shear stress doesn't vary in the same proportion and same direction. The viscosity of this fluid changes as the shear rate varies [6-7].

The flow of paste, mortar, and concrete is assumed to follow the non-Newtonian equation of viscous flow, where viscosity of the fluid is the ratio of shear stress to shear rate (Shear strain rate). Many scientists had proposed different equations to describe the shear stress and the shear strain. Some of the equations are shown in Table 2.1

2.2.1 Bingham model

Paste, mortar, and concrete are considered as non-Newtonian fluid. The most commonly used model for paste, mortar, and concrete is the Bingham model. This model requires two parameters, ie. yield stress and plastic viscosity. The yield stress is the stress above which the material becomes fluid. In other words, the yield stress corresponds to the intercept on the shear stress axis. The plastic viscosity is the measure of how easily the material will flow, once the yield stress is overcome. The plastic viscosity is the slope of shear stress-shear rate plot as shown in Fig. 2.1 [6].

Table 2.1: Equations related to shear stress and shear strain [6].

Equation name	Equation
Newtonian	$\tau = \eta \gamma$
Bingham	$\tau = \tau_o + \eta \gamma$
Hurchel & Bulkley	$\tau = \tau_o + k \gamma^n$
Power	$\tau = A \gamma^n$
Vorn Berg	$\tau = \tau_o + B \sinh^{-1}(\gamma/C)$
Eyring	$\tau = a \gamma + B \sinh^{-1}(\gamma/C)$

Variable definitions:

τ = Shear stress η = Viscosity
τ_o = Yield stress γ = Shear rate
A, a, B, C, K = constants
n = 1 Newtonian flow n > 1 Shear thickening n < 1 Shear thinning

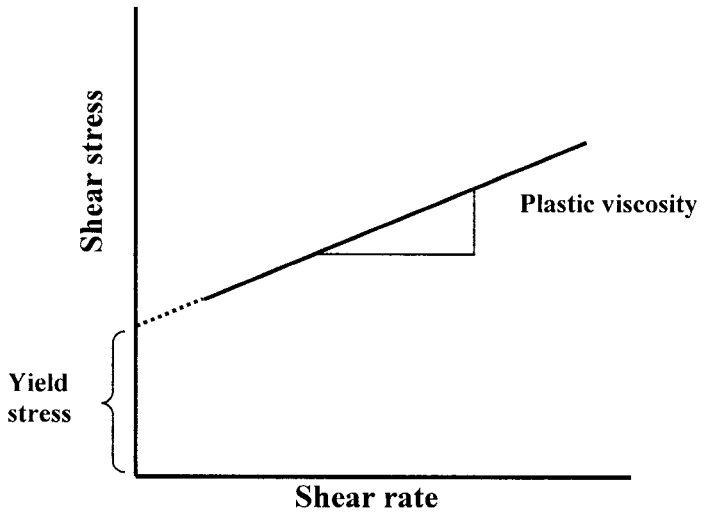

Fig. 2.1: Bingham model for fluid [6]

The Bingham equation is represented as follow:

$$\tau = \tau_o + \eta \gamma \qquad (2.1)$$

Where,

τ = Shear stress η = Viscosity

τ_o = Yield stress γ = Shear rate

The lower yield stress gives less resistance to start the flow of concrete. Higher viscosity prevents segregation but provides high resistance to the flow of concrete. It is important for SCC to have low yield stress and optimal viscosity to ensure enough flow and to prevent segregation [5, 8]. The measurement of only one parameter (either yield stress or plastic viscosity) does not fully characterize SCC rheology. Fig. 2.2 shows how two concretes could have one identical parameter and a very different second parameter. These concretes may be very different in their flow behaviors. Therefore, it is important to use a test or combination of tests that will describe the concrete flow, by measuring both factors [6].

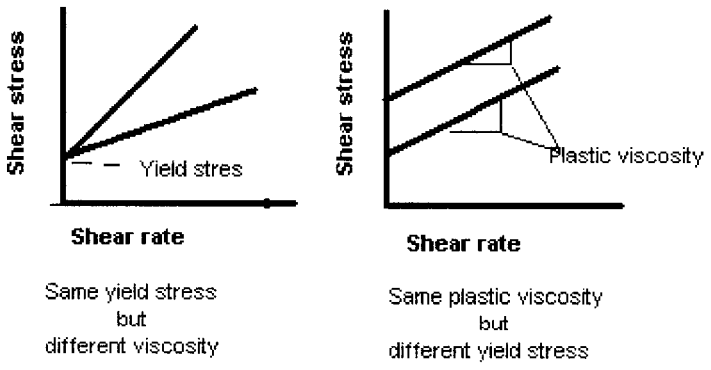

Fig. 2.2: Concrete rheology for different flow behavior [6]

2.2.2 Herschel-Bulkley model

In some cases, it has been found that the Herschel-Bulkley (HB) is suitable to describe the flow of SCC [6]. This model equation provides a relationship between shear stress and shear rate based on power law [6]. This equation leads to the calculation of two new parameters, k and n based on the rheological behavior of the concrete. A linear approximation of the HB curve was introduced to define a plastic viscosity [7]. The Herschel-Bulkley (HB) equation is as follow:

$$\tau = \tau_o + k\,\gamma^n \qquad (2.2)$$

τ = Shear stress γ = Shear rate

τ_o = Yield stress

Where k and n are the new characteristic parameters describing the rheological behavior of the concrete.

Ferraris et al. [9] established a relation between the slump flow and the Herschel-Bulkley (HB) yield stress for SCC (Fig. 2.3). It is observed from this figure that there is a good correlation between slump flow and yield stress for SCC. A minimum concrete yield stress of 700 Pa. is required to generate 550 mm of slump flow and slump flow is found to increasing with the decreased yield stress of concrete.

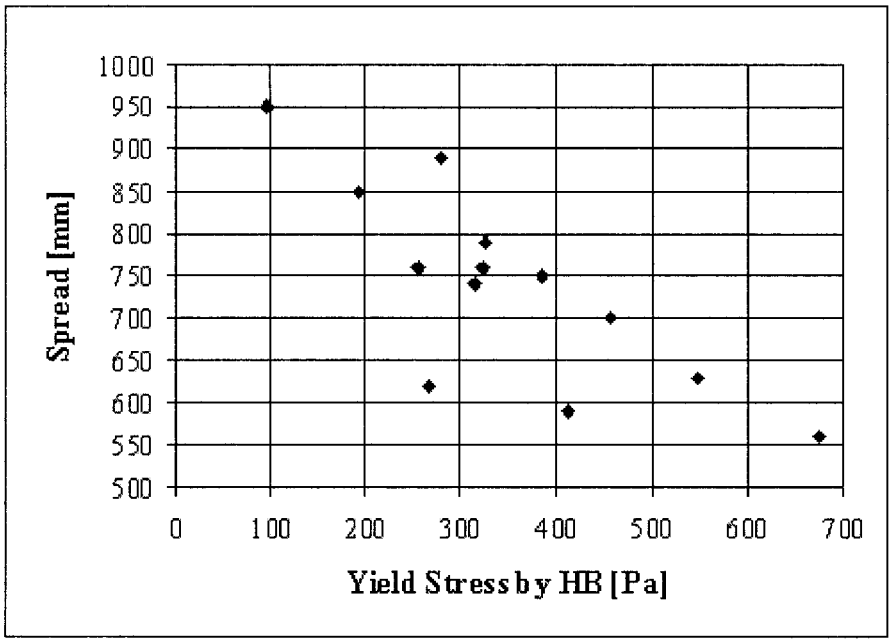

Fig. 2.3: Relationship between yield stress of HB model and slump flow of SCC [9].

2.2.3 Test apparatus for rheology

Tattersall rheometer is the first and most widely known instrument for measuring the rheological parameters of SCC (Fig. 2.4). The apparatus consists of a bucket containing the concrete to be tested. A vane of special geometry, or spindle, is lowered into the sample. The resistance on the spindle due to the material against the rotation of spindle, ie. torque is measured. As the speed of rotation of the spindle is increased, a curve of the torque versus the speed is recorded. The graph obtained is linear; therefore the stress is extrapolated to the torque at zero speed to give the yield stress. The plastic viscosity is related to the slope of the curve [6].

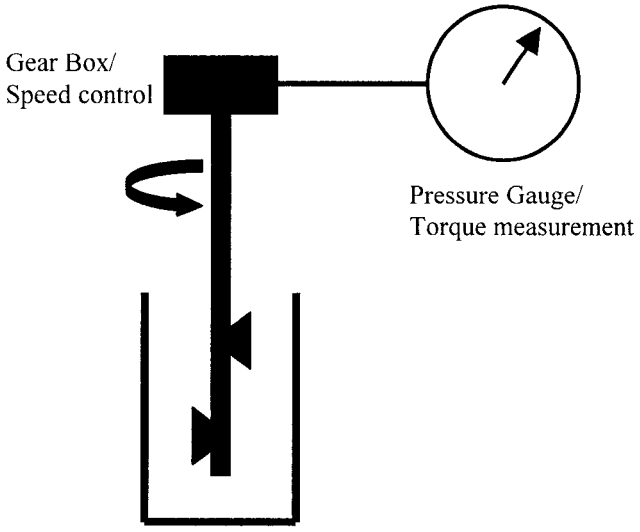

Fig. 2.4: Schematic representation of tattersall rheometer [6].

Tattersall gave the following equation:

$$T = (G / K)\,\tau_o + (G\,\eta)\,N \qquad (2.3)$$

Where,

T = Torque

G = Constant obtained by calibration with non-Newtonian fluid

N = Speed of the impeller

τ_o = Yield stress

η = Viscosity

Tattersall designed the first instrument for measuring the two points rheology (yield stress and plastic viscosity) of concrete, after that, more instruments were developed with more or less the same principles [6, 10]. Some of them are listed below:

- BML Viscometer
- IBB Concrete rheometer
- FHPCM rheometer
- Bertta apparatus

- BTRHEOM Rheometer

Apart from these, Tang et al. [10] used commercially available Brookfield viscometer for rheological measurements of paste and mortar.

2.2.4 Rheological parameters and flow behavior of SCC

The rheological parameters of paste, mortar, and SCC are important to predict flow behavior of SCC. Not much information is available on the correlation between the rheological parameters of paste/mortar and the flow behavior of SCC. The problem comes from the fact that the range of the particle size of binder and fine aggregate is very wide and difficulty in matching the testing conditions of rheology of paste/mortar and SCC. It is important to measure the rheology of paste/mortar in the same conditions that normally exist in concrete to achieve a reliable correlation. Tang et al. [10] concluded that the fresh concrete made with mortar of low viscosity might cause aggregate segregation; whereas mortar with high viscosity might reduce the flowability. A mortar viscosity ranging from 3500 to 5500 mPa.s was found to be suitable for the production of SCC. The volumetric fraction of coarse aggregate was varied from 30 to 40% for their study.

2.3 Fresh properties of SCC

2.3.1 Deformability

Deformability can be defined as the ability of a SCC to flow in a heavily reinforced section and other restricted areas. Highly flowable SCC should have relatively low yield stress to ensure good deformability [11]. Inter-particle friction between coarse aggregate,

sand, and binder increases the internal resistance of flow, limiting the deformability and speed of flow of SCC. Such friction can be high when concrete flows through restricted spacing because of greater chances of collision between the various solids [11]. The deformability of SCC can be increased by increasing the W/B, increasing the dosage of SP, and by incorporating very fine supplementary cementing materials (SCM) [11-12]. Increase in the W/B can secure high deformability but it may affect the mechanical and durability properties of SCC in the long run. Increasing W/B can also reduce cohesiveness and can cause segregation that may leads to blockage during flow. Inter particle friction between binder grains can be reduced by using SP to disperse the cement grains. A high dosage of SP can however lead to the segregation and blockage of the SCC flow [11]. Very fine and glossy textured particle of SCM can reduce the inter-particles friction and lead to higher deformability.

The Slump flow test can be used to evaluate the free deformability of SCC in absence of obstructions while the V-funnel test is suitable to evaluate deformability through restricted areas [13]. Filling capacity and L-box tests are more relevant to determine the deformability of SCC among closely spaced obstacles [11, 14].

2.3.2 Stability and segregation

The stability of fresh concrete is characterized by its resistance to washout loss, segregation, and bleeding and is affected by the mixture proportioning, aggregate shape and gradation, and the placement conditions. When a mixture does not possess an adequate level of stability, the cement paste may not be cohesive enough to retain

individual aggregate particles in a homogeneous suspension. This causes the concrete constituents to separate, thus resulting in a significant reduction in mechanical properties and durability [15].

There are two kinds of segregation. The first is the separation of mortar from coarse aggregates and second is bleeding. Bleeding is defined as a phenomenon whose external manifestation is the appearance of water on the top surface after concrete has been placed but before it has set. Bleeding is the form of segregation where solids in suspension tend to move downward under the force of gravity. Bleeding occurs due to the inability of the constituent materials to hold all the mixing water in a dispersed state. Some bleeding water reaches to the surface; large amount of it gets trapped under large pieces of aggregates, and horizontal reinforcing bars, which affect the mechanical performance of concrete such as strength and bond [16].

Improper consistency, excessive amount of large particles in coarse aggregates with either too high or too low density, presence of less fines (due to low cement and sand contents or the use of poorly graded sand) can cause segregation and bleeding in SCC. The concrete without mineral admixtures may suffer segregation and bleeding in concrete. Fujiwara [17] had developed a test method to measure segregation index and it was used in this research project. Some of the measures that can be used to enhance the stability of fresh SCC are:

- The reduction in water-to binder ratio (W/B);
- The increase of cementing material content such as fly ash, slag and other fines;

- The incorporation of viscosity modifying admixture (VMA).

A large decrease in aggregate volume or an increase in water content can reduce the cohesiveness and lead to segregation. A relative high sand-to-total aggregate content of 42 to 52 % is often used to enhance cohesiveness and reduce the risk of segregation and water dilution [15].

2.4 Test procedures for fresh properties of SCC

Several tests to evaluate consistency, deformability, stability, bleeding and segregation for SCC are available in the literature. Some of the important tests are discussed in the following sections:

Slump flow

The deformability and flowability of fresh SCC in absence of obstructions can be evaluated by using slump flow test. The fresh SCC can be filled in one layer in the standard slump cone without any consolidation. The slump flow value represents the mean diameter (measured in two perpendicular direction) of SCC spread after lifting the standard slump cone and concrete stopped flowing. According to Nagataki et al. [18], the slump flow value of concrete should be ranged between 500 and 700 mm to qualify for the SCC. Tang et al. [10] suggested a slump value of 500 mm or more for SCC under conditions that no aggregate segregation. Xie et al. [4] suggested limit of 650 to 750 mm for SCC. The SCC may segregate at slump flow higher than 750 mm and less than 550 mm slump flow may be insufficient to pass through highly congested reinforcement.

V-funnel test

The deformability of SCC through restricted areas can be evaluated by using V-funnel test [13]. The schematic representation of V-funnel test apparatus is shown in Fig. 2.5. In this test, V-shaped funnel is filled completely with fresh SCC without any consolidation and the bottom outlet is opened, allowing concrete to fall out under gravity. The time of flow from the opening of bottom outlet to the complete seizure of flow is considered as a V-funnel flow time. The V-funnel flow time could be high if paste viscosity and inter-particle friction are high.

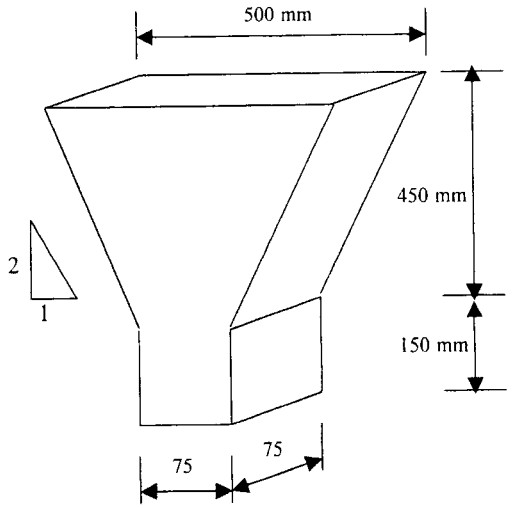

Fig. 2.5: Schematic representation of V-funnel test apparatus

Filling capacity test

The filling capacity test evaluates the capability of SCC to deform in areas with highly congested reinforcing bars. The filling capacity can be determined by casting the concrete in a transparent box of 300 x 500 x 300 mm that has closely spaced smooth horizontal 16

mm diameter copper tubes as shown in Fig. 2.6 [14]. The concrete is introduced through a funnel into the section that is free of obstacles until the concrete reaches 220 mm height. Once the flow of concrete among the bars ceased, the relative area occupied by the concrete in the restricted section is noted to calculate the filling capacity [14]. According to Khayat et al. [14], the filling capacity ranging from 50% to 95% indicates moderate to excellent deformability among closely spaced obstacles.

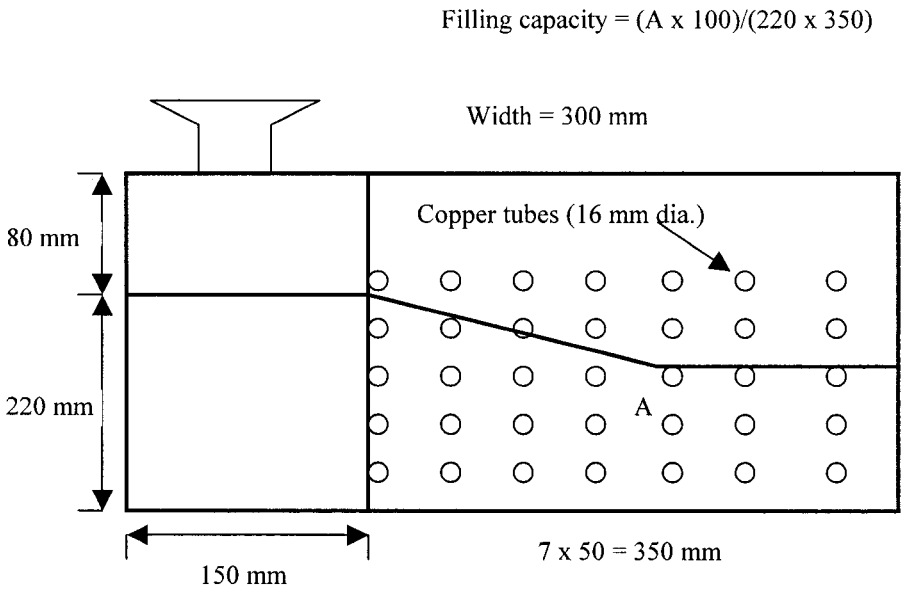

Fig. 2.6: Schematic representation of a filling capacity apparatus

L-box test

The L-box [19] test is proved to be useful to determine the ability of SCC to flow through the gaps between reinforcing bars. The vertical part of the box is filled with fresh concrete and left to rest for one minute (Fig. 2.7). After that, the gate is opened to allow the concrete to flow out of vertical part through three reinforcing bars (12 mm diameter

with 34 mm gap). The times for the leading edge of concrete to reach a distance of 200 and 400 mm along the horizontal part, and the height H_1 and H_2 of concrete are measured and used to determine the h_2/h_1 ratio [19].

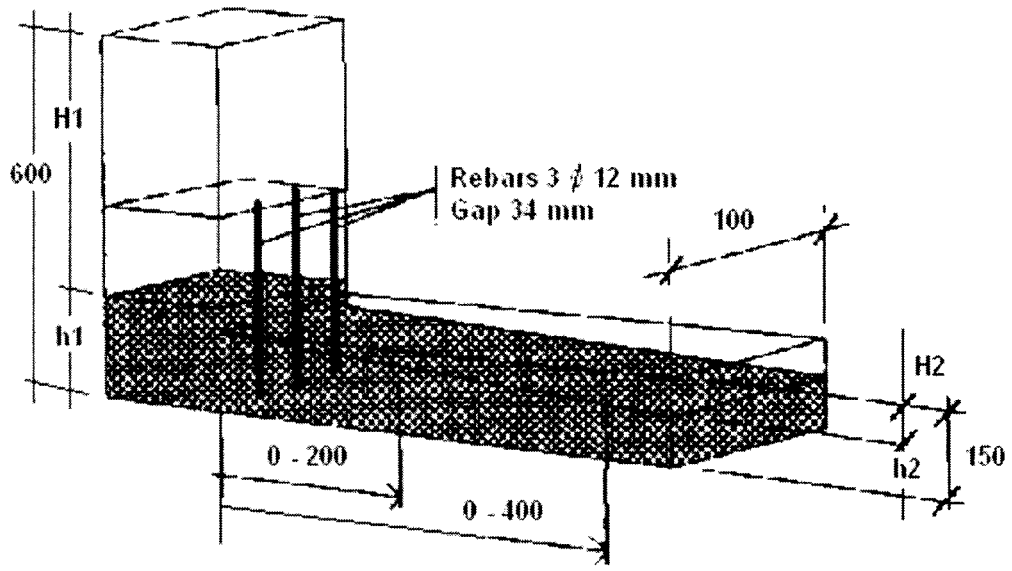

Fig. 2.7: Schematic representation of a L-box test apparatus

Segregation test

Fujiwara [17] had developed a segregation test on fresh concrete. It consists of gently pouring a 2-litre container with fresh concrete over a 5 mm mesh, and then measuring the mass of mortar passing through the screen after 5 minutes. The segregation index is taken as the ratio of mortar passing through the screen to the mass of mortar contained in the 2-litre concrete container. A stable concrete should exhibit a segregation index value lower than 5%. However, due to simplicity of above test, the results are not reproducible, and are very sensitive to the way the concrete is poured. According to Khayat et al. [11], the limit of 5 % is considered to severe, and a limit of 10% appears more realistic.

U-flow test

U-flow test [20] is another test used to determine deformability of SCC through reinforcing bars. A schematic representation of U-flow test is shown in Fig. 2.8 [7]. The test is performed by first completely feeling the left chamber with concrete while the sliding door between the two chambers is closed. The door is then opened and the concrete flows pass the re-bars in to the right chambers. If the filling height is more than 70% of maximum height possible, the concrete is considered as SCC [7].

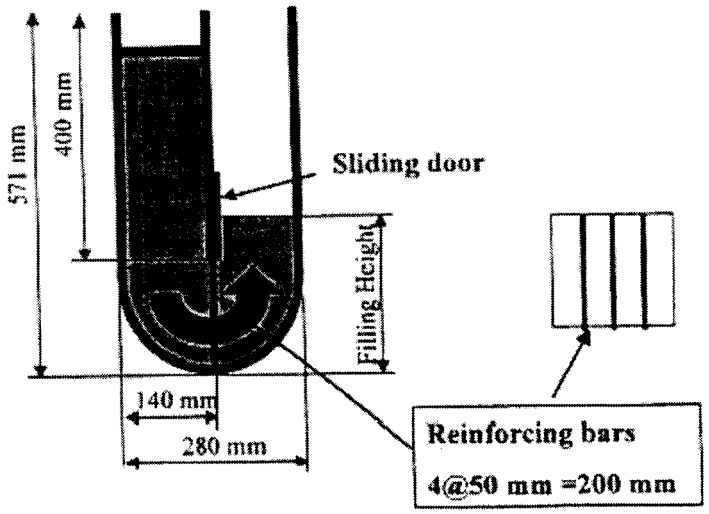

Fig 2.8: Schematic representation of U-flow test.

2.5 Hardened properties of SCC

The segregation and bleeding in SCC can severely affect the hardened properties of SCC. The SCC without segregation and bleeding could have more or less the same hardened properties as normal concrete. The comprehensive study of hardened properties was carried out by Sonebi et al. [19] and the outcome is as follow:

- No significant difference in the pattern of strength development at various ages was observed between SCC mixes and normal mixes.
- The SCC mixes and the reference mixes (normal concrete mixes) had the same relationship between modulus of elasticity and compressive strength.
- The drying shrinkage of SCC mixes at 7 days was slightly higher than that of normal concrete mixes but at 28 days and later the normal mixes exhibited higher shrinkage than SCC mixes.

Persson [21] studied and compared salt scaling and freeze and thaw cycle resistance of SCC and normal concrete with W/B of 0.39 and air content of 6%. The outcome of the study is as follow:

- No significant difference was found between salt scaling of SCC and normal concrete.
- SCC exhibited better freeze and thaw cycle resistance than normal concrete. This may be due to the vibrations of concrete (normal concrete) that may have created pockets around the aggregates where frost damage was occurred [21].

2.6 Statistical models for proportioning and optimizing SCC

The optimization of mixture proportions for SCC, which contain many constituents that are often subjected to several performance constraints at fresh and harden stages, can be difficult and time-consuming task. The trial and error or "one factor at a time" approach will be inefficient and costly. More importantly these approaches may not provide the best combination of materials at minimum cost [22]. The best option is to develop

statistical models based on selected variables for the purpose of optimizing mixtures of concrete, in which final product should be economical and technically desirable [22].

The statistical models are developed by some researchers [11, 15, 23] for proportioning and optimizing SCC mixes with different materials. The models are carried out to set influence of model variables on different key properties of SCC and to reduce the test protocol needed for the proportioning of SCC.

Khayat et al. [11] have developed factorial design model with five independent variables such as W/B (limit 0.37 to 0.50), cementing materials (limit 360 to 600 kg/m^3), viscosity modifying admixture (limit 0.05 to 0.2 % of water), SP (limit 0.3 to 1.1 %), and volume of coarse aggregate (limit 240 to 400 lit/m^3). The responses measured are slump flow, rheological parameters, filling capacity, V-funnel flow, surface settlement and compressive strength (7 and 28 days) of SCC. The following conclusions were drawn:

- For any W/B and SP content, the concrete made with higher binder content had higher deformability and filling capacity.
- The decrease in W/B necessitated an increase in the dosage of SP to maintain a fixed slump flow.
- An increase in SP (up to 0.7 %) with a fixed W/B lowered viscosity and increased filling capacity. However, with increase in SP content beyond 0.7% the filling capacity begins to drop.

Statistical models for SCC incorporating limestone filler were also developed [23]. In this model, four independent variables such as W/B (limit 0.38 to 0.72), limestone filler (limit 0 to 120 kg/m^3), cement (limit 250 to 400 kg/m^3), and SP (limit 0.12 to 0.75 % by mass of powder) were used. The responses measured were slump flow, fluidity loss, V-funnel flow time, rheological parameters, surface settlement, and compressive strengths (1-day and 28-day). The summary of the investigation is as follows:

- The replacement of 100 kg/m^3 of cement with finely ground limestone filler improved the deformability and stability without affecting the one-day compressive strength.
- The increase in limestone filler content can reduce the SP demand to secure a given deformability.
- For given dosage of SP, the loss in slump flow is found to decrease with the increase in limestone filler in mixes containing 360 kg/m^3 of cement. The opposite trend is observed for concrete with 290 kg/m^3 of cement.

2.7 Supplementary cementing materials (SCM)

SCM are materials, when used in conjunction with Portland cement contribute to the properties of fresh and hardened concrete through hydraulic, and pozzolanic activity or both. Typical examples of SCM are: fly ash, granulated blast furnace slag, and silica fume. A pozzolan is a finely divided siliceous or aluminosiliceous material and in presence of moisture, chemically reacts with the calcium hydroxide released by the hydration of portland cement to form compound possessing cementing properties [24].

The practice of using SCM in concrete mixes has been growing in the whole world in recent years. The similarity between these materials are that these are by-products of other process, and their judicious use provide solution that are environmentally-friendly and conserve energy [24]. Various industries are producing millions of tones of pozzolanic materials every year. Dumping of these by-products causes serious environmental pollution. With proper quality control, large amount of these by-products can be incorporated into concrete, either in the form of blended Portland cement or as a mineral admixture. Pozzolanic materials can make concrete competitive, cost effective and durable over other construction materials [24].

2.7.1 Fly ash (FA)

A concrete incorporating high volumes of FA (55 to 60 % replacement of portland cement with class F fly ash) with excellent mechanical properties and durability was developed by CANMET [25]. Bouzoubaa and Lachemi [1] had developed SCC incorporating high volumes of class F fly ash (40 to 60 % replacement of cement) and found encouraging results. The SCC incorporating high volumes of FA could be more economical and environmental friendly option for the construction industry.

2.7.1.1 Definition and classification of FA

FA is the finely divided residue that results from the combustion of pulverized coal and is the by-product of coal-fired power generating plants. The coal is pulverized and blown into burning chamber where it immediately ignites to heat the boiler tubes. The volatile matter and carbon are burnt off whereas most of the mineral impurities deposited in coal

during its formation, such as clay, shale, quartz and feldspar generally fuse and remain in suspension in the flue gas. The fuse matter is quickly transported to lower temperature zones where it solidified as spherical particles. Heavier ash particles fall to the bottom of the burning chamber and lighter ash particles (FA) remain suspended in exhaust gases. These FA particles are removed by mechanical separators, electrostatics precipitators, or bag filters [24, 28].

Canadian Standard Association (CSA) classifies fly ash into three classes based on its CaO content. The Class F fly ash normally produced from burning anthracite or bituminous coal and having a low calcium contents (less than 8%). The class C fly ash normally produced from burning lignite or sub-bituminous coal. It further classifies as class CI, having an intermediate calcium content (8-20%) and class CH, having a high calcium contents (greater than 20%) [26].

In Canada, 4.82 million ton of FA was produced in 2001. Out of that only 1.05 million ton (22%) was used for engineering applications. 0.83 million ton (17%) FA was used for cement and concrete products [27]. Due to its fine particles size and generally non-crystalline character, FAs usually show excellent pozzolanic properties. More FA could be consumed every year by cement and concrete industry, provided there is adequate quality control and better understanding of technical requirements for the satisfactory performance of material [29].

2.7.1.2 Physical, Chemical, and mineralogical properties of FA Physical properties

Most of FA particles are solid spheres and some are hollow cenospheres. The particle sizes in FA vary from less than 1μm to more than 100 μm. However only 10 to 30% of the particles by mass are larger than 45 μm [24, 26]. The scanning electron microscope (SEM) of FA and cement is presented in Fig. 2.9 [29]. The surface area is typically 300 to 500 m^2/kg, although some FAs can have low or high surface area. The bulk density of FA can vary from 540 to 860 kg/m^3 and specific gravity generally ranges between 1.9 and 2.8. Generally it contains tan or grey color [26]. It appears that, difference in particle size distribution, morphology, and the surface characteristics of FA would influence water demand and reactivity. FA consisting of clean, glassy, spherical particles should be able to reduce water requirement especially when proportion of fine aggregates is less [24].

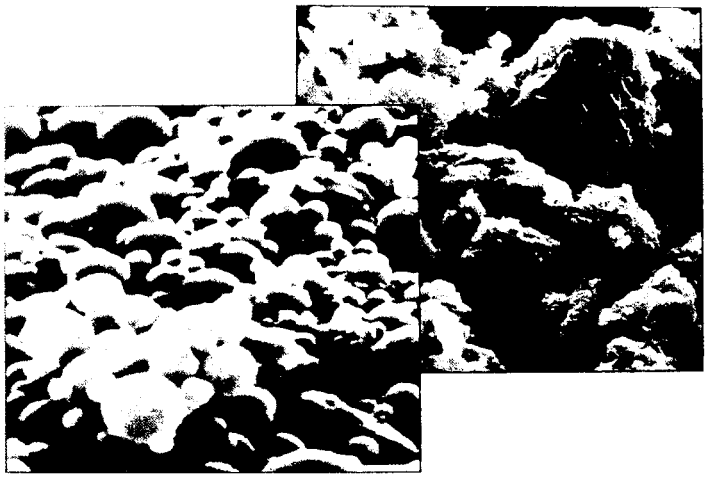

Fig. 2.9: Scanning electron microscope picture of FA (left) and Portland cement (right) [29].

Chemical properties

The FA is primarily silicate glass containing silica, alumina, ion, and calcium. Minor constituents are magnesium, sulpher, sodium, potassium, and carbon. The crystalline compounds are present in small amounts [26]. Typical chemical compositions for class F, class C, and Portland cement are given in Table 2.2 [29]. As per the ASTM standard specification for mineral admixture (ASTM C-618), a minimum 70 % of non calcium oxides (silica + alumina + iron oxide) for class F fly ash, and 50 % for class C fly ash are required. Typically, class C ashes contain 1 to 3 % free lime, which is reactive with water and class F fly ash contains no free lime [30].

Table 2.2: Typical chemical composition of FA and Portland cement [29].

Compounds	Fly ash class		Portland Cement
	Class F	Class C	
SiO_2	54.9	39.9	22.6
Al_2O_3	25.8	16.7	4.3
Fe_2O_3	6.9	5.8	2.4
CaO	8.7	24.3	64.4
MgO	1.8	4.6	2.1
SO_3	0.6	3.3	2.3

Mineralogical properties of FA

FA particles are composed of glass with non-crystalline minerals. However crystalline minerals are present in small amounts. The low calcium FA (class F), due to high proportion of silica and alumina consists principally of aluminosilicate glass. In the

furnace, very large sphere of molten glass may not get cooled rapidly and uniformly, thus the crystallization of aluminosilicate takes place as a slander needles in the interior of glassy sphere, and the same is non-reactive [24]. Mehta [24] noted from the results of Diamond [31] and Mortureux et al. [32] that the principal crystalline minerals in low calcium FA are quartz, mullite, sillimanite, hematite, and magnetite. Since the crystalline minerals are non-reactive at ordinary temperature in the Portland cement solution phase, their presence in large proportion, at the cost of non-crystalline component or glass, reduces the reactivity of ash.

In regards to high calcium FA (class C), it appears that the chemical composition and reactivity of the non-crystalline or glassy phase is different from the low calcium FA. The principal crystalline mineral in high calcium FA is C_3A, which is known to be a most reactive mineral present in the portland cement. It appears that the calcium aluminosilicate glass in high calcium FA would be more reactive than the aluminosilicate glass in low calcium FA [24]. Another important difference is that in the high calcium FA, there is usually a little (less than 2%) unburned carbon. In the low calcium FA, complete removal of carbon is rare and the presence of 2 to 10 % carbon, which can be easily determined by the loss of ignition test. Some of the carbon may be encapsulated in the glass, but the major portion appears to occur as cellular, or lacy particles, which have high internal surface, and are therefore capable of adsorbing large amount of water. If the proportion of cellular or lacy particles of carbon (larger than 45 mili. Micron size) is higher in FA, the use of such FA as a mineral admixture in concrete increases the water requirement and consumption of air-entering admixture [24, 30].

2.8 Influence of FA on the fresh properties of SCC

2.8.1 Effect on the workability/ flowability

Workability is an important property of plastic concrete; it depends mainly on the cohesiveness. Cohesiveness is largely controlled by the volume of the paste in the concrete. FA can be added to concrete by three ways, firstly as a partial replacement of cement by mass, secondly as a partial replacement of aggregates, and thirdly as a partial replacement of both cement and aggregates. The fine particles of FA, generally improve the workability and flowability by reducing the size and volume of voids, thus requiring less water to produce a concrete of given consistency [30].

Berry et al. [33] reported that the concrete made by substituting 30% of cement with class F fly ash required 7% less water than the control concrete of equal slump. In another case involving investigation of concrete materials for construction of south Saskatchewan river dam, it was found that with the addition of FA, the resulting concretes, with a lower ratio of water to total cementatious materials (Portland cement + FA), showed improved cohesiveness and workability and reduction in segregation [33]. Many investigators observed that the use of coarse FA, or a FA with high loss on ignition (usually 10 % or more) caused an increase in water requirement instead of reducing it. It is now known that this would happen only when a considerable amount of carbon, which are usually large in size, is present in the FA. Again, some high calcium fly ashes may contain significantly large amount of C_3A, which tends to increase the water requirement due to loss of consistency, caused by the rapid formation of calcium aluminate hydrates or sulfoaluminate hydrates. When FA is added to concrete by partial replacement of

aggregates, workability will be slightly reduced, because of increase in water demand and increase in viscous drag due to presence of additional particles [24].

The study of SCC [1] incorporating high volumes of class F fly ash confirmed that the dosage of SP increased with the decrease in the percentage of FA for achieving desire deformability. Xie et al. [4] developed a SCC incorporating ultra-pulverized fly ash (UPFA) (30 to 40 %). The chemical composition was similar to that of class F fly ash but Blaine fineness was very high ranging from 550 to 1100 m^2/kg. The effect of UPFA on the fresh SCC was to improve the viscosity of fresh SCC, and its effect was similar to those of viscosity modifying agents [4].

2.8.2 Effect on the setting time of concrete

FA concrete mixtures set more slowly than corresponding Portland cement concrete. For high carbon FA, the water requirement for given consistency is higher and thus retards the setting times also [24, 35]. Lane and Best [40] stated that FA generally slows the setting of concrete and the retardation may be affected by the proportion, fineness, and chemical composition of ash.

In a study undertaken by Bouzoubaa and Lachemi [1], it was found that the initial setting time of SCC with 60% class F fly ash was 7.26 h:m while the final setting time was 10.04 h:m. The initial and final setting time of control concrete (without FA) were 4:48 h:m and 6:28 h:m respectively. The setting times of SCC incorporating 40 to 60% class F fly ash were found to be 3 to 4 hours longer than the control concrete [1]. It is advisable that

before using an unknown FA, the influence on the setting time of concrete should be investigated.

2.9 Influence of FA on the mechanical properties and durability of concrete

2.9.1 Effect on compressive strength

Due to economic and durability considerations, FA is generally used as a partial replacement of Portland cement in concrete. Compressive strength is one of the important property of concrete. Most of the other properties directly or indirectly, depend on the compressive strength. Both the strength development rate and the ultimate strength are controlled by different inter related parameters including the kinetics of hydration reaction of compound of Portland cement and mineralogical phase of admixture and its characteristics. This is because the strength development is a function of pore-filling process, which takes place with the formation of hydration products [24].

The high calcium FA may start its cementitious and pozzolanic activity as early as 3 days after initiation of hydration. The low calcium FA decreases the strength at early age (7 days) and increases it at later age (56 days). It seems that the availability of hydroxyle, sulfate and calcium ions in the surrounding solution triggers the hydration of high calcium FA relatively quickly, and the process is self-sustaining due to the supply of these ions from the hydration of FA itself [24].

When FA is used as a partial replacement for fine aggregates, it increases the strength of concrete at both early and late ages. The strength gain at early ages is in part due to a

slight acceleration in Portland cement hydration. The strength gain at later ages, which can be substantial, is mostly due to the pozzolanic reaction, causing pore refinement, and replacing the weaker component (calcium hydroxide) with the stronger one (C-S-H) [16, 24].

If the elimination of large pores and the reduction of calcium hydroxide are necessary elements for producing concretes with a high compressive strength, FA and other mineral admixtures are most suited, irrespective of their use as cement replacement, aggregate replacement, or both [16].

2.9.2 Effect on modulus of elasticity

The modulus of elasticity is greatly influenced by the strength of concrete, the stiffness of aggregates, the cement paste matrix, the transition zone, and the testing parameters. The elastic modulus of cement paste matrix is determined by the porosity. The factors controlling porosity are W/B, air content, mineral admixture, and degree of cement hydration [16].

It is well established that FA has great influence in controlling the porosity of concrete by pore refinement and consuming the calcium hydroxide from the cement paste matrix [16]. In general, void spaces, micro cracks, and oriented calcium hydroxide crystals are relatively more common in transition zone than in the bulk cement paste; therefore they play a very important role in determining the modulus of elasticity of concrete. It has been reported that the strength and elastic modulus of plain concrete seems to be

proportionate to each other during early ages (before 3 months), but they do not show the same behavior at later age (3 months to 1 year). The elastic modulus increases at a higher rate than the compressive strength. The elastic modulus of concrete containing FA is reported to be higher after the age of 90 day, compared to plain Portland concrete [16].

2.9.3 Effect on drying shrinkage

Many studies have been carried out to investigate the influence of FA on shrinkage of concrete. It is observed that the replacement of cement by FA has very little or no influence on the shrinkage [24, 34]. In regard to drying shrinkage, Mehta [24] noted from the results of Lane et al. [40] that the drying shrinkage of plain and FA concrete prisms was essentially the same after 400 days.

Robert et al. [30], studied the drying shrinkage of concrete with different percentage of FA as cement replacement. The results indicate that the shrinkage strain for the FA and controlled concrete are essentially equal at any given time. At the end of one-year, the drying shrinkage strain for 0, 20, 30, 50 % fly ash specimens was around 600 of micro-strain.

Bouzoubaa and Lachemi [1] made the same conclusion from their study on the drying shrinkage of SCC incorporating high volumes of FA. The drying shrinkage for SCC incorporating FA are low and do not exceed 600 micro-strain at 224 days. No difference is noticed between the drying shrinkage of the control concrete and SCC incorporating FA.

2.9.4 Effect on the freezing and thawing cycles resistance

Concrete containing FA must be sufficiently air entrained to provide freezing and thawing resistance. As the quantity of FA increases the requirement of air-entrained admixture increases. The major factor affecting air entrainment of FA concrete is the carbon content. High surface area of carbon adsorbs air-entraining agent from the concrete mix, resulting in the requirement of higher dosage to obtain a specified air content. Once the adequate air content is established, the FA concrete should resist the freezing and thawing cycles [21, 24, 33].

Robert et al. [30] studied the freeze and thaw resistance for FA concrete after 14 days of curing. The non-entrained concretes were damaged after few cycles. The durability was found to increase with the increase in percentage replacement of cement by FA at W/B of 0.38 and 0.45. The concrete with 20% FA replacement was found to have better durability than the control mix. After 400 cycles, more scaling damage was noted on the 50 percent FA replacement specimens than those on the 20 and 30 percent replacement specimens.

2.9.5 Effect on scaling resistance

Aside from causing steel corrosion, the repeated application of deicing chemicals has the potential to cause scaling of concrete surface. The exact cause of this problem is not completely understood [16]. However deicing chemicals are used to melt ice and following process occurs: the ice melt, the concrete thaws, the melt water is absorbed, the surface concrete become more saturated, the melt water is diluted, and the concrete

surface freezes. This freezing and thawing cycle is repeated again and again causing scaling on the concrete surface [16, 37].

Researchers at CANMET [25] evaluated the scaling resistance to high volumes of fly ash concrete to deicing salts. Both visual examination and weight loss indicated severe scaling of the surfaces of the test specimens with coarse aggregate visible over the entire surface. According to ASTM C 672 scale of visual rating of 0 to 5, the test specimens were rated 5. In general, the scaling resistance decreases with the increase in FA content.

2.9.6 Effect on the chloride permeability

The permeability of concrete is the fundamental parameter to determine the rate of mass transfer related to the destructive chemical action such as chloride, sulfate, carbon dioxide, and alkali aggregate expansion and greatly affect the durability of concrete [38]. The two factors, which adversely affect the impermeability of concrete, are [38]:

1. The presence of large voids in hydrated cement paste.
2. The micro cracks at the aggregate-cement paste transition zone.

FA can improve the permeability of concrete due to its capability of transforming large pores of concrete into small pores and reducing micro cracking in the transition zone [16].

In concrete, it is now known that the transition phase between the aggregate and hydrated cement paste plays a very important part in determining the mechanical properties and long term durability characteristics of concrete [38]. In normal Portland cement concrete,

the transition zone is generally less dense and contains a large amount of crystals of calcium hydroxide than concrete containing FA. It is more prone to micro cracking due to tensile stresses induced by normal thermal and humidity changes. The presence of high calcium FA reduced the degree of orientation of calcium hydroxide crystals in the transition zone. On the other hand, the addition of low calcium FA increased both the thickness of the transition phase and the degree of orientation of calcium hydroxide at the same hydration age. Therefore, high calcium FA shows better resistance to permeability than low calcium FA [24]. Papadakis [39] studied the chloride permeability of cement mortar having different percentages of fly ash. The rapid chloride permeability decreased with the use of FA either by replacing cement or aggregates. The electric charge passed through the control specimens was higher than 4000 coulombs. All the specimens incorporating FA, whether it substitutes cement or aggregates, exhibited lower electrical charge. The charge passed through a specimen was found inversely proportional to FA content in the mortar volume [39].

It may be concluded that the use of FA can reduce the water demand and bleeding in fresh concrete, decrease the size and number of large voids in hydrated cement paste, lower the amount and degree of orientation of crystalline calcium hydroxide as well as micro cracking in transition phase, and improve the impermeability of concrete.

Chapter 3 Experimental Program

3.1 Introduction

The experimental program was carried out in three phases. In phase I, the measurement of flowability of pastes with Marsh cone and rheological parameters of pastes were carried out. The rheological parameters of mortars were investigated in phase II. In phase III, the tests on fresh and mechanical properties as well as durability of SCC were carried out.

Four independent variables such as total binder content, percentage of FA replacing cement by mass in total binder content, percentage of solid content of superplasticizer with respect to total binder content (% of SP), and W/B are selected for the tests on paste, mortar, and SCC. The amount of fine aggregate in the case of mortar and the amount of fine and coarse aggregates in the case of SCC were kept constant for all mixes. A total of twenty-one mixes were prepared for paste, mortar, and concrete.

3.2 Materials

3.2.1 Cement

CSA Type 10, equivalent to ASTM Type I, normal Portland cement was used. Its physical properties and chemical compositions are presented in Table 3.1.

Table 3.1: Physical properties and chemical analysis of cement and fly ash (FA)

	Cement (CSA Type 10)	FA, ASTM Class F
Physical properties		
Specific gravity	3.1	2.1
Fineness		
Passing 45 micron %	87.1	83.6
Specific surface, Blain, cm^2/g	3740	3060
Compressive strength MPa		
7- day	33.8	-
28-day	41.0	-
Water requirement, %		99.2
Pozzolanic activity index		
7-day	-	94.5
28-day	-	106.9
Setting time, Minutes		
Initial setting time	121	-
Final setting time	-	-
Air content of mortar, volume %	8.1	-
Chemical analysis, %		
Silicon dioxide, (SiO_2)	19.4	52.4
Alluminium Oxide (Al_2O_3)	5.3	23.4
Ferric Oxide (Fe_2O_3)	2.3	4.7
Calsium oxide (CaO)	61.8	13.4
Magnesium oxide (MgO)	2.3	1.3
Sodium oxide (Na_2O)	0.2	3.6
potassium oxide (K_2O)	1.1	0.6
Equivelent alkali (Na_2O+0.658 K_2O)	1.0	4.0
Phosphorous oxide (P2O5)	0.1	0.2
Titanium oxide (TiO_2)	0.3	0.8
Chloride (Cl)	0.1	-
Sulfure trioxide (SO_3)	3.8	0.2
Loss on ignition	2.1	0.3
Bogue potential compound composition		
Free CaO	0.8	-
Tricalsium silicate (C_3S)	53.8	-
Dicalcium silicate (C_2S)	15.2	-
Tricalsium aluminate (C_3A)	10.2	-
Tetra calcium aluminoferritte (C_4AF)	7.1	-

3.2.2 Aggregates

Natural gravel with nominal maximum size of aggregate (MSA) of 12.5 mm and natural sand were used as coarse and fine aggregate respectively, in concrete mixes. The grading or particle size distribution of coarse and fine aggregates was determined in accordance with ASTM C 136 and the results are presented in Table 3.2. The specific gravity, bulk density, moisture absorption, and surface moisture content of coarse and fine aggregates calculated as per ASTM standards are tabulated in Table 3.3.

3.2.3 Fly ash

ASTM class F (CSA class CI) fly ash from Alberta, was used. Its physical properties and chemical compositions are presented in Table 3.1

3.2.4 Superplasticizer (SP)

The poly-naphthalene sulfonic acid based SP was used for all the mixtures. The SP is in accordance with ASTM C 494 type F specifications. The physical characteristics provided by manufacturer are presented in Table 3.4.

Table 3.2: Grading, fineness modulus, and MSA of coarse and fine aggregate

Sieve size	Percentage retained by mass	Cumulative percentage retained by mass
Coarse aggregate		
19 mm (3/4-in.)	0	0
12.5 mm (1/2-in.)	5.4	5.4
9.5 mm (3/8-in.)	20.1	25.5
4.75 mm (No.4)	70.2	95.7
Total		
Nominal MSA	**12.5 mm**	
Fine aggregate	Percentage retained by mass	Cumulative percentage retained by mass
9.5 mm (3/8-in.)	0	0
4.75 mm (No.4)	0.72	0.72
2.36 mm (No. 8)	9.13	9.85
1.18 mm (No. 16)	10.35	20.2
600 micron (No.30)	23.64	43.8
300 micron (No. 50)	36.22	80
150 micron (No.100)	15.48	95.54
Total		250.11
Fineness modulus	**2.5**	

Table 3.3: Physical test results of aggregates

Test	Coarse Aggregate	Fine aggregate
Dry loose bulk density Kg/m^3	1.59	1.78
Specific gravity- SSD	2.68	2.78
Specific gravity- Bulk	2.64	2.73
Moisture absorption %	1.74	1.83
Wash test-% loss	2.00	-

Table 3.4: Physical characteristics of superplasticizer

Characteristic	Result
Physical test	Liquid
Specific gravity at 25^0 C	1.21
% of solid by weight	40.5
pH	8.5
Color	Dark brown
Sulphates, %	1.2

3.3 Methodology

3.3.1 Design of experiments

At present time, there is no theoretical approach available that can be used to design SCC with optimum SCM content. Normally a pre-decided proportion of SCM is used in trial batches. If it gives satisfactory results, that proportion is used for SCC. For all successful SCC compositions that can be found in the literature, there comes a time when trial batches have to be made using the pre-selected materials in order to produce SCC fulfilling all the specified requirements [38]. Without optimizing SCM, most economical SCC cannot be produced. It is a very heavy task to develop an optimized composition using trial batches. With a minimum number of a well planed trial batches, it is possible to explore a large area of composition in order to find the optimized composition fulfilling the specified requirement. It involves some sophisticated mathematics,

probability and statistical concept [38].

Statistically balanced design of experiment is desired to understand relationships between input factors and responses, to build mathematical models relating the input factors and responses, and to optimize the responses with minimum cost and optimum engineering properties. Some methods for the design of experiments are available in the literature; Box-Wilson Central Composite Design (CCD) method was found most convenient and used in this project. The CCD method efficiently reduces the number of runs compared to other methods, and is considered best when quantitative variables are used in experiments [41].

3.3.1.1 Box-Wilson Central Composite Designs (CCD) [41]

A CCD method is very flexible and an efficient second order modeling design for quantitative factors. Four input factors were used in the test program such as X_1 as total binder content, X_2 as percentage of FA replacing cement content, X_3 as percentage solid mass of superplasticizer with respect to total binder content, and X_4 as W/B. The limit of the experiment of study as shown in Table 3.5 is set 350 to 450 kg/m^3 for X_1, 30 to 60% for X_2, 0.1 to 0.6 % for X_3, and 0.33 to 0.45 for X_4.

The CCD consisted of three portions as follow:

Fraction factorial portion (n_f)

The fractional factorial method is an efficient alternative of full factorial method, where the factors are set at 2 levels and the number of runs (mixes) is decided by 2^{k-1}, where k is

the number of factors. In this study, the total number of runs (mixes) for fraction factorial portion is kept $2^{4-1} = 8$ with different combination of coded value varying between +1 and –1 as shown in Table 3.6

Center point portion (n_c)

Enough numbers of runs for center points are needed to get good estimation of pure experimental error and to maintain orthogonality. According to Schmidt et al. [40], minimum number (nc) can be obtained from the following equation:

$$4 \times \sqrt{n_f + 1} - 2k \qquad (3.1)$$

A total of 5 runs (mixes) was kept for center point portion (Table 3.6) with '0' coded value.

Axial Portion

The numbers of runs for axial portion were set 2k = 8 for the experimental program. The coded value of portion is set at $(n_f)^{1/4} = (8)^{1/4} = 1.68$, where n_f is the number of runs in fraction factorial portion of the design. The final coded value is set at five different levels such as –1.68, -1, 0, +1, +1.68. The detail is shown in Table 3.5.

The total numbers of runs (mixes) were twenty-one and the sequence of mixes was randomized as shown in Table 3.6

Table 3.5: Limit and coded value of factors (variables)

Factor	Detail	Limit	Coded value				
			-1.68	-1	0	+1	+1.68
X_1	Total binder content kg/m^3	350 to 450	350	370	400	430	450
X_2	% of fly ash	30 to 60 %	30	36	45	54	60
X_3	S.P % of solid mass w.r to total binder	0.1 to 0.6%	0.1	0.2	0.35	0.5	0.6
X_4	W/B	0.33 to 0.45	0.33	0.355	0.39	0.425	0.45

Table 3.6: Center composite design for four variables

Run #	Mix #	Factors				Remarks
		X_1	X_2	X_3	X_4	
1	6	+1	+1	-1	-1	Fractional factorial portion
2	8	-1	-1	-1	-1	
3	10	-1	-1	+1	+1	
4	11	+1	-1	+1	+1	
5	13	-1	+1	-1	+1	
6	17	+1	+1	+1	-1	
7	20	-1	+1	+1	+1	
8	21	+1	-1	-1	+1	
9	1	0	0	0	0	Center point portion
10	2	0	0	0	0	
11	9	0	0	0	0	
12	15	0	0	0	0	
13	18	0	0	0	0	
14	7	+1.68	0	0	0	Axial portion
15	4	-1.68	0	0	0	
16	3	0	+1.68	0	0	
17	12	0	-1.68	0	0	
18	14	0	0	+1.68	0	
19	16	0	0	-1.68	0	
20	5	0	0	0	+1.68	
21	19	0	0	0	-1.68	

3.3.2 Measurement of flowability of paste with Marsh cone

The Marsh cone apparatus was used to determine the flowability of cement paste. Marsh cone is being used for different industrial sectors to appreciate the flowability of different types of grout or mud. The principle of the method consists in the preparation of a grout and the measurement of the time needed for a certain volumes of grout to flow through a funnel having a given diameter. The cones that are used may have different geometric features and the diameter of the funnel may range from 5 mm to 12.5 mm [38].

A total of twenty-one cement paste mixtures were prepared from cement, FA, water, and SP in the laboratory using a portable blender machine. Mixture proportions of the ingredients are shown in Table 3.7. The mixing sequence used for preparation of pastes is as follows:

The water and SP were placed in a bowl. Cement and fly ash were added to the bowl and mixed for 1 minute with a blender speed set to speed # 4 (4000 rpm), the blender was then stopped and the side of the bowl was scraped. Finally, the paste was mixed for additional 2 minutes at speed # 4 (4000 rpm).

The methodology of Marsh cone test was as follows [42]:

- 1.2 liter of paste was poured into the Marsh cone while the bottom opening was closed.
- The flowing time (S_p) in second was recorded for all the mixes as a time required by the paste, which passed through the Marsh cone, to fill 300-cm^3 bottle.

3.3.3 Experimental procedures for rheology of paste and mortar

Flow behaviors of cement paste and mortar are complex rheological phenomenon involving shear stress and shear rate (shear strain rate) as described by Newton's law of viscous flow. The concrete flow is considered to follow the Bingham model. The flow behavior of the test sample can be quantified by the measurable parameters of shear stress and shear rate, which have linear relationship, as demonstrated by the Bingham model and depends on the torque 'T' and the rotational speed 'N' respectively.

Table 3.7: Mix proportioning for paste

Mix. No.	Binder content (Kg/m^3) *X_1	% of Fly ash *X_2		% of S.P X_3	W/B X_4	Cement Content *(kg/m^3)	Water content *(Kg/m^3)
		%	Kg/m^3				
1	1200	45	540.0	0.35	0.39	660.0	468.0
2	1200	45	540.0	0.35	0.39	660.0	468.0
3	1200	60	720.0	0.35	0.39	480.0	468.0
4	1050	45	472.5	0.35	0.39	577.5	409.5
5	1200	45	540.0	0.35	0.45	660.0	540.0
6	1290	54	696.6	0.2	0.335	593.4	457.9
7	1350	45	607.5	0.35	0.39	742.5	526.5
8	1110	36	399.6	0.2	0.355	710.4	394.0
9	1200	45	540.0	0.35	0.39	660.0	468.0
10	1110	36	399.6	0.5	0.425	710.4	471.8
11	1290	36	464.4	0.5	0.425	825.6	548.3
12	1200	30	360.0	0.35	0.39	840.0	468.0
13	1110	54	599.4	0.2	0.425	510.6	471.8
14	1200	45	540.0	0.6	0.39	660.0	468.0
15	1200	45	540.0	0.35	0.39	660.0	468.0
16	1200	45	540.0	0.1	0.39	660.0	468.0
17	1290	54	696.6	0.5	0.355	593.4	457.9
18	1200	45	540.0	0.35	0.39	660.0	468.0
19	1200	45	540.0	0.35	0.33	660.0	396.0
20	1110	54	599.4	0.5	0.425	510.6	471.8
21	1290	36	464.4	0.2	0.425	825.6	548.2

* The contents based on kg/m^3 of paste

The rheological measurement of paste and mortar were conducted using a Brookfield viscometer (model RVDV- II +). The viscometer is equipped with disc type spindles with guard leg. The viscometer measured the torque required to rotate the standard spindles in paste and mortar. The Brookfield viscometer model RVDV- II + gives only apparent viscosity and torque at a given spindle speed. The torque and spindle speed-readings were converted into viscosity functions such as shear stress and shear rate [43].

Table 3.8: Mix proportioning for mortar

Mix. No.	Binder content (Kg/m^3) *X_1	% of Fly ash *X_2		% of S.P X_3	W/B X_4	Cement Content *(kg/m^3)	Water content *(Kg/m^3)	Fine Aggregate *(kg/m^3)
		%	Kg/m^3					
1	600	45	270.0	0.35	0.39	330.0	234.0	1374
2	600	45	270.0	0.35	0.39	330.0	234.0	1374
3	600	60	360.0	0.35	0.39	240.0	234.0	1329
4	525	45	236.3	0.35	0.39	288.7	204.7	1536
5	600	45	270.0	0.35	0.45	330.0	270.0	1275
6	645	54	348.3	0.2	0.335	296.7	228.9	1311
7	675	45	303.7	0.35	0.39	371.3	263.2	1212
8	555	36	199.8	0.2	0.355	355.2	197.0	1551
9	600	45	270.0	0.35	0.39	330.0	234.0	1374
10	555	36	199.8	0.5	0.425	355.2	235.9	1440
11	645	36	232.2	0.5	0.425	412.8	271.1	1240
12	600	30	180.0	0.35	0.39	420.0	234.0	1419
13	555	54	299.7	0.2	0.425	255.3	235.9	1395
14	600	45	270.0	0.6	0.39	330.0	234.0	1374
15	600	45	270.0	0.35	0.39	330.0	234.0	1374
16	600	45	270.0	0.1	0.39	330.0	234.0	1374
17	645	54	348.3	0.5	0.355	296.7	228.9	1308
18	600	45	270.0	0.35	0.39	330.0	234.0	1374
19	600	45	270.0	0.35	0.33	330.0	198.0	1473
20	555	54	299.7	0.5	0.425	255.3	235.9	1392
21	645	36	232.2	0.2	0.425	412.8	274.1	1245

* The contents based on kg/m^3 of mortar

The cement paste was prepared as discussed in section 3.3.2. The cement mortar was mixed in a Hobart paddle mixer with the mixture proportion shown in the Table 3.8. The water and SP were placed in a mixing bowl. The cement, FA, and fine aggregate were added at 1-minute interval with the mixer set to speed # 1 (140 rpm). The mortar was then mixed for 2.5 minutes at speed # 2 (285 rpm). The mixer was stopped and the side of the mixing bowl was scraped. Finally, the sample was mixed for an additional 2.5 minutes at speed # 2. The temperature was kept at 23 ± 2° C during the mixing and testing of the cement paste and mortar. The methodology followed for converting torque and spindle speed into rheological functions such as shear stress and shear rate is as given by Mitschka [43].

- The torque values were noted for different spindle speeds of 5, 6, 10, 12, 20, 30, 50, 60, and 100 rpm.
- The values of torque were then converted to shear stress (Pa.) using the following equation:

$$\tau_i = k_{\alpha t}\, \alpha_i \qquad (3.2)$$

Where

τ_i = Shear stress in Pa. for i^{th} speed

$k_{\alpha t}$ = Coeffi.

α_I = Torque for i^{th} speed

- The shear stress and spindle rotation speed-readings were plotted on log-log form. The slope of the curve is considered as the flow index of fluid 'n'
- Shear rate values (in S^{-1}) were then calculated from the following equation:

$\gamma_i = k_{ny}\,(n)\,N_i$ (3.3)

Where

γ_I = Shear rate for i^{th} speed

k_{ny} (n) = Coeffi.

N_i = Spindle speed rpm

The shear stress and shear rate were then plotted on chart and slope and intercept of regression line represented plastic viscosity (Pa.s) and yield stress (Pa.), respectively.

3.3.4 Mixture proportion of SCC

The proportions of the SCC mixtures are presented in Table 3.9. A total 21 mixtures were prepared with varying proportion of four independent variables as shown in Table 3.5 and Table 3.6. The proportion of course aggregate was kept constant at 900 kg/m^3 while the proportion of fine aggregate was varied a little as mix design procedure is based on the absolute volume method.

All concrete mixtures were prepared in 0.07 m^3 (70 liter) batches in a fixed horizontal pan mixer. The batching sequence consisted of homogenizing of coarse aggregate and fine aggregate for 30 seconds then approximately 75 % of the water was added and mixed for 30 seconds. Cement and FA were then added and the mixing was done for 1 more minute. The remaining water along with SP was added and concrete was mixed for 3 minutes, and after 2-minute rest, the mixing was resumed for 2 more minutes.

Immediately after mixing the concrete, fresh concrete tests have started. The fresh

concrete tests consisted of slump and slump flow, V-funnel, filling capacity, L-box, segregation, bleeding, air content, 45-minute slump and slump flow, and setting times.

Table 3.9: Mix proportioning for SCC

Mix. No.	Binder content Kg/m^3 *X_1	Fly ash *X_2		% of S.P X_3	W/B X_4	Cement Content *(kg/m^3)	Water content *(kg/m^3)	Coarse Aggregate *kg/m^3)	Fine Aggregate *(kg/m^3)
		%	Kg/m^3						
1	400	45	180	0.35	0.39	220	156	900	916
2	400	45	180	0.35	0.39	220	156	900	916
3	400	60	240	0.35	0.39	160	156	900	886
4	350	45	157	0.35	0.39	193	137	900	1024
5	400	45	180	0.35	0.45	220	180	900	850
6	430	54	232	0.2	0.335	198	153	900	874
7	450	45	202	0.35	0.39	248	176	900	808
8	370	36	133	0.2	0.355	237	131	900	1034
9	400	45	180	0.35	0.39	220	156	900	916
10	370	36	133	0.5	0.425	237	157	900	960
11	430	36	155	0.5	0.425	275	183	900	827
12	400	30	120	0.35	0.39	280	156	900	946
13	370	54	200	0.2	0.425	170	157	900	930
14	400	45	180	0.6	0.39	220	156	900	916
15	400	45	180	0.35	0.39	220	156	900	916
16	400	45	180	0.1	0.39	220	156	900	916
17	430	54	232	0.5	0.355	198	153	900	872
18	400	45	180	0.35	0.39	220	156	900	916
19	400	45	180	0.35	0.33	220	132	900	982
20	370	54	200	0.5	0.425	170	157	900	928
21	430	36	155	0.2	0.425	275	183	900	830

* The contents based on kg/m^3 of concrete

3.3.5 Preparation and casting of test specimens for SCC

From each of the concrete mixtures, the following test specimens were cast:

- Ten 100 x 200 mm cylinders (Nine cylinders for the compressive strength at 1, 7, 28 days), and one cylinder for rapid chloride permeability test at 28 days);

- One 150 x 300 mm cylinder for the modulus of elasticity test;
- One 75 x 75 x 300 mm prism for the freezing and thawing resistance test;
- One 150 x 300 x 75 mm sample for the scaling resistance test;
- Three 75 x 100 x 300 mm prisms for shrinkage measurements;
- One 75 x 100 x 380 mm prism for the flexural strength test;

One standard cylindrical container of approximately 14-liter capacity with 255 mm inside diameter was filled with fresh concrete to determine the bleeding. One 150 x 150 mm cylinder was filled with mortar obtained by sieving the fresh concrete to determine the setting time of concrete. All SCC specimens were cast in one layer without any hand compaction or mechanical vibration.

After casting, all the molded specimens were covered with plastic sheets and water saturated burlaps, and left in the humidity room for 24 hours. They were then demolded and the cylinders and prisms were placed to the humidity room at 23 ± 2° C and 100 % relative humidity until required for testing. The prisms for the drying shrinkage test were stored in lime-saturated water for 28 days prior to their transfer to the conditioned chamber of 22° C and 50 % relative humidity. The specimen for scaling resistance was placed in moist curing room for 14 days and stored in the air for 14 days at 23 ± 2° C and 45 to 55% relative humidity.

3.4 Tests on SCC

The tests on fresh and mechanical properties were carried out for each of 21 mixtures of SCC.

3.4.1 Tests on the fresh properties of SCC

Slump and slump flow tests

The slump test was carried out as per ASTM C 143 procedure. The deformability and flowability of fresh SCC in absence of obstructions was evaluated by using the slump flow test. The fresh SCC was filled in one layer in the standard slump cone without any consolidation. The slump flow value represents the mean diameter (measured in two perpendicular direction) of SCC after lifting the standard slump cone and concrete is stopped flowing. The slump and slump flow after 45 minutes were also measured and recorded to evaluate the slump loss of SCC with time.

V-funnel test

The deformability of SCC through restricted areas was evaluated using the V-funnel test [13]. In this test, the V-shaped funnel was filled completely with fresh SCC and the bottom outlet was opened to allow concrete to fall out under gravity. The time of flow from the opening of bottom outlet to the complete seizure of flow was measured as a V-funnel flow time.

Segregation test

The segregation test suggested by Fujiwara [17] was used in this study. This test was

conducted by gently pouring a 2-litre container of fresh concrete over a 5 mm mesh, and the mass of mortar passing through the screen after 5 minutes was measured. The segregation index was taken as a ratio of the mortar passing through the screen to that mortar volume contained in the 2-litre concrete sample.

Filling capacity test

The filling capacity was determined by casting the concrete in a transparent box of 300 x 500 x 300 mm that had closely spaced smooth horizontal 16 mm diameter copper tubes. The concrete was introduced through a funnel into the section that was free of obstacles until the concrete reaches 220 mm height. Once the flow of concrete among the bars ceased, the relative area occupied by the concrete in the restricted section was noted to calculate the filling capacity [14].

L-box test

The L-box test was performed to evaluate the ability of SCC to flow through gaps between reinforcement blocking. It consisted of three reinforcing bars with gaps of 35 mm. The vertical part of the box was filled with fresh SCC. After that, the gate was opened to allow the concrete to flow out of the vertical part into the horizontal part through the reinforcing bars. The time for the leading edge of the concrete to reach a distance of 200 mm and 400 mm along the horizontal part, and the height H_1 and H_2 of vertical part and horizontal part respectively were measured. The L-box test results were evaluated by the ratio of h_2/h_1, where $h_1 = 600-H_1$ and $h_2 = 150-H_2$ (Fig. 2.7) [19].

Air content test

The air content of freshly mixed concrete by the pressure method was carried out as per ASTM C 231 procedure.

Setting time test

Initial and final setting times of SCC were determined as per ASTM C 403 procedure. A mortar sample was obtained by sieving SCC through 4.75 mm sieve. The mortar was placed in a plastic container of internal 150 mm diameter and 150 mm height. The sample was stored at 23 ± 2° C throughout the test period.

Bleeding of concrete

Bleeding of fresh concrete was measured as per ASTM C 232 procedure, method A. This method determines the relative quantity of mixing water that will bleed on the top surface from SCC sample. The cylindrical container 255 mm internal diameter and 280 mm inside height was used for the test. The volume of bleeding water per unit surface area was calculated.

3.4.2 Test on the mechanical properties and durability of concrete

Compressive strength test

The compressive strength of concrete was carried out as per ASTM C 39. 100 x 200 mm cylinders were used to test the compressive strength of SCC. A total of nine cylinders were tested for each mix. The compressive strength was measured at 1, 7, and 28 days. The average compressive strength of three cylinders was considered for each age.

Modulus of elasticity test

ASTM C 469 test method was used to determine the Young's modulus of elasticity. 150 x 300 mm cylinders were used for this purpose.

Flexural strength test

The 28-day flexural strength of SCC was determined by using 75 x 100 x 400 mm prism with third point loading as per ASTM C 78.

Shrinkage test

ASTM C157 procedure was used to determine the drying shrinkage. Three 75 x 100 x 275 mm prisms were used to measure the drying shrinkage. After demolding, all the specimens were cured in the lime-saturated water for 28 days and after then stored in the controlled storage room at 23 ± 2° C and 50 ± 4 % relative humidity. The drying shrinkage for each specimen was measured after 7, 28, 56 and 112 days of controlled curing.

Rapid Freezing and Thawing durability test

The resistance of SCC specimen to rapidly repeated cycles of freezing and thawing was carried out in presence of water as per ASTM C 666, procedure A. ASTM C 215 method was used to measure fundamental transverse resonant frequencies for concrete prism to calculate relative dynamic modulus of elasticity and durability factor.

75 mm x 75 mm x 300 mm prisms were used for this test. The specimens were cured for

14 days. After completion of the curing period, the weight, and the fundamental transverse frequency conforming to ASTM C 215 were recorded. The procedure A was followed where specimens were completely surrounded by 1 mm to 3 mm water all the time during the test.

Scaling resistance test

This test method covers the determination of the resistance to scaling of horizontal concrete surface exposed to freezing and thawing cycles in the presence of deicing chemicals. It was intended to evaluate this surface resistance qualitatively by visual examination. The ASTM C 672 test procedure was followed for this test. The specimen with a size of 300 x 150 x 75 mm was used for this test. The test specimens were kept in moist curing room for 14 days and then stored in the air for another 14 days at 23 ± 2° C. After completion of moist and air curing, the specimens were covered with approximately 6-mm layer of solution of calcium chloride and water (100 ml solution contains 4 g of anhydrous calcium chloride). The specimens were kept in the freezer for 50 cycles and the visual rating of surface was determined in a scale of 0 to 5. The qualitative rating was done as per ASTM C 672.

Rapid chloride permeability (RCP) test

The RCP test was carried out as per ASTM C 1202. This method covers the determination of the electrical conductance of concrete to provide a rapid indication of its resistance to the penetration of chloride ions. The concrete cylinder of 102 mm diameter was prepared and cured in moist room for 28 days. After 28 days of curing, the

specimens were cut into 51 mm thick slices. Side surface of the specimens were coated with the epoxy and coating was cured until it was no longer sticky to touch. The specimens were then placed in a vacuum desiccator for 3 hours. After that, water was allowed to drain in the desiccator while vacuum desiccator was running. The water stopcock was closed and vacuum pump was run for one additional hour.

The specimen was then placed between the two cells and sealed watertight with silicon. The positive cell was filled with a 0.3 N NaOH solution and negative cell was filled with a 3.0% NaCl solution. The test was terminated after 6 hours. The current in amperes after each 30 minutes and charge passed in coulombs after 6 hours were recorded. The total charge passed, in coulombs, was considered as an indication of the resistance of the specimen to chloride ion penetration.

Chapter 4 Results and Discussions

4.1 Introduction

The results of the experimental program are presented and discussed in this chapter. The correlation between rheological parameters of paste/mortar and fresh properties of SCC are also discussed. The results of fresh and hardened properties of SCC are presented and discussed.

4.2 Results

4.2.1 Paste

The results for plastic viscosity (Pa.s), yield stress (Pa.), and marsh cone flow of twenty one paste mixes are presented in Table 4.1. The mix proportioning of paste was same as SCC except the coarse aggregate and fine aggregate were discarded.

In the literature, different marsh cones with different geometry and sometimes different quantities of paste were passed through the cone to measure flow time [38, 42]. The marsh cone flow time could be different for the same paste, if different geometry of cones or different quantities of paste were used to measure the flow time. To standardize the test, specific flow time S_{sp} is proposed. The specific flow time is the ratio of time required in seconds to fill the fix volume of a container by paste to the time required in seconds to fill the same volume of container by water. The specific flow times for twenty-one mixes are also presented in Table 4.1. It should be noted that the total binder content (X_1) was considered based on kg /m^3 of paste.

Table 4.1: Rheological parameters and marsh cone flow time of paste mixes

Mix #	Total binder content X1	% of FA X2	% of SP X3	W/B X4	Plastic viscosity (Pa.s)	Yield stress (Pa.)	Marsh cone flow (Sec.)	Specific flow time
1	1200	45	0.35	0.39	0.021	0.60	18.5	2.00
2	1200	45	0.35	0.39	0.017	0.40	18.5	2.00
3	1200	60	0.35	0.39	0.029	1.67	18.0	1.96
4	1050	45	0.35	0.39	0.020	7.12	30.5	3.32
5	1200	45	0.35	0.45	0.015	0.62	14.5	1.58
6	1290	54	0.20	0.355	0.145	8.45	36.4	3.96
7	1350	45	0.35	0.39	0.018	0.75	19.5	2.12
8	1110	36	0.20	0.355	0.068	10.15	41.0	4.46
9	1200	45	0.35	0.39	0.023	0.67	19.0	2.06
10	1110	36	0.50	0.425	0.018	0.04	15.3	1.66
11	1290	36	0.50	0.425	0.016	0.08	15.4	1.67
12	1200	30	0.35	0.39	0.058	6.53	32.2	3.50
13	1110	54	0.20	0.425	0.016	1.83	15.6	1.70
14	1200	45	0.60	0.39	0.019	0.00	15.2	1.65
15	1200	45	0.35	0.39	0.020	0.94	18.5	2.01
16	1200	45	0.10	0.39	0.059	9.67	27.5	2.99
17	1290	54	0.50	0.355	0.021	0.35	17.0	1.85
18	1200	45	0.35	0.39	0.019	0.81	24.5	2.66
19	1200	45	0.35	0.33	0.054	8.65	29.5	3.21
20	1110	54	0.50	0.425	0.020	0.25	15.3	1.66
21	1290	36	0.20	0.425	0.035	1.54	24.5	2.66

4.2.2 Mortar

The plastic viscosity (Pa.s) and yield stress (Pa.) of all twenty-one mortar mixes are presented in Table 4.2. The statistical analysis of mortar was carried out in order to establish the influence of four variables on plastic viscosity and yield stress of mortar. The detail statistical analyses for plastic viscosity and yield stress of mortar are presented in Appendix A. It should be noted that the total binder content (X_1) was considered based on kg/m^3 of mortar.

Table 4.2: Rheological parameters of mortar mixes

Mix #	Total binder content X1	% of FA X2	% of S.P X3	W/B X4	Plastic viscosity (Pa.s)	Yield stress (Pa.)
1	600	45	0.35	0.39	0.478	4.06
2	600	45	0.35	0.39	0.480	4.23
3	600	60	0.35	0.39	0.321	3.26
4	525	45	0.35	0.39	1.450	8.35
5	600	45	0.35	0.45	0.217	1.16
6	645	54	0.20	0.355	1.261	2.73
7	675	45	0.35	0.39	0.460	1.20
8	555	36	0.20	0.355	3.262	10.28
9	600	45	0.35	0.39	0.472	4.93
10	555	36	0.50	0.425	0.224	2.64
11	645	36	0.50	0.425	0.213	1.64
12	600	30	0.35	0.39	0.757	4.80
13	555	54	0.20	0.425	0.792	5.64
14	600	45	0.60	0.39	0.444	3.10
15	600	45	0.35	0.39	0.468	5.22
16	600	45	0.10	0.39	2.150	11.89
17	645	54	0.50	0.355	0.560	2.05
18	600	45	0.35	0.39	0.492	4.35
19	600	45	0.35	0.33	3.597	10.68
20	555	54	0.50	0.425	0.299	1.49
21	645	36	0.20	0.425	0.462	5.30

4.2.3 Fresh properties of SCC

The results of initial slump, slump after 45 minutes, initial slump flow, and slump flow after 45 minutes along with slump loss and slump flow loss for 21 SCC mixes are presented in Table 4.3. The V-funnel, L-box (T_{20} and T_{40} time, and h_2/h_1), and filling capacity test results for SCC are presented in Table 4.4. Test results of setting times, bleeding, air content, and segregation index are presented in Table 4.5

Table 4.3: Properties of fresh SCC with regards to slump and slump flow

Mix #	Initial slump (mm)	Slump after 45 minutes (mm)	Initial slump flow (mm)	Slump flow after 45 minutes (mm)	Slump loss		Slump flow loss	
					(mm)	%	(mm)	%
1	290	275	590	460	15	5.2	130	22.0
2	280	270	590	460	10	3.6	130	22.0
3	290	220	630	430	70	24.1	200	31.7
4	180	150	410	na	30	16.7	na	na
5	290	285	760	650	5	1.7	110	14.5
6	275	260	540	440	15	5.5	100	18.5
7	285	270	680	540	15	5.3	140	20.1
8	230	175	330	na	65	28.2	na	na
9	285	270	570	470	15	5.3	100	17.5
10	285	275	650	550	10	3.5	100	15.4
11	295	290	810	720	5	1.7	90	11.1
12	265	250	510	430	15	5.7	80	15.7
13	285	275	600	510	10	3.5	90	15.0
14	295	280	770	650	15	5.1	120	15.0
15	285	275	600	475	10	3.5	125	15.6
16	250	200	380	310	50	20.0	70	18.4
17	290	280	710	610	10	3.4	100	14.1
18	280	260	580	430	30	10.7	150	25.9
19	215	160	350	280	55	25.6	70	20.0
20	290	285	760	670	5	1.7	90	11.8
21	265	210	480	na	45	17.0	na	na

Table 4.4: Properties of fresh SCC with regards to V funnel, L-box, and filling capacity tests

Mix #	Total binder content X1	% of FA X2	% of SP X3	W/B X4	Initial slump flow (mm)	V-Funnel time (sec.)	L-box T20 (Sec.)	L-box T40 (sec.)	L-box h2/h1 ratio	Filling Capacity %
1	400	45	0.35	0.39	590	3.50	1.00	2.00	1.00	64.94
2	400	45	0.35	0.39	590	3.25	1.00	2.00	1.00	75.00
3	400	60	0.35	0.39	630	3.50	1.00	2.00	0.91	52.46
4	350	45	0.35	0.39	410	na	na	na	na	na
5	400	45	0.35	0.45	760	2.50	0.75	1.25	1.00	94.97
6	430	54	0.20	0.355	540	3.25	1.00	2.00	0.87	79.22
7	450	45	0.35	0.39	680	2.25	1.00	2.00	1.00	84.77
8	370	36	0.20	0.355	330	na	na	na	na	na
9	400	45	0.35	0.39	570	3.00	1.00	2.00	1.00	70.45
10	370	36	0.50	0.425	650	3.00	0.75	1.50	0.94	77.21
11	430	36	0.50	0.425	810	2.00	0.75	1.50	0.95	96.00
12	400	30	0.35	0.39	510	4.50	1.25	2.50	0.96	61.11
13	370	54	0.20	0.425	600	2.75	1.00	2.00	1.00	75.65
14	400	45	0.60	0.39	770	3.50	0.75	1.50	1.00	94.94
15	400	45	0.35	0.39	600	3.00	1.00	2.00	1.00	75.06
16	400	45	0.10	0.39	380	7.00	na	na	na	26.88
17	430	54	0.50	0.355	710	4.00	1.00	2.00	1.00	89.09
18	400	45	0.35	0.39	580	3.00	1.00	2.00	1.00	74.67
19	400	45	0.35	0.33	350	na	na	na	na	na
20	370	54	0.50	0.425	760	2.50	0.75	1.50	1.00	93.02
21	430	36	0.20	0.425	480	2.50	1.50	3.00	0.60	44.74

Table 4.5: Properties of fresh SCC with regards to setting times, air content, segregation and bleeding.

Mix #	Total binder content X1	% of FA X2	% of SP X3	W/B X4	Initial setting time (h:m)	Final setting time (h:m)	Bleeding (ml/cm^2)	Air content %	Segregation Index %
1	400	45	0.35	0.39	6:35	8:20	0.014	2.5	1.52
2	400	45	0.35	0.39	7:18	8:50	0.012	3.0	0.81
3	400	60	0.35	0.39	8:56	11:06	0.019	3.1	1.28
4	350	45	0.35	0.39	6:20	7:24	0	3.0	0
5	400	45	0.35	0.45	7:35	9:50	0.141	2.5	12.50
6	430	54	0.20	0.355	7:00	9:10	0	2.2	0
7	450	45	0.35	0.39	6:18	7:56	0.114	2.5	4.93
8	370	36	0.20	0.355	4:50	6:20	0	3.4	0
9	400	45	0.35	0.39	6:12	8:15	0.009	1.9	1.28
10	370	36	0.50	0.425	6:10	8:08	0.029	2.1	3.26
11	430	36	0.50	0.425	7:54	9:50	0.176	2.4	21.75
12	400	30	0.35	0.39	5:32	7:28	0	3.4	0
13	370	54	0.20	0.425	7:28	9:50	0.196	2.4	1.62
14	400	45	0.60	0.39	8:54	11:05	0.489	2.1	24.43
15	400	45	0.35	0.39	7:20	9:38	0.012	2.8	1.01
16	400	45	0.10	0.39	5:20	7:56	0	3.1	0
17	430	54	0.50	0.355	8:04	10:18	0	2.9	5.68
18	400	45	0.35	0.39	6:34	8:40	0.010	2.4	1.20
19	400	45	0.35	0.33	5:20	7:38	0	2.8	0
20	370	54	0.50	0.425	10:03	12:15	0.029	2.4	3.77
21	430	36	0.20	0.425	5:20	7:38	0	3.1	0.81

4.2.4 Hardened properties of SCC

The compressive strength of SCC mixes at 1, 7, and 28-days is presented in Table 4.6. The modulus of elasticity and the flexural strength of SCC are also presented in Table 4.6. The test results on drying shrinkage of SCC at the age of 7, 28, 56, and 112 days are presented in Table 4.7. The test results on freezing and thawing (relative dynamic modulus of elasticity and durability factor) of SCC are presented in Table 4.8. The results on ratings of scaling resistance test at 5, 10, 15, 25, 50 cycles and rapid chloride permeability are presented in Table 4.9

Table 4.6: Compressive strength, modulus of elasticity, and flexural strength of SCC

Mix #	Modulus of elasticity (GPa.)	Flexural strength (MPa.)	1-day compressive strength (MPa.)	7-day compressive strength (MPa.)	28-day compressive strength (MPa.)
1	30	7.4	12	27	49
2	31	7.2	13	28	49
3	31	6.9	7	28	44
4	29	6.6	11	25	44
5	28	6.0	8	19	38
6	29	6.7	9	25	46
7	31	7.2	12	29	50
8	27	7.2	17	34	49
9	28	6.3	13	28	49
10	27	6.0	16	30	46
11	31	6.7	15	27	48
12	27	6.9	16	29	45
13	23	5.2	6	17	31
14	29	6.5	12	29	43
15	30	6.5	12	28	47
16	27	6.9	11	27	44
17	32	6.5	13	28	52
18	29	7.1	13	28	45
19	29	7.2	14	30	51
20	26	6.7	5	20	33
21	24	7.2	13	28	36

Table 4.7: Drying shrinkage development for SCC

Mix #	Drying shrinkage strain x 10^{-6}			
	7-day	28-day	56-day	112-day
1	133	273	333	330
2	306	380	460	620
3	166	266	473	533
4	306	380	587	630
5	253	490	517	657
6	136	193	267	387
7	140	336	400	448
8	240	430	507	667
9	260	203	253	350
10	180	323	377	460
11	210	656	663	643
12	263	620	643	597
13	193	260	350	470
14	153	300	380	430
15	210	283	433	457
16	160	280	430	477
17	100	220	443	463
18	130	146	413	423
19	113	193	417	403
20	103	246	383	407
21	143	400	467	487

Table 4.8: Freezing and thawing cycles resistance of SCC

Mix #	Weight (kg.)	Weight loss after 300 cycles %	R D M E after 300 cycles %	Durability Factor %	Remarks
1	4.006	1.15	68	68	
2	3.929	0.23	75	75	
3	4.029	1.04	77	77	
4	4.075	0.49	78	78	
5	3.895	2.46	62	62	
6	3.971	4.66	60*	43	* RDME after 216 cycles
7	3.984	2.00	71	71	
8	4.130	0.26	80	80	
9	3.982	0.05	78	78	
10	4.004	0.27	71	71	
11	3.874	0.10	79	79	
12	4.018	0.20	81	81	
13	4.016	0.25	66	66	
14	4.119	1.40	70	70	
15	4.077	1.72	71	71	
16	4.036	2.23	70	70	
17	3.897	3.05	65	65	
18	4.034	2.45	70	70	
19	4.042	0.27	95	95	
20	3.854	4.04	61*	44	* RDME after 216 cycles
21	3.979	2.13	67.40	67	

RDME = Relative dynamic modulus of elasticity

Table 4.9: Scaling resistance and rapid chloride permeability of SCC

Mix %	Visual rating in a scale of 0 to 5 for scaling resistance (ASTM C 672)					Rapid chloride permeability (coulombs)
	Cycle 5	Cycle 10	Cycle 15	Cycle 25	Cycle 50	
1	1	2	3	4	5	804
2	1	2	2	3	4	839
3	2	3	4	5	5	1150
4	0	2	3	4	4	1099
5	1	2	2	3	4	827
6	1	2	3	4	5	942
7	1	2	3	4	5	942
8	1	2	3	3	4	892
9	1	2	3	4	5	852
10	2	3	4	4	5	1168
11	0	2	3	3	4	1042
12	2	3	4	4	5	1255
13	1	2	3	4	5	1127
14	1	2	3	4	5	903
15	1	2	3	4	5	924
16	1	2	3	4	5	954
17	1	2	3	4	5	865
18	1	2	3	4	5	984
19	1	2	3	4	5	772
20	1	2	3	4	5	1379
21	1	2	3	4	5	1099

4.2.5 Statistical analysis for models

The statistical details such as model equation, summary of fit, analysis of variance and parameters estimates for model 1, model 2, model 3, model 4, and model 5 are presented in Appendix B to F respectively.

4.3 Discussions

Various tests for fresh properties of SCC such as slump flow, V-funnel flow, filling capacity, L-box, segregation and bleeding were carried out to access the deformability

and stability of concrete. The concrete needs 550 to 750 mm of slump flow [18], less than 6 sec. of V-funnel flow time [14], 50 to 95% of filling capacity [14], greater than 0.8 of h_2/h_1 ratio of L-box test [19, 45], less than 10% of segregation index [11] and less than 0.08 ml/cm^2 of bleeding [26] to qualify for SCC.

From the results of the present study, the mixes 4, 8, 16, 19, and 21 exhibited low deformability, hence not qualified for SCC. The mixes 5, 11, 14 are considered segregated mixes due to high bleeding and high segregation index than the prescribe limits. The mixes 1, 2, 3, 6, 7, 9, 10, 12, 13, 15, 17, 18, and 20 were qualified for SCC. It should be noted that the mix # 12 exhibited slump flow of 510 mm (lower than prescribed limit of 550 mm) but it showed satisfactory results for other deformability tests, hence qualified for SCC. The mix # 7 and 13 have higher bleeding (more than prescribed limit of 0.08 ml/cm^2) but exhibited low segregation index and satisfactory results for deformability tests, hence these mixes are considered as SCC mixes.

4.3.1 Rheology of Paste

The paste consists of a mixture of cement, FA, SP, and water. When cement is mixed with water, ion dissolution and chemical reaction occurs, which forms thin layers of hydrated product surrounding non-reacted cement particles. This thin layer may create mechanical force and hold all particles together. To break down these agglomerates and to induce flow, some amount of shear stress is required [44]. The addition of FA as a replacement of cement and the addition of SP may cause less shear stress to generate flow in the paste. The plastic viscosity and the yield stress of paste (Table 4.1) are

correlated with the slump flow of SCC (Table 4.3). While correlating the rheological parameters of paste with fresh properties of corresponding SCC, it is important to note the importance of the volumetric fraction of aggregate 'V_{fa}' in SCC mixes. The 'V_{fa}' for all twenty-one concrete mixes were ranging from 63 to 71% while the ratio of the volume of coarse aggregate to the volume of total aggregate was kept constant at 0.33. The V_{fa} is the ratio of combined volume of fine and course aggregates to the volume of all ingredients of concrete.

The plastic viscosity and yield stress of paste are correlated with the slump flow of SCC and illustrated in Fig. 4.1 and Fig. 4.2 respectively. No significant correlation between the viscosity of paste and the slump flow of SCC is observed. The yield stress of paste has shown reasonably good linear correlation with the slump flow of SCC as illustrated in Fig. 4.2.

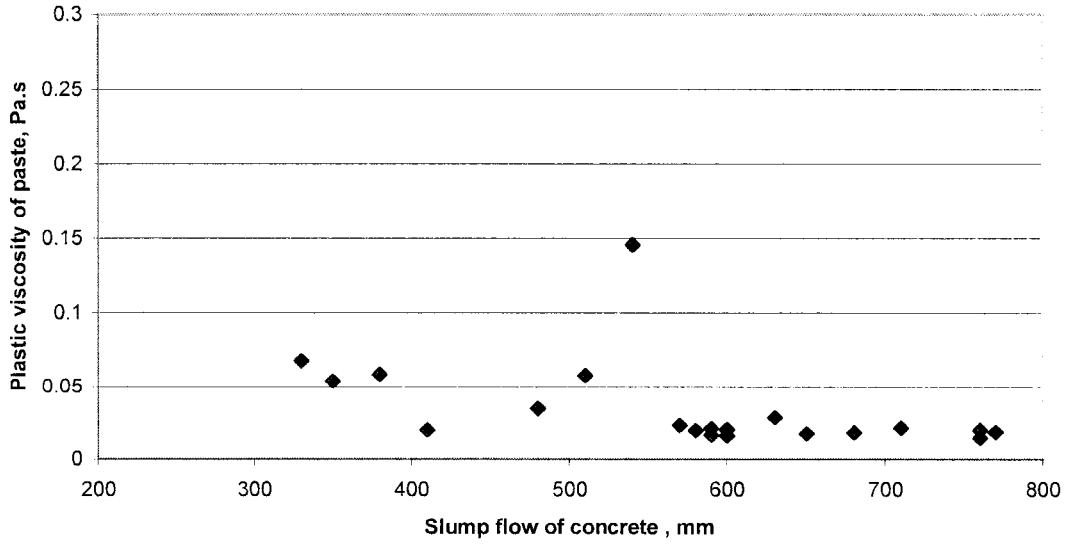

Fig. 4.1: Slump flow of concrete v.s Plastic viscosity of paste

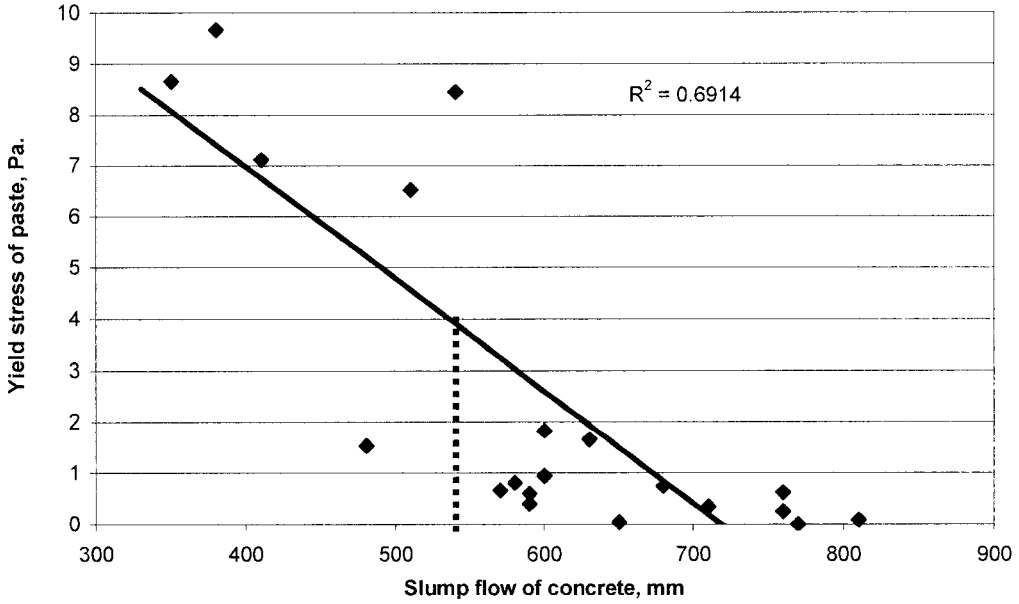

Fig. 4.2: Slump flow of concrete v.s yield stress of paste

The slump flow of concrete is found to increase with the decrease of yield stress of corresponding paste. When a paste has a yield stress below 4 Pa., the corresponding SCC should exhibit a slump flow above the level of 550 mm. However, SCC mix # 6 and Mix # 12, were qualified for SCC (even though, the corresponding paste had high yield stress) as they were accompanied by low plastic viscosity of paste. Even if the yield stress is more related to deformability, it is necessary to consider both the yield stress and the plastic viscosity for predicting the flow characteristics of SCC. From Figs. 4.1, 4.2 and Tables 4.1, 4.3, 4.4 and 4.5 it can be concluded that the concrete may qualify for SCC, if the corresponding paste has a plastic viscosity ranging between 0.02 and 0.08 Pa.s and a yield stress ranging between 0.02 and 4 Pa. However, it can be noted that if the paste has a viscosity slightly higher than 0.08 Pa.s and accompanied by a low yield stress, the corresponding concrete may exhibit good deformability to qualify for SCC.

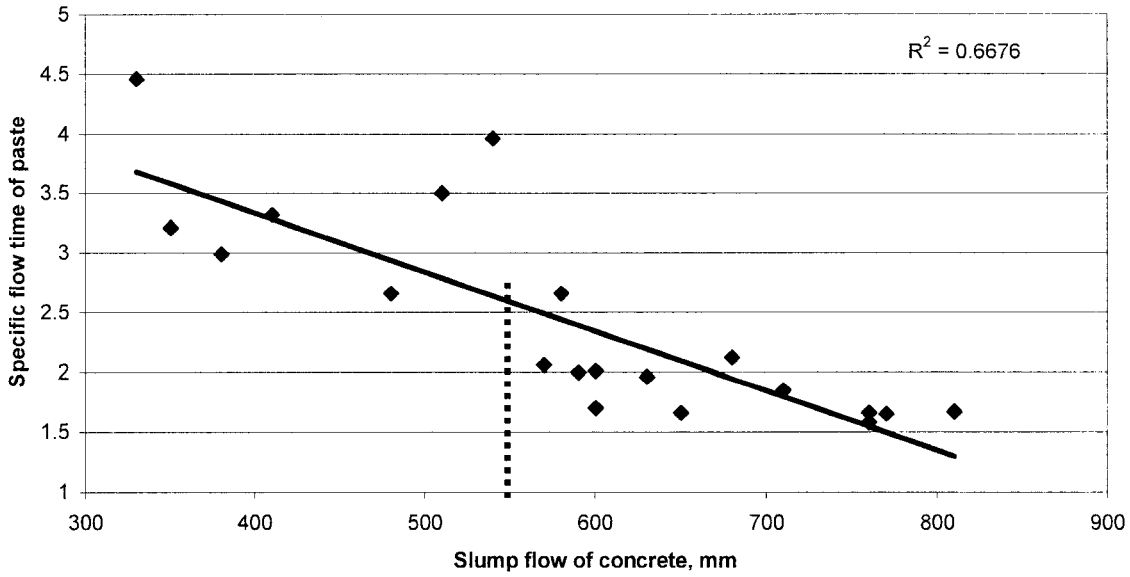

Fig. 4.3: Relation between slump flow of concrete and specific marsh cone flow time of paste

Fig. 4.3 shows that the slump flow of SCC increases with the decrease of specific flow time of the corresponding paste. The concrete containing a paste of specific flow time less than 2.6 exhibited a slump flow higher than 550 mm (Fig. 4.3), a flow time less than 6 sec., a h_2/h_1 higher than 0.8, and a filling capacity more than 50% (Table 4.4). However it is difficult to predict the segregation in SCC from the results of specific flow time of paste as the resistance to segregation is governed by the plastic viscosity. The yield stress (responsible for generating the flow), has good correlation with specific flow time of paste. The coefficient of correlation (R^2) is found to be 0.81 as indicated in Fig. 4.4.

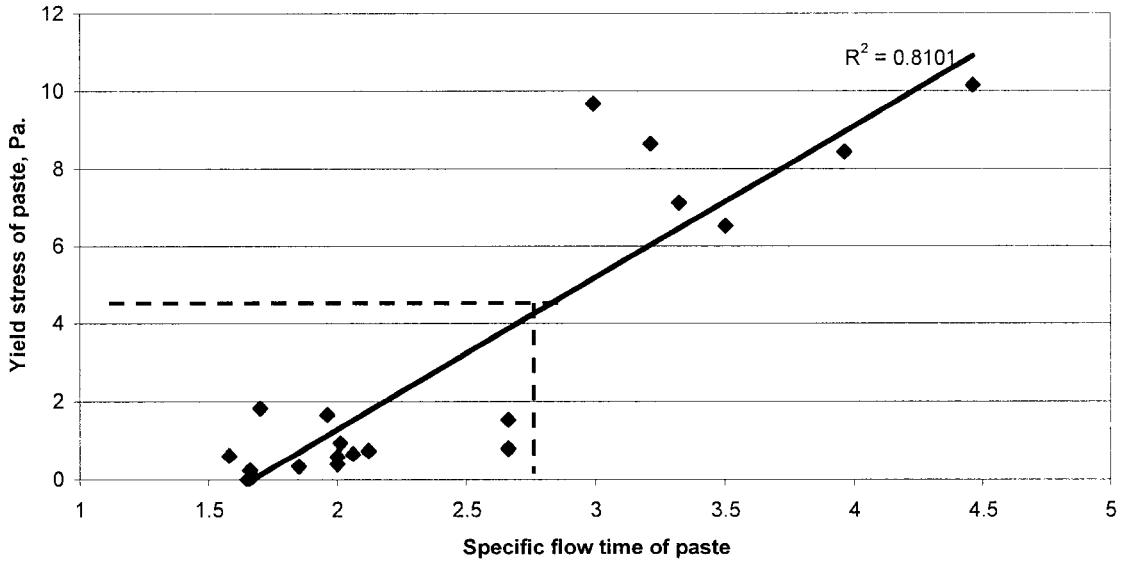

Fig. 4.4: Relation between the specific flow time of paste and the yield stress of paste

From Fig. 4.2, 4.3,and 4.4, it can be established that a paste having a yield stress of less than 4 Pa. and specific flow time of less than 2.6 can generate sufficient flow in the corresponding concrete to qualify for SCC.

4.3.2 Rheology of mortar

The mortar consists of cement, FA, SP, water, and fine aggregate. It can be noted that the volumetric fraction of aggregate 'V_{fa}' for all twenty-one concrete mixes were varied from 63 to 71% while the ratio of volume of coarse aggregate to volume of total ingredient was kept constant at 0.33. The rheological parameters of mortar are more relevant than those of paste to predict the flow behavior of the corresponding concrete as fine aggregates are incorporated in the mortar.

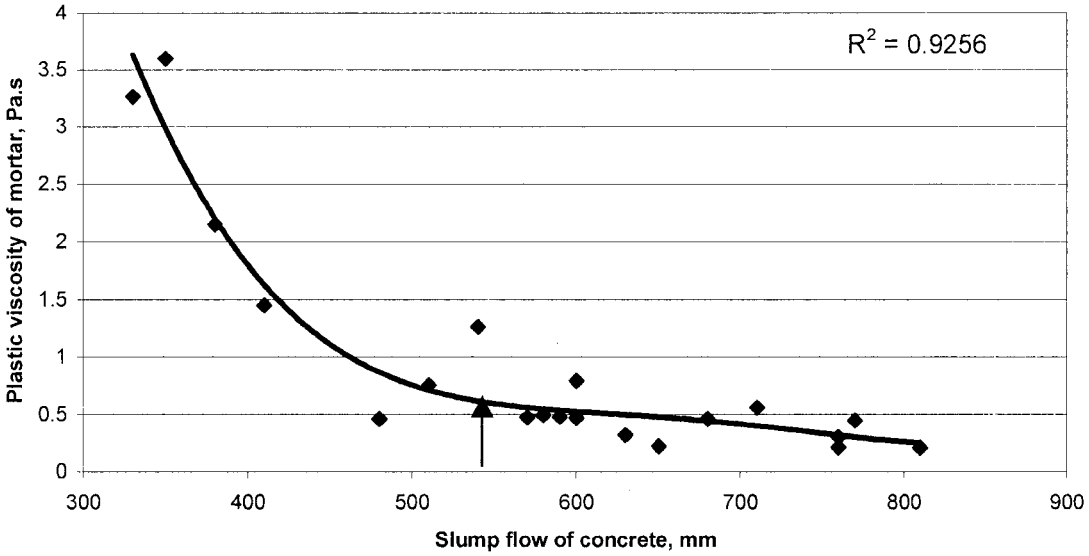

Fig. 4.5: Relation between slump flow of concrete and plastic viscosity of mortar

It can be observed from Fig. 4.5 that the slump flow of SCC increases with the decrease of plastic viscosity of the corresponding mortar. A good polynomial correlation (R^2 = 0.93) is found between the plastic viscosity of the mortar and the slump flow of SCC (Fig. 4.5). It should be noted that a concrete with a slump flow between 550 and 750 mm is supposed to qualify for SCC. It is observed from Fig. 4.5 that the plastic viscosity of the mortar is found high at low slump flow of the corresponding concrete and it has a rapid drop until the slump flow reaches about 550 mm. The plastic viscosity of mortar between 0.6 and 0.25 Pa.s can achieve slump flow of 550 to 750 mm in the corresponding SCC. It can be concluded that an optimum mortar viscosity between 0.25 and 0.6 Pa.s is needed to generate the necessary slump flow for SCC without segregation. However, if the mortar viscosity is higher than 0.6 Pa.s and it accompanied by a low yield stress, the concrete mix may generate enough slump flow without segregation. Mix

6 is an example of these combinations (plastic viscosity 1.26 Pa.s, yield stress 2.72 Pa., and slump flow 540 mm). Fig. 4.6 indicates that the yield stress of mortar has good correlation with the slump flow of the concrete with a correlation coefficient of 0.85. The slump flow of SCC is found to increase with the decrease of yield stress of the corresponding mortar. It can be observed from Fig. 4.6 that concrete mixes containing a mortar having a yield stress of less than 6 Pa are more likely to have a good deformability to qualify for SCC. There are more chances of segregation of concrete mixes containing a mortar whose yield stress is less than 1.5 Pa., and plastic viscosity is less than 0.25 Pa.s.

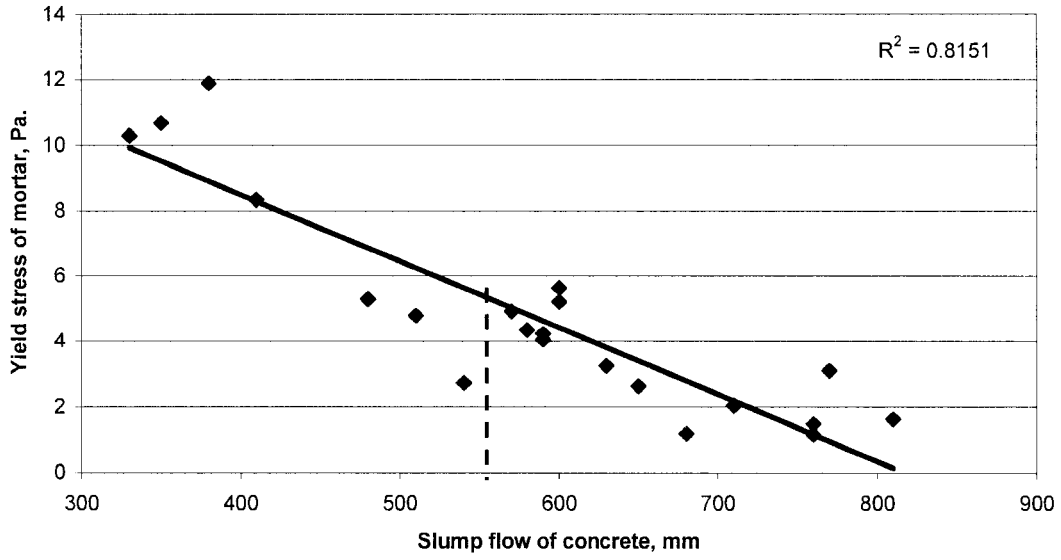

Fig. 4.6: Relation between slump flow of concrete and the yield stress of mortar

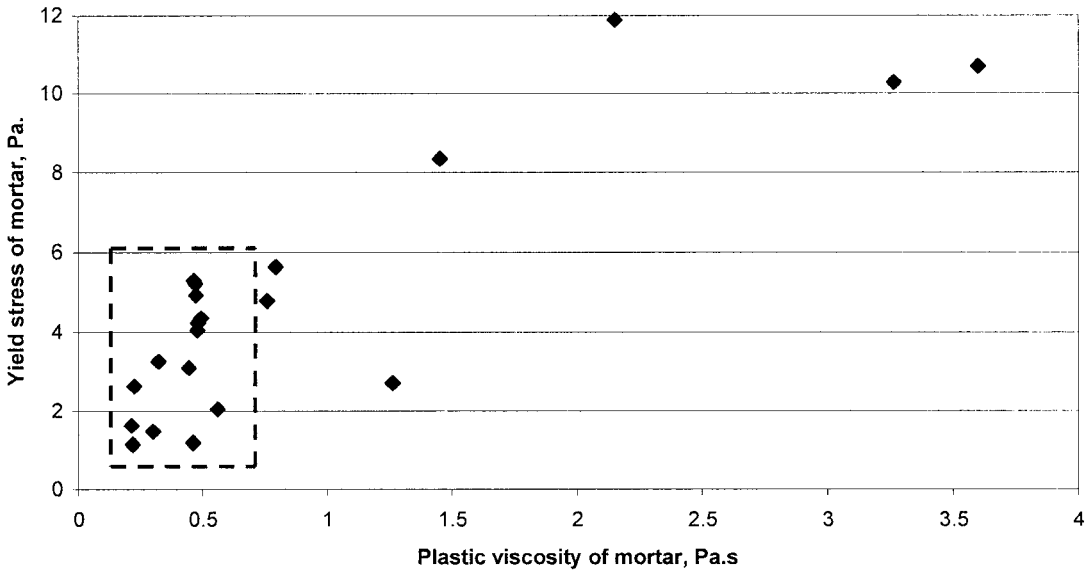

Fig 4.7: Relation between the plastic viscosity of mortar and the yield stress of mortar

It can be concluded that the critical rage of the mortar yield stress is 1.5 to 6 Pa. and the plastic viscosity is 0.25 to 0.6 Pa.s for qualifying the corresponding concrete as a SCC.

4.3.3 Influence of variables on the rheological behavior of mortar

The statistical analysis by ANOVA (Analysis of Variance) technique was carried out for the plastic viscosity and the yield stress of mortar mixes to determine if the four selected variables are statistically significant or not. In other words, it can be determined that the variation in these variables have influence on the plastic viscosity and the yield stress or not. The value of all the variables were set to coded value such as +1.68, +1, 0, -1, -1.68 to assess the degree of impact of each variable on responses. It is important to note that the higher the value of estimate for each variable coefficient, the greater the influence is on the response.

From Table 4.10 (detail given in Appendix A), it can be concluded that the all four variables are statistically significant with more than 91.2% confidence level. The four variables, which are the total binder content (X_1), the percentage of FA (X_2), the percentage of S.P (X_3), and the water-to-binder ratio W/B (X_4) have influence on the plastic viscosity of mortar. The negative nature of estimated parameter for all the variables indicates that the increment of any variable can decrease the plastic viscosity of mortar. The W/B (X_4) has highest negative influence on the plastic viscosity of mortar followed by % of S.P (X_3), and total binder content (X_1). The % of fly ash (X_2) has least negative influence on the plastic viscosity of mortar. An increase of W/B, % of S.P, total binder content, and % of FA can increase the flow of mortar or concrete. It is important to note that increasing the % of FA (X_2) will increase the mortar flow but the drop in viscosity will be less compared to the other three variables. This is particularly beneficial since an optimum amount of plastic viscosity is essential in SCC to avoid segregation.

Table 4.10: Statistical analysis of mortar for plastic viscosity

Variable	Coefficient	Confidence level, %	Remarks
X4	-0.8066	99.99	Stat. significant
X3	-0.4346	98.7	Stat. significant
X1	-0.4064	97.8	Stat. significant
X2	-0.2777	91.2	Stat. significant

Table 4.11: Statistical analysis of mortar for yield stress

Variable	Coefficient	Confidence level, %	Remarks
X4	-2.2312	99.95	Stat. significant
X1	-1.1724	99.68	Stat. significant
X3	-0.6238	99.49	Stat. significant
X2	-0.7847	86.79	Not sure

The statistical analysis for the yield stress of mortar as illustrated in Table 4.11 (more detail in Appendix A) indicates that the variables X_1, X_3, and X_4 are statistically significant with more than 99.5% confidence level. The null hypothesis that X_1, X_3, and X_4 have no influence on the yield stress can be rejected. It can be concluded that X_1, X_3, and X_4 have great influence on the yield stress of mortar. The negative nature of estimated parameters indicates that increment of variables X_1, X_3, and X_4 can reduce the yield stress. The W/B (X_4) has highest negative influence on the yield stress compared to the total binder content (X_1) and % of S.P (X_3).

The confidence level of variable X_2 is 86.79% (Table 4.11). As per the rule of accepting of null hypothesis, if the confidence level is more than 90%, the variable is considered as statistically significant. The statistically significant means that the variable has positive or negative influence on the response. If the confidence level is less than 85%, the variable is not considered to be statistically significant. In other words, the variable has no

influence on the response. If the confidence level is between 85% and 90%, neither the null hypothesis can be accepted nor rejected. As the variable X_2 has confidence level of 86.79%, it can not concluded whether % of FA (X_2) has influence on yield stress or not.

4.3.4 Fresh properties of SCC

4.3.4.1 Slump, Slump flow and Slump loss

The initial slump, slump after 45 minutes, initial slump flow, slump flow after 45 minutes, slump loss and slump flow loss are tabulated for all twenty-one concrete mixtures in Table 4.3. The mixes 4, 8, 16, 19, and 21 have exhibited an initial slump flow of less than 550, hence not qualified for SCC. Mixes 5, 11 and 14 have very high initial slump flow with notable segregation of aggregate. All other mixers are qualified for SCC as they exhibited satisfactory slump flow. The statistical model for the slump flow is developed and will be discussed later in this chapter.

Fig. 4.8 compares the initial slump flow and the slump flow after 45 minutes for all the mixes. The initial slump flow of mixes 4, 8, and 21 are 410, 330, 480 mm respectively and considered to be low. These concretes exhibited no flowability after 45 minutes, hence the slump flow after 45 minutes were not recorded. The mixes with very low initial slump flow showed high slump flow loss. For all SCC qualified mixes, slump flow loss ranged between 11% and 25% except for the mix # 3, which showed a slump flow loss of 31%.

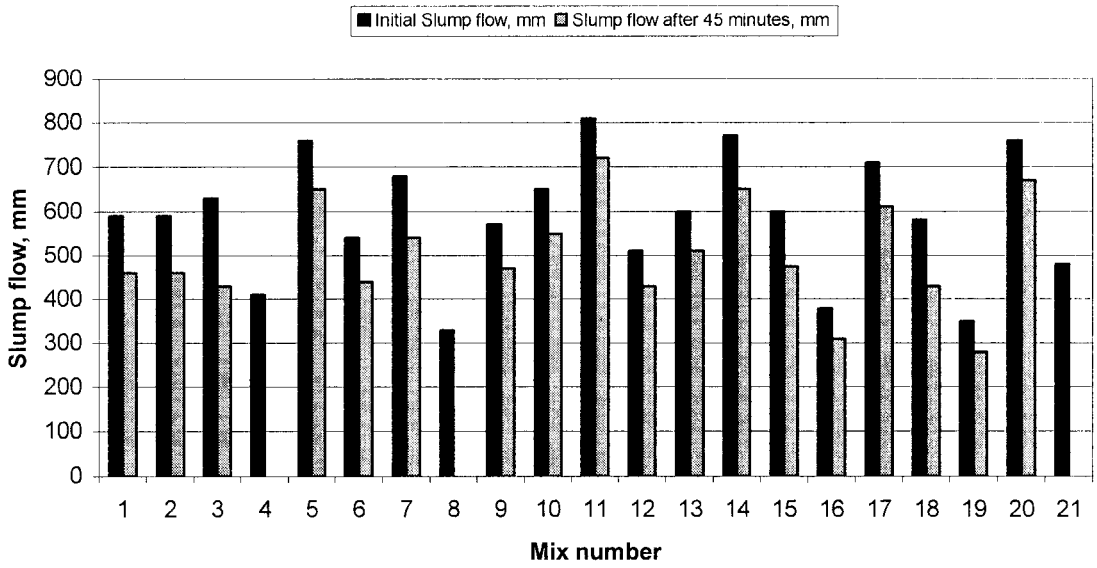

Fig 4.8: Comparison between the initial slump flow and the slump flow after 45 minutes

4.3.4.2 V-funnel test, filling capacity test, and L-box test

The results of the V-funnel, the filling capacity, and the L-box tests are presented in Table 4.4. All the mixes qualified for SCC had exhibited V-funnel flow time of less than 4.5 seconds except mix # 21. Mix # 21 indicated a flow time of 2.5 seconds, but did not qualify for SCC. V-funnel flow time of this project seems to be in good agreement with other research studies [1, 14, 23]. Bouzoubaa and Lachemi [1] found 3 to 7 seconds V-funnel flow time for SCC, while Khayat et al. [14] found 2.2 to 5.4 seconds, Ghezal et al. [23] found 2.1 to 4.2 seconds from different studies on SCC.

L-box test indicates the concrete's ability to flow through the gaps between the reinforcing bars. The T_{20} time for all qualified SCC mixes varied from 0.75 to 1.25 second and T_{40} time ranged between 1.25 and 2 seconds. No significant difference for T_{20}

and T_{40} time was observed in all mixes. T_{20} time of 0.6 to 1 second and T_{40} time of 1.2 to 2 seconds were reported for SCC mixes in construction projects [19].

The h_2/h_1 was found to vary ranging from 0.87 to 1.00 for all qualified SCC mixes. Sufficient data is not available in the literature to evaluate the h_2/h_1 ratio for SCC used in heavily reinforced sections. However, Sonebi at el. [19] and Petersson [45] reported that the h_2/h_1 of SCC greater than 0.8, exhibited good results without blocking in the structures hence, they considered the h_2/h_1 of 0.8 as a lower critical limit for SCC [19, 45]. According to author's opinion, h_2/h_1 of L-box test and the result of filling capacity test should be considered together to evaluate the concrete ability to pass through heavily reinforced bars without the need of any compaction.

The filling capacity test is more relevant for assessing the deformability of SCC among closely spaced obstacles. The filling capacities of all the mixes are illustrated in Fig. 4.9. The filling capacities of mixes 4, 8, and 19 were not recorded as the flow of concrete was too low to measure. The mixes 16 and 21 are not qualified for SCC (filling capacity less than 45 %). Mix # 3 has exhibited moderate filling capacity (52.5%). All other qualified mixes have exhibited excellent filling capacity between 61 and 96%. According to Khayat and Assaad [14], a filling capacity between 50 and 95% indicates moderate to excellent deformability among closely spaced obstacles.

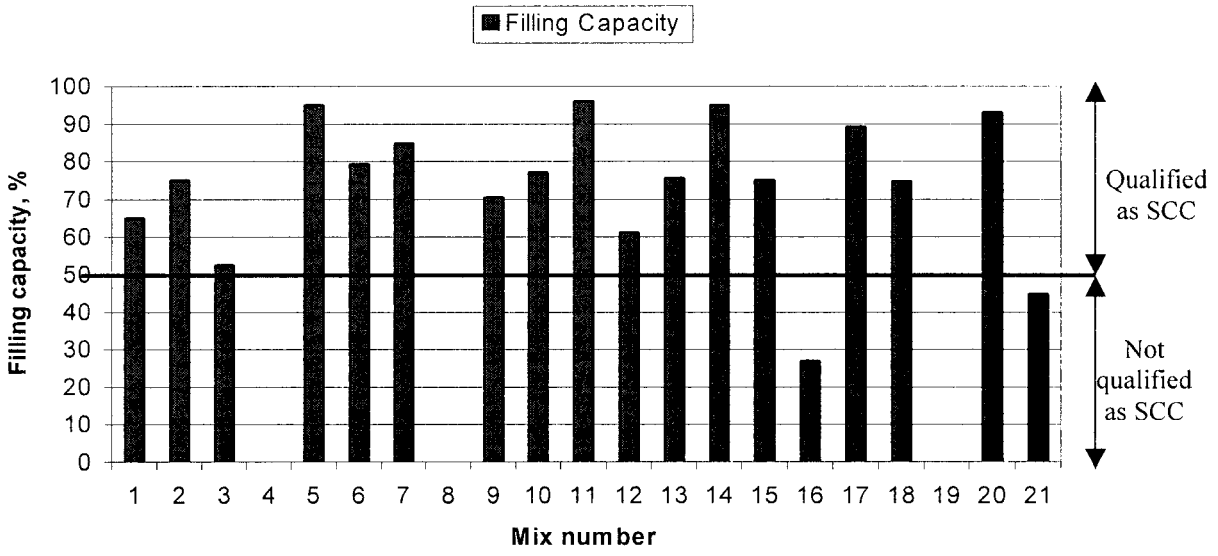

Fig. 4.9: Filling capacity of SCC

The filling capacity of concrete has good correlation with the yield stress of mortar (R^2 = 0.68) as shown in Fig 4.10. The lower the yield stress of mortar, the higher is the filling capacity. The SCC containing a mortar with yield stress of less than 6 Pa., exhibited filling capacity of more than 62% for corresponding concrete for most of the mixes. It is one more evidence that the concrete can qualify for SCC, if its mortar has a yield stress of less than 6 Pa. While establishing this relation, it is important to note that the ratio of volume of coarse aggregate to volume of total ingredient was kept constant at 0.33 for all 21 mixes.

4.3.4.3 Segregation and Bleeding

One of the most important requirement for any SCC is that the aggregate should not segregate from the paste and the mix should remain homogeneous during the production and placing. It is also equally important that the particles move with the matrix as a

cohesive fluid during the flow of SCC. Unfortunately there are no fundamentally sound theoretical models and experimental procedures available in the literature to quantify the amount of segregation [5]. As discussed in the previous chapter a test developed by Fujiwara was used in this study to evaluate the segregation of aggregate.

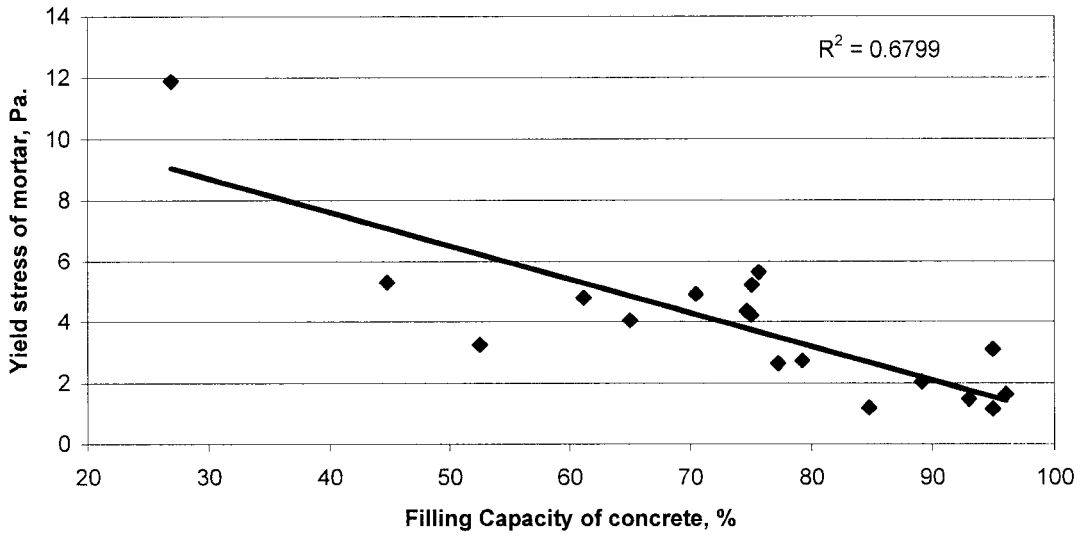

Fig. 4.10: Relation between the filling capacity of concrete and the yield stress of mortar

Using this test, Khayat et al. [46] stated that a stable SCC should exhibit a segregation index value lower than 10 %. In the present study, all the SCC qualified mixes (except mix # 5) exhibited a segregation index lower than 10 %. The relation between the slump flow and the segregation index of concrete is illustrated in Fig. 4.11. From this figure, it can be observed that no segregation was found up to a concrete slump flow of 540 mm. The chances of segregation are very high beyond a slump flow of 750 mm, as the segregation index tends to be more than 10% (Fig. 4.11). It is always advisable to keep the slump flow between 550 and 750 mm for a stable and homogeneous SCC. Plastic

viscosity plays a very important role in the segregation resistance. As discussed earlier in this chapter, all the four variables have influence on the plastic viscosity of mortar. The increase of all variables, results in the drop of the plastic viscosity. However the drop in viscosity is less significant when % of FA increases compared to other variables. Mix # 3 and Mix # 20 are the example of such phenomenon. Mix # 3 (60 % fly ash) had a slump flow of 630 mm, and a segregation index of only 1.28%. Mix # 20 (54 % fly ash) had a slump flow of 760 mm and segregation index of only 3.77%.

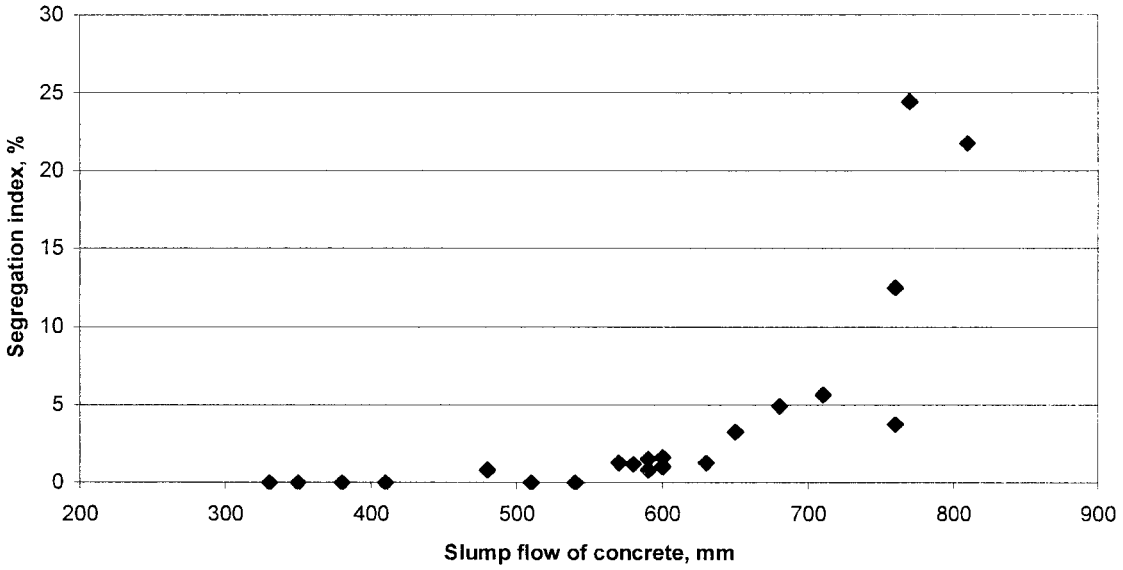

Fig 4.11: Relation between slump flow of concrete and segregation index

The total amount of bleeding water observed for all qualified SCC mixes ranged from 0 to 0.19 ml/cm^2 (Table 4.5). It was observed from the results that the W/B and the % of SP had high influence on the surface bleeding. The bleeding of SCC increases with the increasing W/B and SP content.

4.3.4.4 Setting time

The initial setting time of concrete was found to be ranging from 290 minutes (4:50 h:m) to 603 minutes (10.03 h:m), while the final setting time was found to be in the range of 440 minutes (7:20 h:m) and 735 minutes (12.15 h:m). The comparisons of setting times for all the mixes are shown in Fig. 4.12. From the results, it appears that the % of FA and the % of SP have high influence on the setting times. Mix # 3 with 60 % FA exhibited very high initial as well as final setting times of 536 minutes and 666 minutes respectively. Mix # 20 had a combination of high % of FA and high % of SP. It exhibited very high initial and final setting times of 603 and 735 minutes respectively.

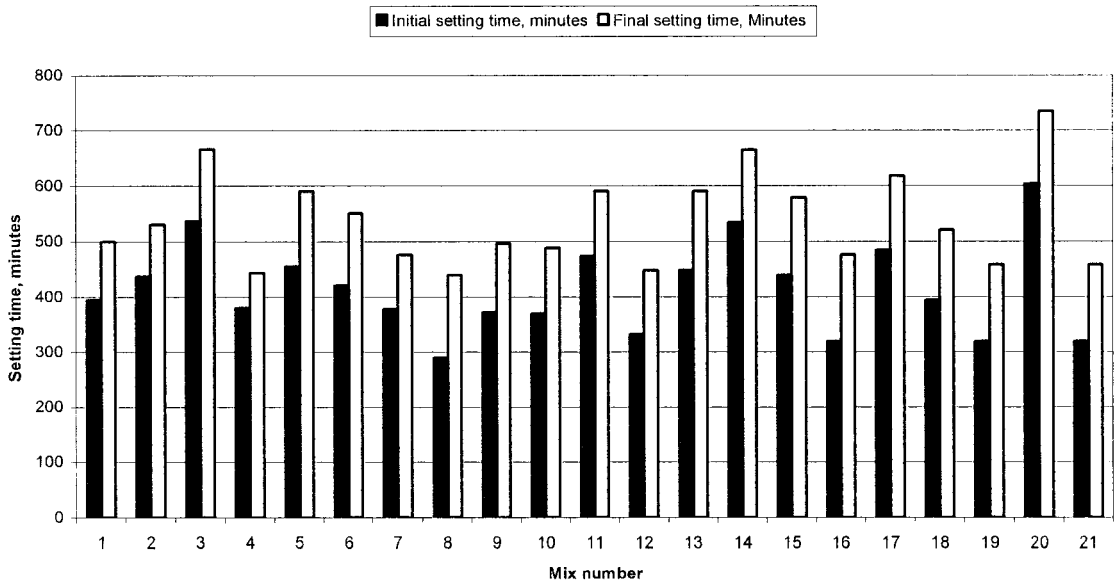

Fig. 4.12: Initial and final setting times of concrete

4.3.5 Hardened properties of SCC

4.3.5.1 Compressive strength

The compressive strength at the age of 1, 7, and 28 days of all concrete mixtures is presented in Fig. 4.13. The SCC with higher % of FA exhibited low 1-day compressive strength (mix 3, 13, 20). The 28-day strength appeared to be relatively low for SCC with combination of higher % of FA, lower binder content, and higher W/B (Mix 13 and 20). No influence of the % of SP on compressive strength was observed.

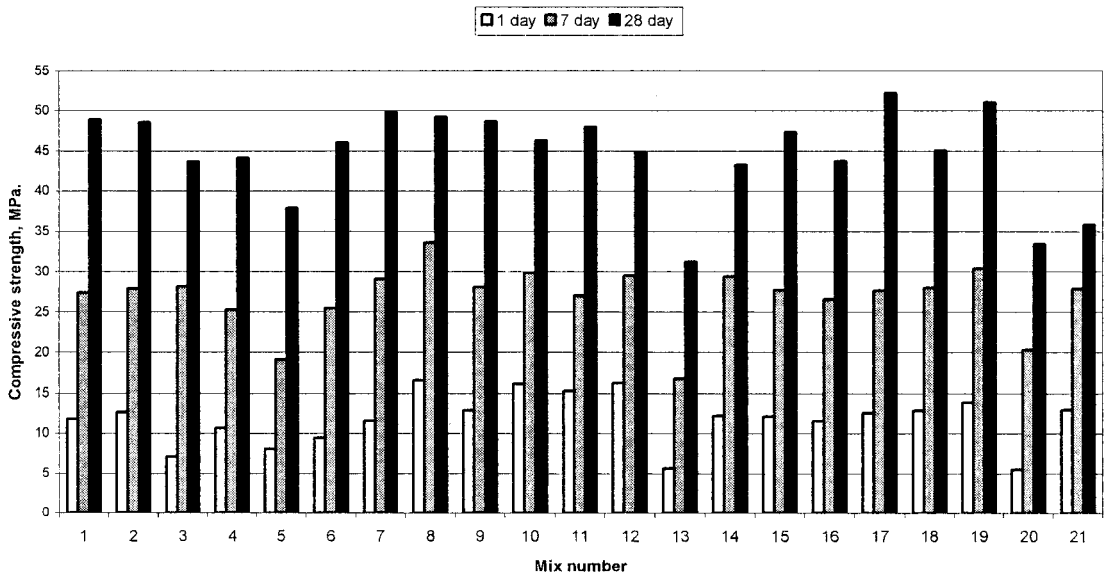

Fig. 4.13: Comparison of compressive strengths at different ages

4.3.5.2 Modulus of elasticity

The modulus of elasticity of all 21 mixtures is tabulated in Table 4.6. The results show that the modulus of elasticity of SCC investigated ranges between 23 and 32 GPa. To avoid the direct measurement of the modulus of elasticity, many engineers and

researchers have tried to find out empirical approach relating this parameter to the 28-day compressive strength f'_c to the 28-day modulus of elasticity [52]. An attempt to correlate the modulus of elasticity to the compressive strength of SCC is illustrated in Fig. 4.14. The linear correlation is not excellent (R^2 = 0.62). However the best-fit equation for modulus of elasticity in terms of 28-day compressive strength is derived as follow:

$$E = 4208\sqrt{f'_c} + 298 \qquad (4.1)$$

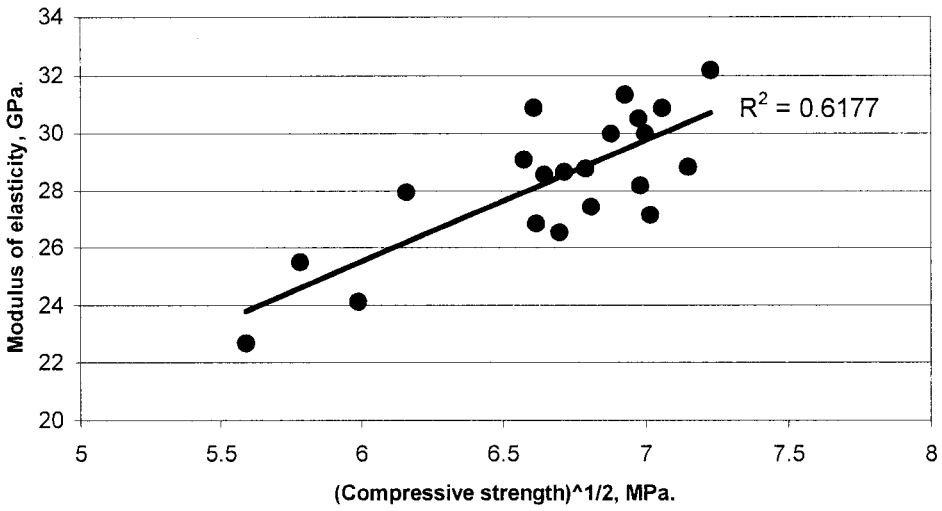

Fig. 4.14: Relation between the modulus of elasticity and the compressive strength

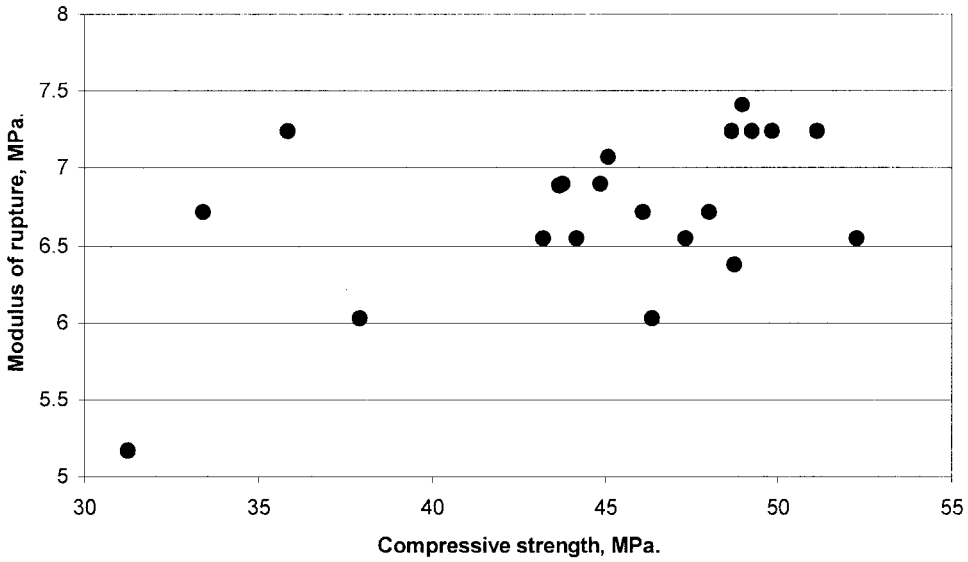

Fig. 4.15: Relation between the compressive strength and the flexural strength

4.3.5.3 Flexural strength

The 28-day flexural strength for all SCCs is tabulated in Table 4.6. The flexural strength ranges from 5.1 to 7.2 MPa. The relation between the 28-day flexural strength and the 28-day compressive strength is presented in Fig. 4.15. No good correlation is found between the 28-day compressive strength and the 28-day flexural strength. More experimental data is needed to establish the relation.

4.3.5.4 Drying shrinkage

The comparative drying shrinkages of all the SCCs is illustrated in Fig. 4.16. The drying shrinkage strain at the age of 112 days ranged between 330 and 667 micro strain. No significant difference was observed between concrete qualified for the SCC and those not qualified for the SCC. Mix # 12 (total binder content 400, % of FA replacement 30 %,

SP=0.35 %, and W/B=0.39) had exhibited 112-day drying shrinkage of 597 micro strain, and Mix # 3 (total binder content 400, % of replacement of FA 60 %, SP=0.35 %, and W/B=0.39) had exhibited a lower drying shrinkage (at 112 days) of 533 micro strain. The increase in FA replacement from 30% (mix # 12) to 60% (mix # 3) did not significantly affect the drying shrinkage of SCC. Bouzoubaa and Lachemi [1] had not found any significant difference for drying shrinkage between normal concrete and SCC incorporating FA.

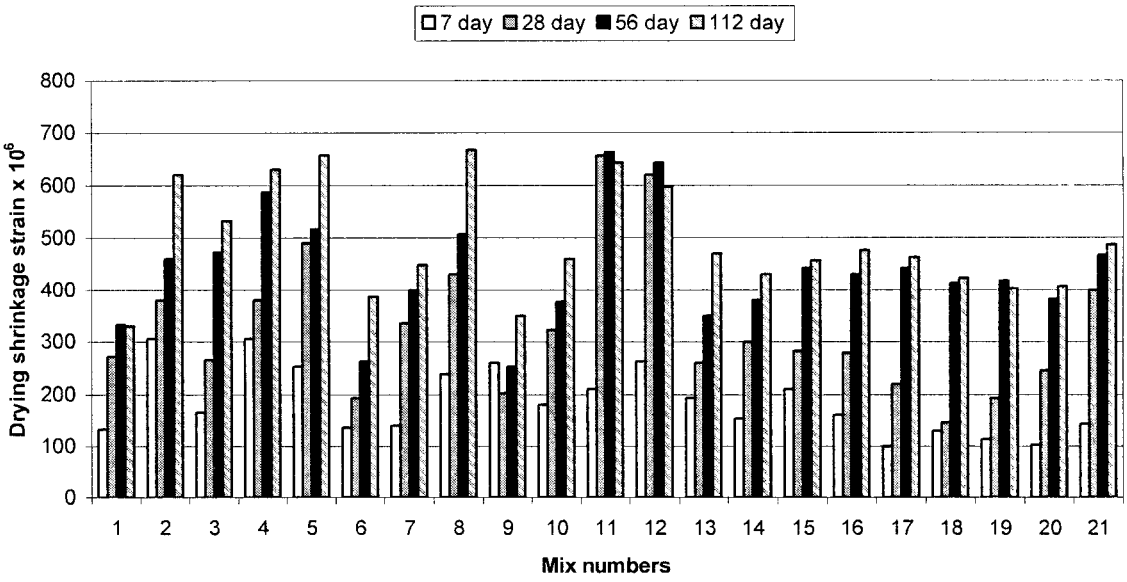

Fig. 4.16: Comparison of drying shrinkage at different ages

4.3.5.5 Freezing and thawing cycles resistance

The relative dynamic modulus of elasticity, the weight loss and the durability factor at 300 cycles are presented in Table 4.8. The durability factors (DF) for various SCCs are illustrated in Fig. 4.17. The SCC mixes developed in this project are non-air entrained

hence relatively low freezing and thawing cycles resistance is expected. Entraining air in the SCC should enhance its freezing and thawing resistance.

The DF for mixes # 6 and 20 was relatively low and found to be around 43%, respectively. This may be due to the use of higher % of FA without established adequate air content [24, 30, 33]. The mix # 19 had an excellent durability factor of 95 %. All other mixes had exhibited a DF within the range of 62 to 81 %. No significant difference was found between low deformability and segregated mixes.

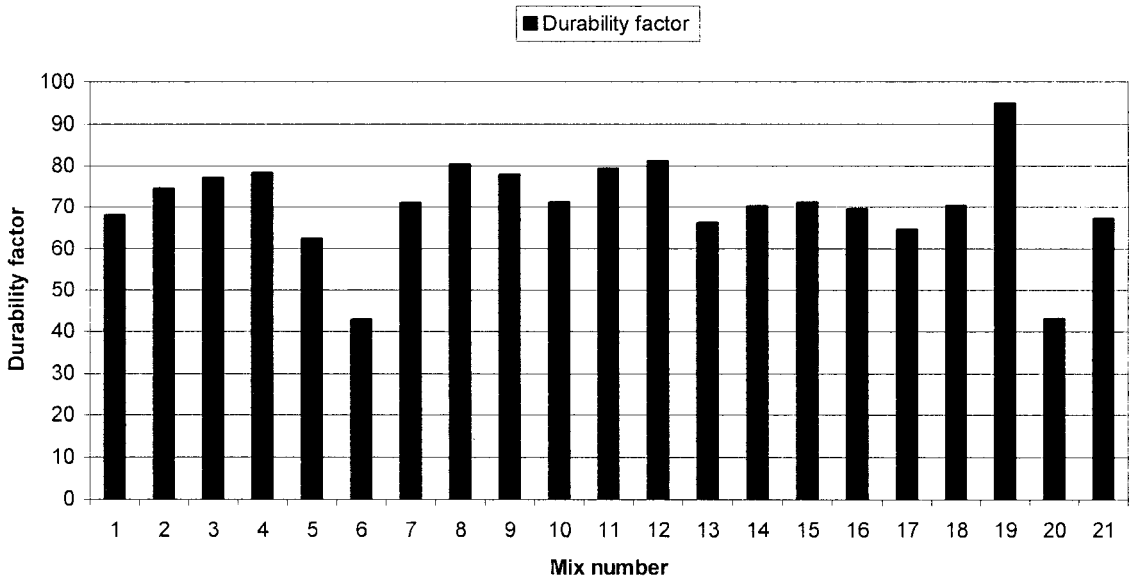

Fig. 4.17: Comparison of durability factor

The relative dynamic modulus of elasticity (RDME) is illustrated in Fig 4.18 to 4.20. Except for mixes # 6 and 20, all other mixes were sustained up to 300 freezing and thawing cycles. The RDME after 180 cycles is found to be more than 80 % for all the mixes.

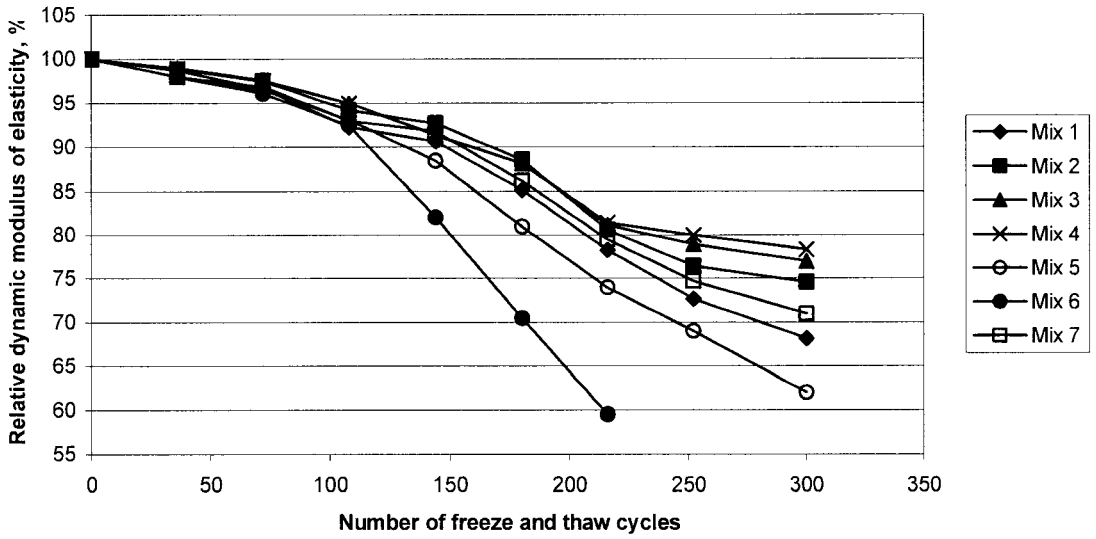

Fig. 4.18: Freezing and thawing cycles resistance for mix # 1 to 7

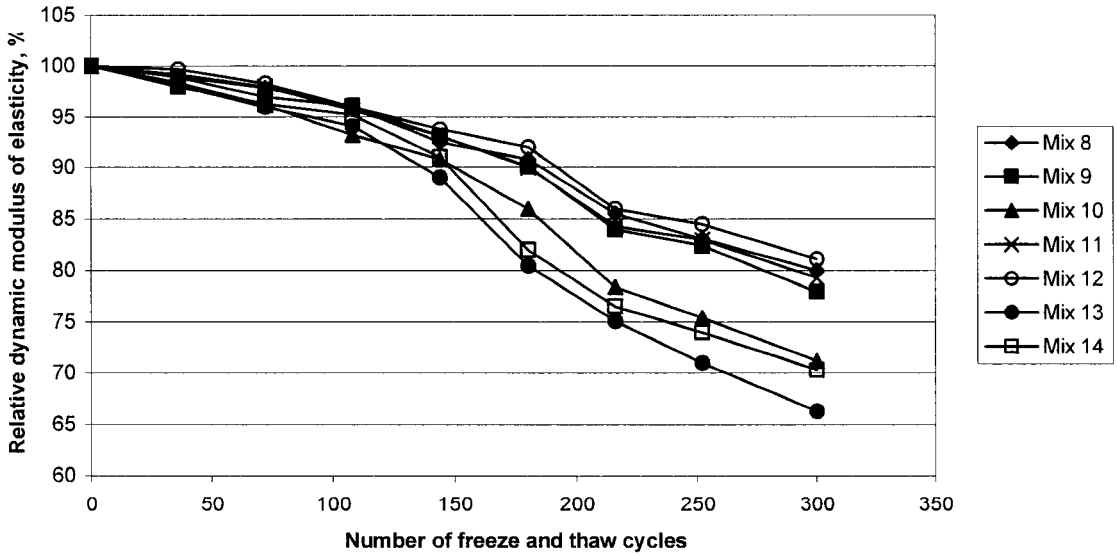

Fig. 4.19: Freezing and thawing cycle resistance for mix # 8 to 14

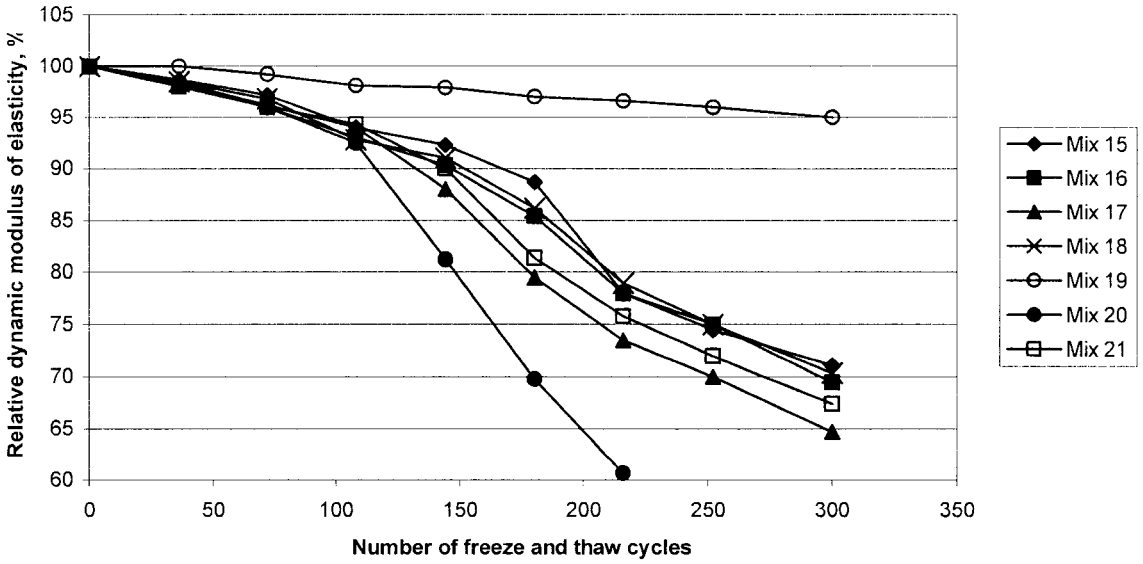

Fig. 4.20: Freezing and thawing cycle resistance for mix # 15 to 21

4.3.5.6 Rapid chloride permeability (RCP)

The results of the RCP test for all the mixture are illustrated in Fig. 4.21. The RCP of the SCC investigated appeared to be low or very low (ASTM 1202-97) and ranges from 772 to 1379 coulombs. The chloride ion permeability based on charge passed is very low for 100 to 1000 coulombs and low for 1000 to 2000 coulombs [ASTM C 1202-97]. This was expected as the percentage of FA replacement in the mixes ranges from 30 to 60%. FA generally improves the permeability of concrete due to its capability of transforming large pores of concrete into small pores and reducing micro cracking in the transition zone [16].

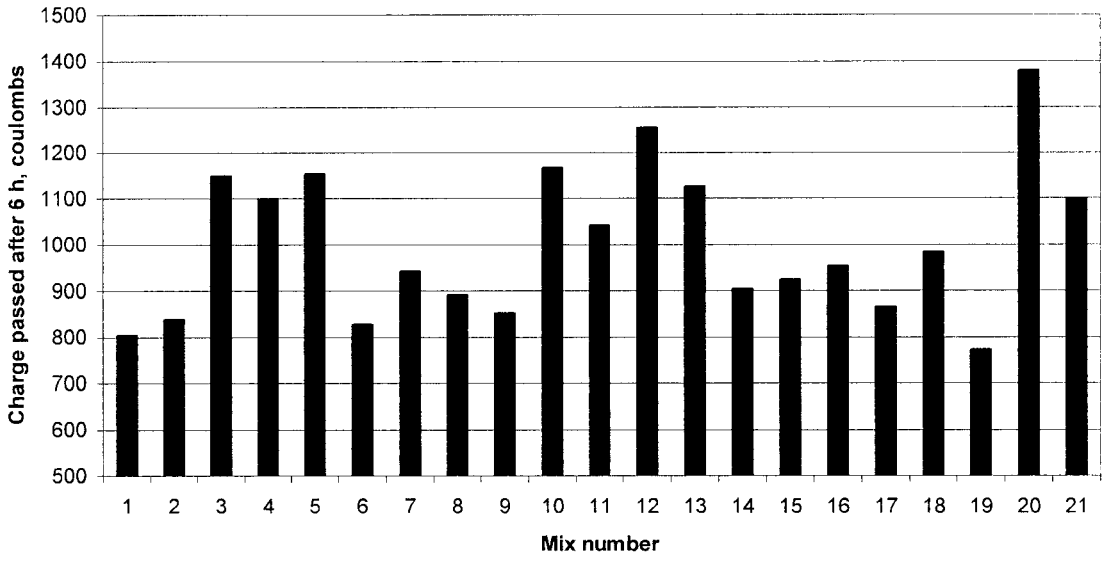

Fig. 4.21: Comparison of chloride ions charge passed in coulombs

4.3.5.7 Scaling resistance

The scaling resistance represents physical rather than chemical effect and is qualitative as well. ASTM C 672 provides an evaluation of surface scaling in a rating of 0 to 5. Pigeon et al. [48] noted that "It is generally believed that this procedure tends to be too severe. Many concretes that failed in the laboratory can have an extremely good service life." The results of the surface scaling resistance determined according to ASTM C 672 are presented in Table 4.9. The results show the scaling rate of 4 and 5 for all the SCC mixes subject to cycles of freezing and thawing in the presence of deicing salt. The poor performance of the SCC investigated can particularly be due to the absence of air entraining in the concrete. However the scaling resistance of SCC can be improved by entraining air in concrete with proper air void stability.

Chapter 5 Statistical models

5.1 Introduction

In order to estimate model parameters effectively, CCD method was used for the design of experiments. The coded value and limit of the four factors (variables) are presented in Table 3.4 and 3.5 in Chapter 3. The four variables that can have significant influence on the characteristic of SCC were selected to derive statistical models and ultimately to evaluate the properties of SCC. The limits of the variables were decided by conducting some preliminary tests and from past experience. The four variables selected are as follows:

X_1 = Total binder content per cubic meter of concrete, kg/m^3

X_2 = Percentage of fly ash replacing cement by mass, %

X_3 = Percentage of solid mass in superplasticizer with respect to the total binder content. (Hereinafter this variable will be refer as % of SP)

X_4 = Water-to-binder ratio (W/B)

The five selected models are as follows:

Model 1: Slump flow, mm (Y_1)

Model 2: 1-day compressive strength, MPa (Y_2)

Model 3: 28-day compressive strength, MPa (Y_3)

Model 4: Rapid chloride permeability, Coulombs (Y_4)

Model 5: Material cost, Canadian $ (Y_5)

The SAS statistical software was used to derive five models by the least square approach. The structure of the statistical models is as follows:

$$Y = a_0 + a_1X_1 + a_2X_2 + a_3X_3 + a_4X_4 + a_{12}X_1X_2 + a_{13}X_1X_3 + a_{14}X_1X_4 + a_{23}X_2X_3 + a_{24}X_2X_4 + a_{34}X_3X_4 + a_5X_1^2 + a_6X_2^2 + a_7X_3^2 + a_8X_4^2$$

Where, Y represents the model response and X_1, X_2, X_3, and X_4 represent the independent variables.

The interaction between the four variables (X_i X_j) and the quadratic effect (X_i^2) of variables were also considered in the proposed models. By trial and error method, the best-fit models were identified from different probability distribution functions such as Normal (Gaussian), Gaussian inverse, Gamma, Poison and Binomial with different link functions such as identity, log, and power. The 't' test and/or 'chi square' test were carried out to decide the statistical significance of variables. The null hypothesis was checked for all estimated coefficients such as a_0, a_1, a_3 etc. The null hypothesis is a presupposition that the true value of coefficient is zero. In other words, the variable or variables associated with that coefficient are statistically not significant and it has no influence on the response Y. If the probability greater than 't statistics' or 'chi square statistics' is less than 0.1 (10%), the null hypothesis (the coefficient value is zero), can be rejected and established that the variable or variables with the estimated coefficient has significant influence on the response. If the probability greater than 't statistics' or 'chi square statistics is more than 0.15 (15%), the null hypothesis (the coefficient value is

zero), can be accepted and it can established that the variable or variables with the estimated coefficient has no influence on the response and hence that variable or variables can not be included in the model. In the proposed models, the probability greater than 't statistic' or 'chi square statistic was found less than 0.05 (with few exceptions where value was between 0.05 to 0.1). This signifies that there is less than 5% probability that the contribution of a given variable with the respective coefficient to the tested response exceeds the value of the specified estimated coefficient. A possible higher value of correlation coefficient (R^2) was considered while selecting the proposed models. After many trials with SAS software, best-fit five models were found out for various SCC properties.

The derived statistical models are useful tools in understanding the effect of various variables (ingredients) and their interaction on the SCC properties. The influence of high replacement of cement by FA is the particular interest of the study. The proposed models can predict the influence and major trends of variables on important properties of SCC. By using these models one can reduce the time, cost, and efforts associated with the selection of trial batches. The variables of models and response properties of SCC can be optimized and simulated by using response surface diagrams or optimization software such as LINGO 7.

5.2 Model 1: Slump flow

The slump flow is one of the most important properties of SCC. If the slump flow of concrete is between 550 and 750 mm without any segregation, the concrete can be

qualified for SCC. Of course, other fresh concrete tests such as V-funnel flow time, L-box, filling capacity are also important to evaluate thoroughly the fresh SCC properties. However, one can take decision from slump flow test, if other test set-ups are not available. The proposed slump flow model is as follows:

Slump flow Y_1 = -1793 + 2.0542 X_1 + 5.9456 X_2 + 710.476 X_3 + 2648.08 X_4

The statistical detail of the model is presented in Appendix B. The model was fit in Normal (Gaussian) probability distribution function with Identity link function. The nature of the model is linear and all the four variables have positive influence on the response (slump flow, Y_1). The R^2 value is 0.92, which indicates the excellent goodness of fit. From the ANOVA analysis, it appears that the probability greater than F statistics (Fisher statistics) is less than 0.0001. The model is highly statistically significant with a confidence level more than 99.99 %. All the variables are also tested individually for t statistics. The probability greater than t for intercept is less than 0.0001 (confidence level more than 99.99 %), for X_1 is 0.0001 (confidence level 99.99 %), for X_2 is 0.0004 (confidence level 99.6 %), for X_3 and X_4 are less than 0.0001 (confidence level 99.99 %). All the four variables are statistically significant and have great influence on the slump flow.

The response surfaces for slump flow with 350, 400, and 450 binder contents and 0.35% of SP are illustrated in Fig. 5.1 to 5.3. At a given binder content and a SP content, a desired slump flow can be achieved by different combinations of FA percentage and

W/B. Fig. 5.4 represents the influence of FA replacement on the slump flow of concrete based on the proposed model 1. At given binder and S.P contents, an increase in FA content can substantially increase the slump flow at any W/B. Fig. 5.4 shows that an increase in FA replacement by 10 % increases the slump flow by approximately 60 mm.

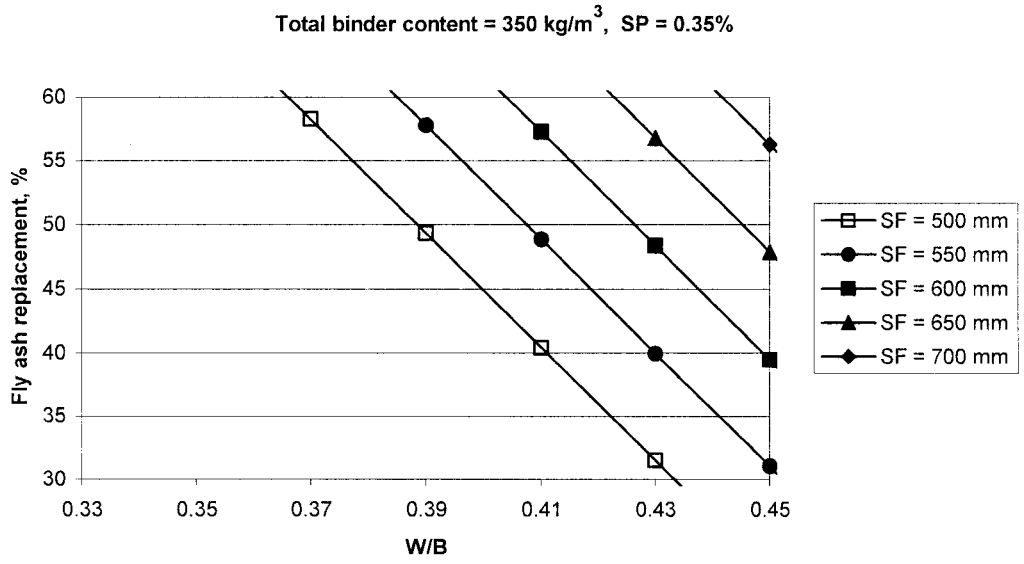

Fig. 5.1: Response surface for variation in slump flow (SF)

SP dosages can be estimated and optimized by using the proposed model 1. FA replacement has great capability to reduce the SP demand to achieve a desired slump flow. Fig 5.5 represents the influence of FA replacement on SP demand to achieve a desired slump flow. Fig. 5.5 indicates that if a 650 mm slump flow is desired for SCC with 400 kg/m^3 binder content and 0.39 W/B, an increase in FA content by 10% (by the total weight of binder) decreases the SP content by 0.09% (by the total weight of binder).

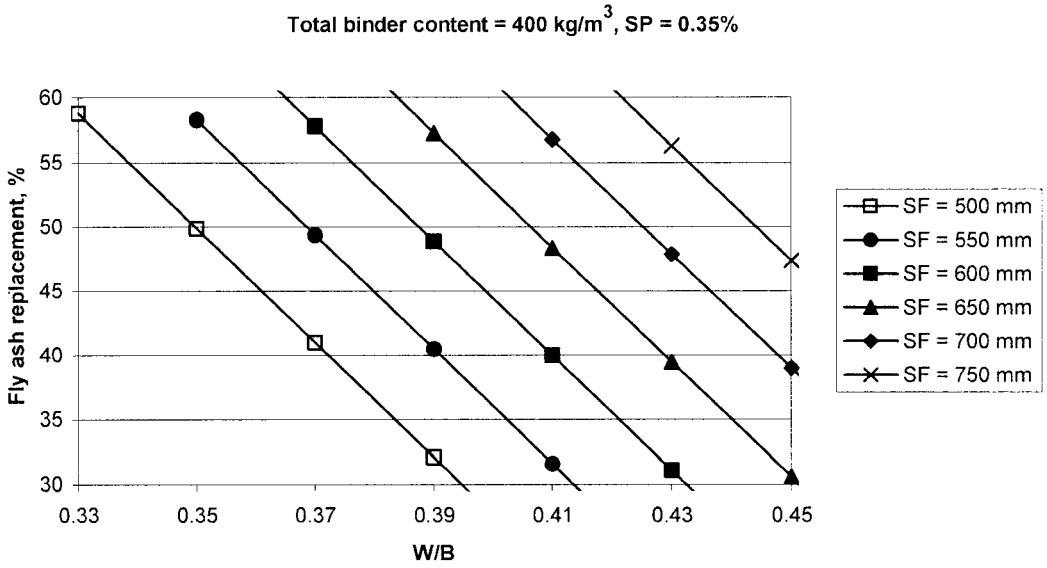

Fig. 5.2: Response surface for variation in slump flow (SF)

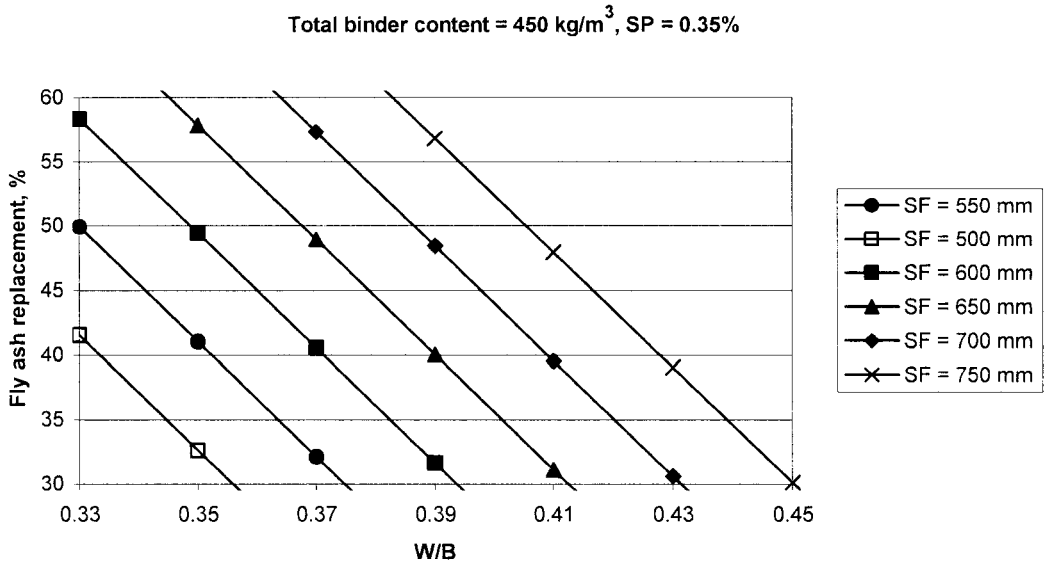

Fig. 5.3: Response surface for variation in slump flow (SF)

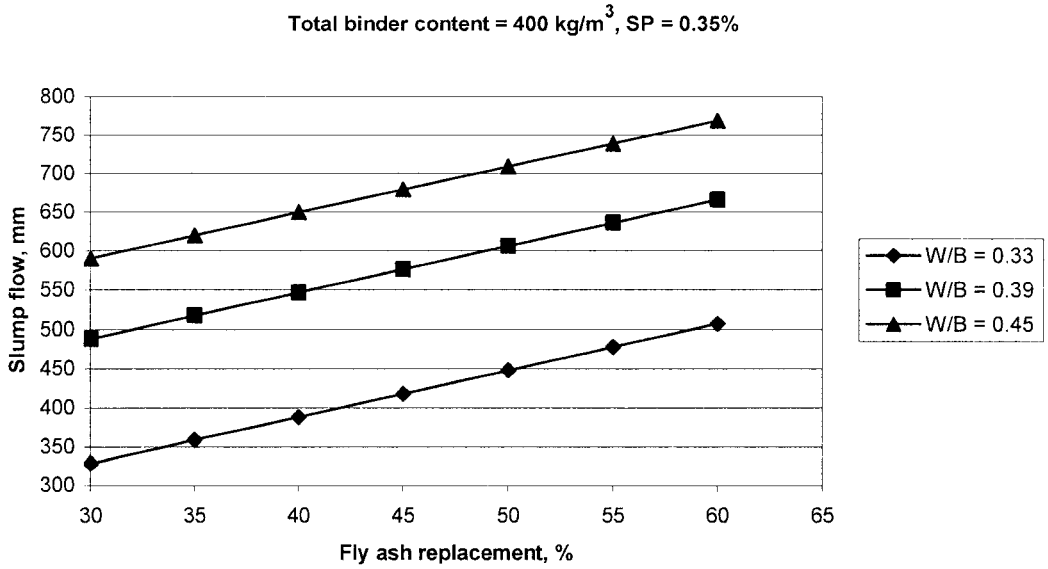

Fig. 5.4: Influence of fly ash replacement on slump flow

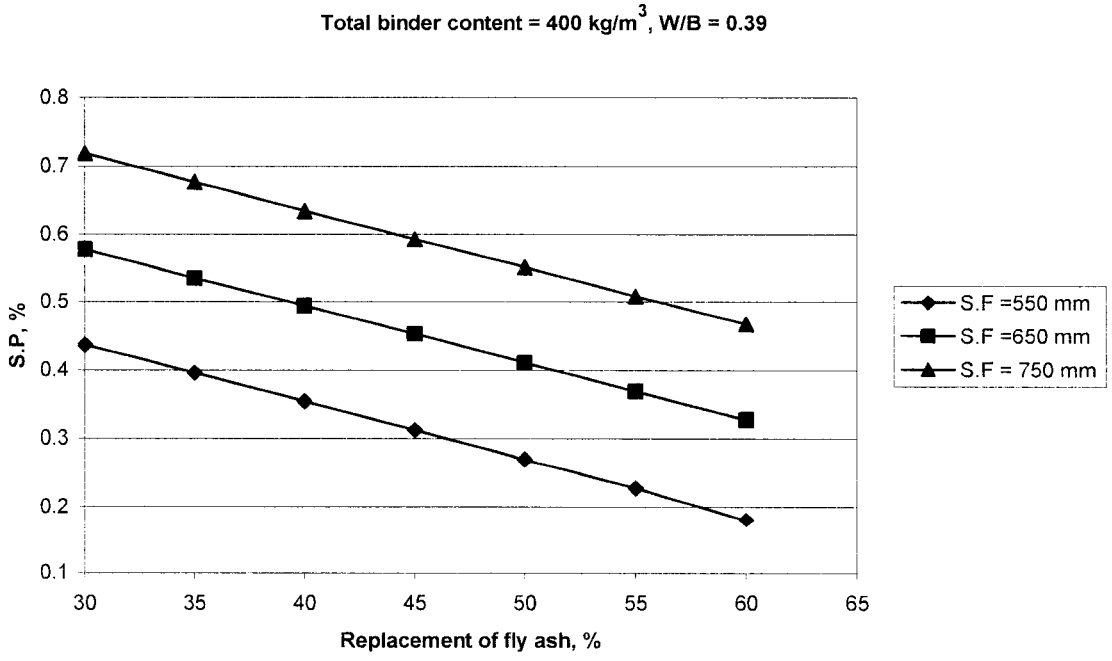

Fig 5.5: Influence of fly ash replacement on superplasticizer demand

5.3 Model 2: 1-day compressive strength

Concrete with high volumes of fly ash can often exhibit high setting time and low early age strength. In this project, SCC is developed by using high volumes of FA hence evaluation of 1-day strength is considered to be essential. The 1-day compressive strength plays a very important role for certain type of works such as road pavement, repair works, and the concrete structure cast at very low ambient temperature. The 1-day strength model is as follows:

$$\textbf{1-d strength } Y_1 = 1786.34 - 3.0317\,X_1 - 29.8364\,X_2 - 2972.19\,X_3 - 3190.45\,X_4 + 0.0391\,X_1X_2 + 3.7161X_1X_3 + 5.1744\,X_1X_4 + 40.6712\,X_2X_3 + 36.9763\,X_2X_4 + 3993.55\,X_3X_4 - 0.2706\,X_1X_2X_3X_4 - 0.0005\,X_1^2 - 363.7157X_4^2$$

The statistical detail of the model is presented in Appendix C. The model is fit in Normal (Gaussian) probability distribution function with Identity link function. The nature of the model is non-linear and all the four variables have influence on the response (1-day compressive strength, Y_2). The four variables are also interacting with each other and impacted on the response. The R^2 value of 0.99 is an indication of the excellent goodness of fit. From the ANOVA analysis, it appears that the probability greater than F statistics (Fisher statistics) is less than 0.0001. The model is highly statistically significant with a confident level of more than 99.99 %. All the variables are also tested individually for t statistics. The probability greater than t for intercept, all variables, and their interaction is indicated in Appendix C. The probability greater than t for all variables is found less than

0.0365 (confidence level of more than 96.35 %). All the variables are statistically significant and have great influence on the 1-day strength.

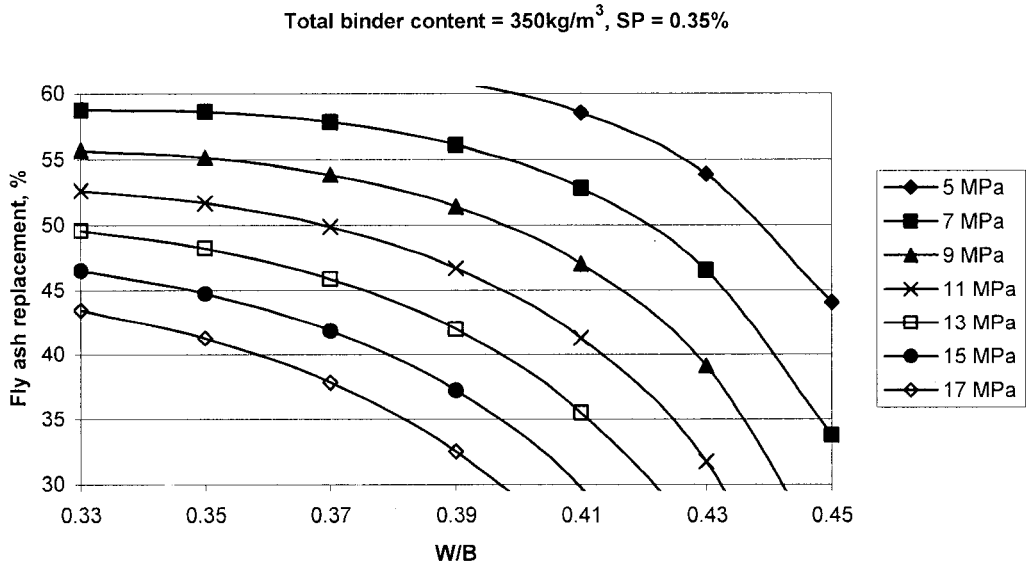

Fig. 5.6: Response surface for variation in 1-day strength

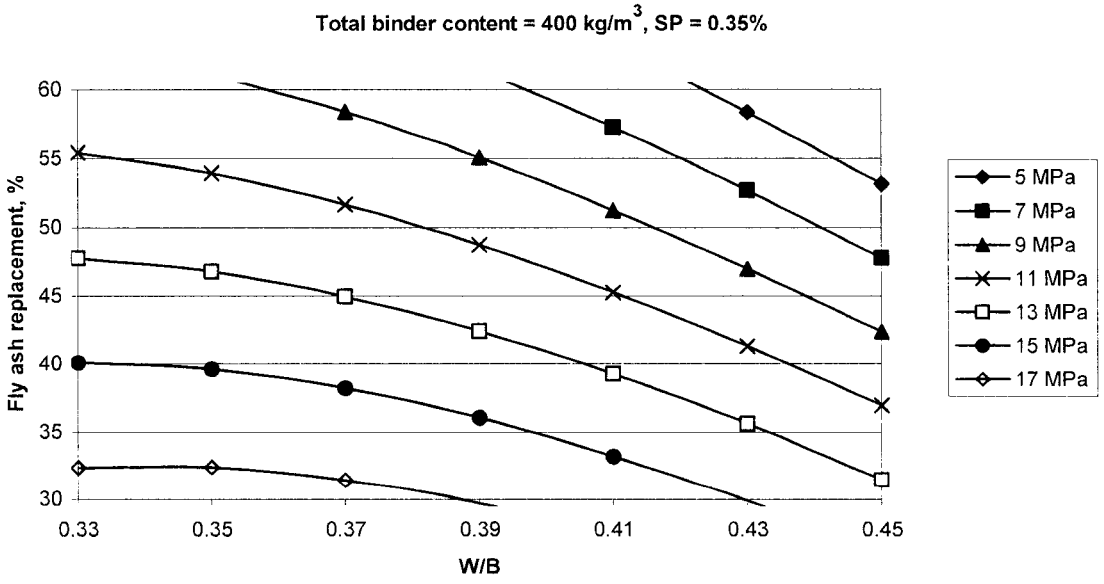

Fig. 5.7: Response surface for variation in 1-day strength

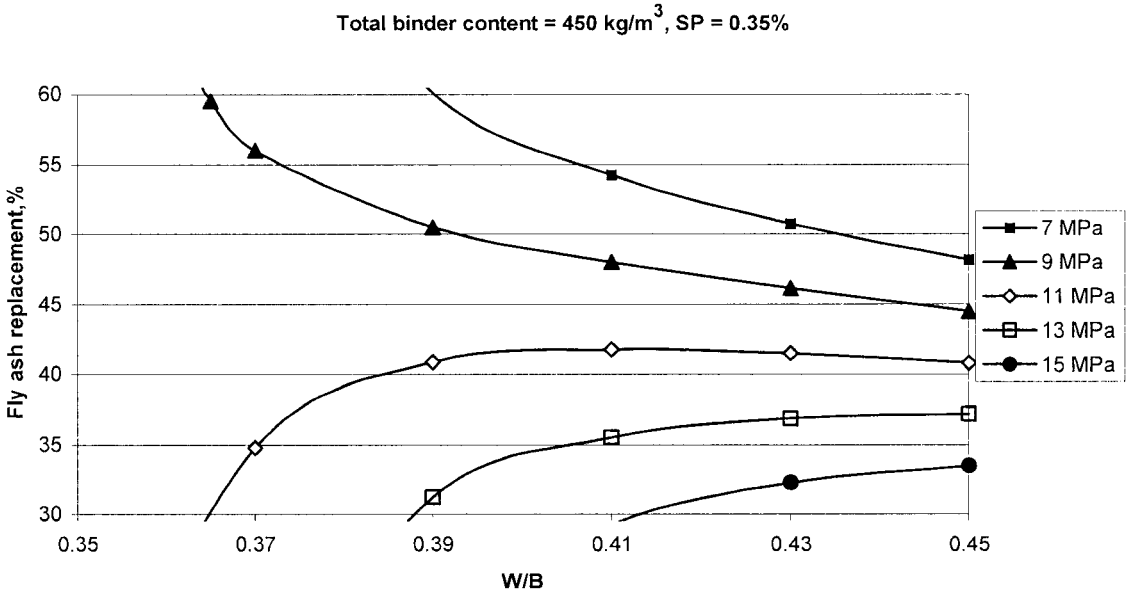

Fig. 5.8: Response surface for variation in 1-day strength

The response surfaces for 1-day strength at 350, 400, and 450 binder contents and SP content of 0.35% are illustrated in Fig. 5.6. to 5.8. At given binder and SP contents, a desired 1-day strength can be achieved by different combinations of FA percentage and W/B. For example, for certain projects, a minimum 13 MPa 1-day compressive strength is desired with binder content of 400, and S.P content of 0.35 %. The result can be achieved by using 47% fly ash and 0.35 W/B or 32% fly ash and 0.45% W/B ratio as indicated in Fig. 5.7. The choice of combinations can be further reduced if specific parameter such as slump flow is also desired.

Fig. 5.9 represents the influence of fly ash replacement on the 1-day compressive strength. At a given total binder and a SP content, an increase in the % of FA can substantially reduce the 1-day compressive strength. It is also observed that 1-day strength reduction with increase of FA is higher at high W/B compared to low W/B (Fig. 5.9). Fig. 5.9 indicates that at W/B of 0.45, the reduction in 1-day strength on every 10 % increment of FA is 3.7 MPa (27.2 %), while at 0.39 W/B ratio it is 3.15 MPa (18.6 %), and at 0.33 W/B it is only 2.6 MPa (14.7 %).

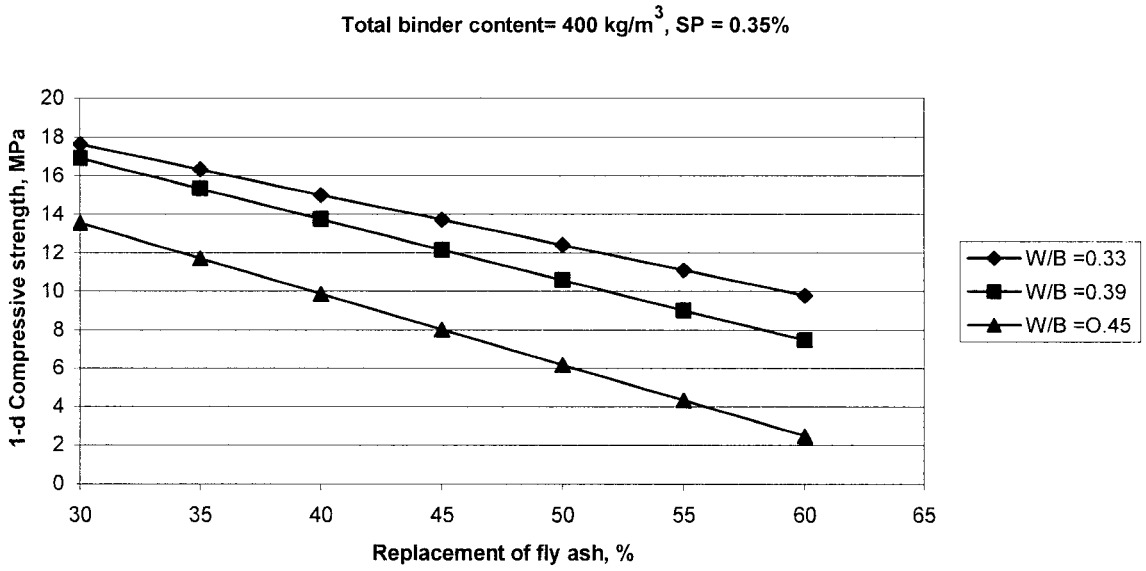

Fig. 5.9: Influence of fly ash fly ash replacement on 1-day strength

5.4 Model 3: 28-day compressive strength

In design and quality control of concrete, 28-day strength is normally specified. The 28-day compressive strength of concrete determined by a standard uniaxial compression test is universally accepted as a greater index of concrete strength [16]. Hence the 28-day compressive strength model was selected to evaluate the quality of SCC. The 28-day strength model is as follows:

28-day strength, $Y_3 = 264.091 - 0.4297\ X_1 - 4.4592\ X_2 - 107.277\ X_4 + 0.0106\ X_1X_2 + 0.0307\ X_1X_3$

The statistical detail of the model is presented in Appendix D. The model is fit in Normal (Gaussian) probability distribution function with Identity link function. The nature of the model is non-linear and all the three variables such as the total binder content (X_1), the percentage replacement of FA (X_2), and the W/B (X_3) have direct influence on the response (28-day strength, Y_3). X_1, X_2 and X_1, X_3 are interacting with each other and have positive influence on the response. The R^2 value of 0.7592; is an indication of reasonably good fitness. From the ANOVA analysis, it appears that the probability greater than F statistics (Fisher statistics) is less than 0.0003. The model is highly statistically significant with confidence level of 99.97%. All the variables individually also tested for t statistics. The probability greater than t statistics for intercept, all variables, and their interaction is indicated in Appendix D. The probability greater than t statistics for all variables is found to be less than 0.087 (confidence level more than 91.3%). All the variables indicated in model are statistically significant and have influence on the 28-day compressive strength.

The response surfaces for the 28-day compressive strength at 350, 400, and 450 kg/m^3 binder content with SP content of 0.35% are illustrated in Figs. 5.10 to 5.12. At a given binder and a SP content, a desired 28-day compressive strength can be achieved by different combinations of % of FA and W/B as indicated in Figs. 5.10 to 5.12. On the

other hand, if the values of all four variables are known, the 28-day compressive strength can be predicted from the response surface charts.

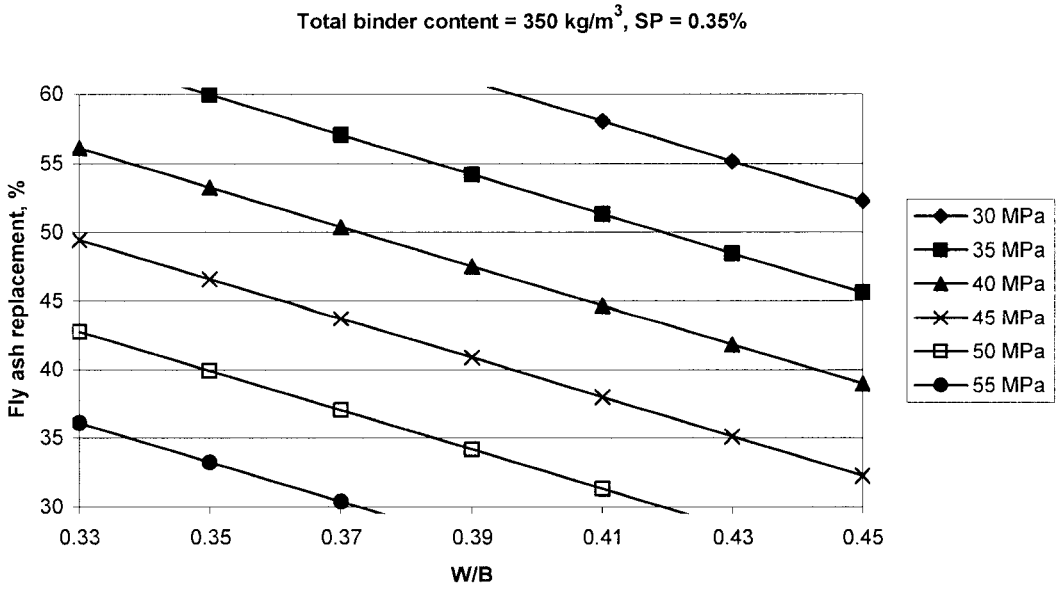

Fig. 5.10: Response surface for variation in 28-day strength

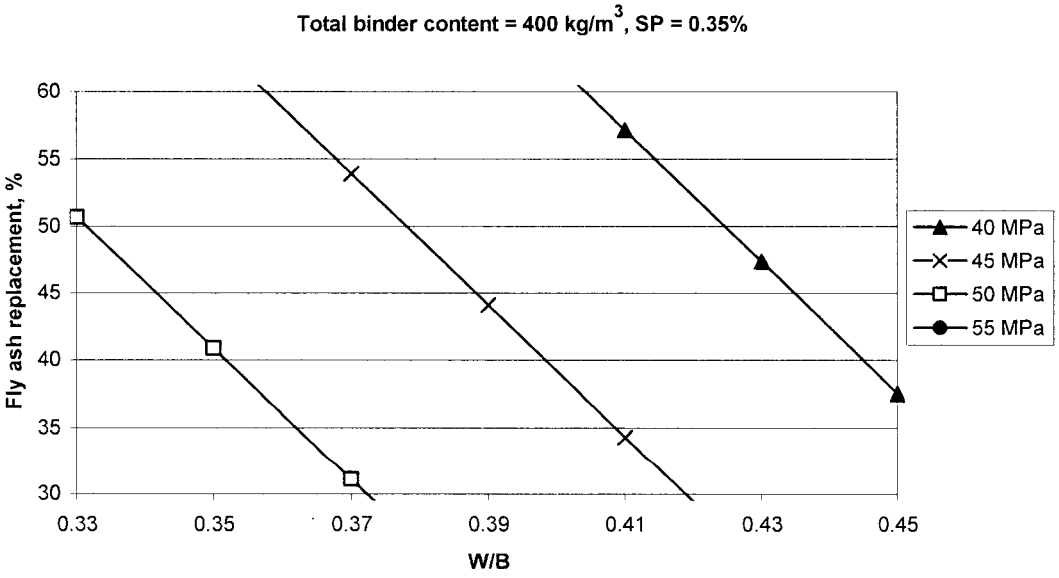

Fig. 5.11: Response surface for variation in 28-day strength

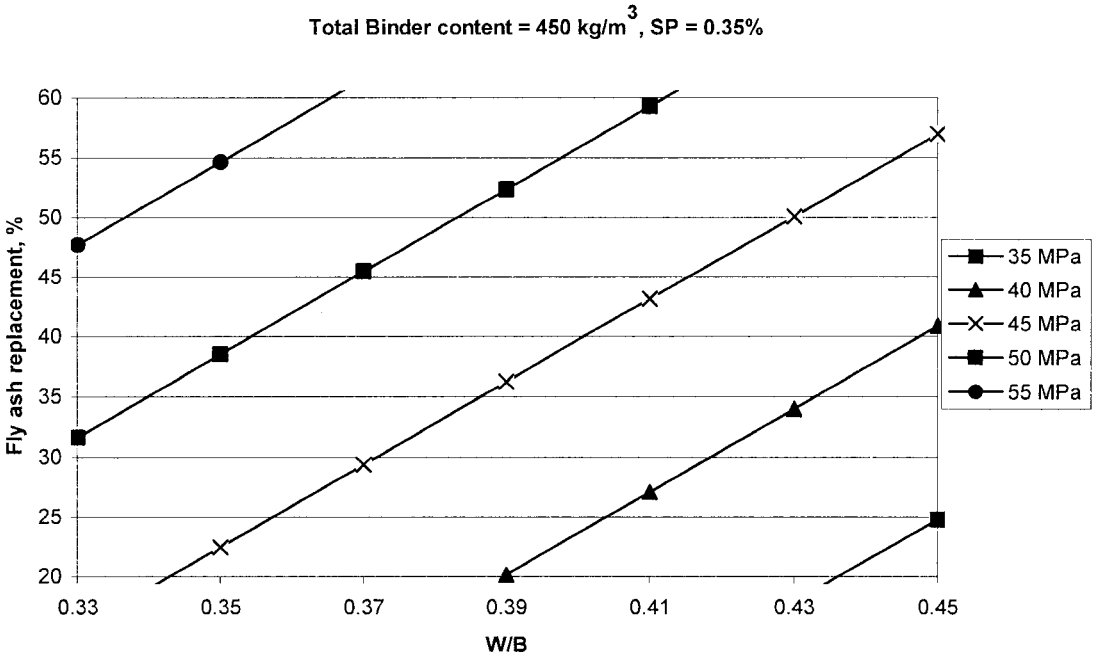

Fig. 5.12: Response surface for variation in 28-day strength

The influence of FA replacement on the 28-day compressive strength is illustrated in Fig. 5.13. At a given total binder and SP content, the 28-day compressive strength decreases with the increase of FA percentage. At a 400-binder content and 0.35% S.P dosage, a 2.19 MPa (5%) decrease in the 28-day compressive strength is observed on every 10% increase in FA replacement. Unlike 1-day compressive strength, this behavior is similar for all W/B.

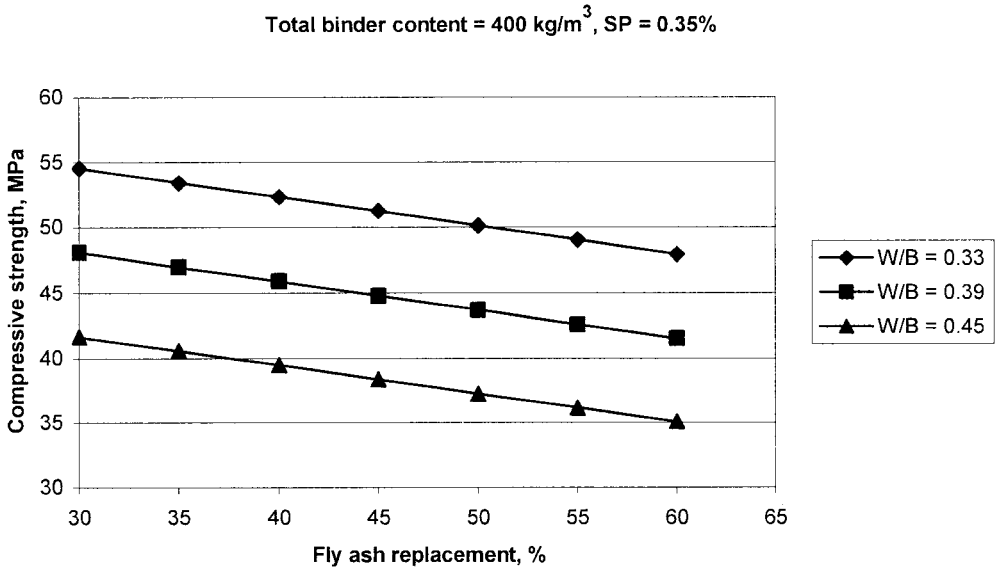

Fig. 5.13: Influence of fly ash replacement on 28-day strength

5.5 Model 4: Rapid chloride permeability (RCP)

The problem of corrosion of reinforcing bars in concrete due to penetration of chloride is well known. The chloride-induced depassivation of steel bars plays major role in the corrosion of reinforcing bars, which results in the deterioration of concrete [39, 49]. The RCP model is developed to evaluate and assess the durability of SCC with high volumes of FA. The RCP model is as follows:

$$\textbf{RCP, } \textbf{Log(Y4)} = 12.0012 - 0.0229\,X_1 - 0.0436\,X_2 + 0.017\,X_2X_3 + 0.0947\,X_2X_4 - 1.6182\,X_3X_4 + 0.0000269\,X_1^2$$

The statistical detail of the model 4 is presented in Appendix E. The RCP (Y_4) is the representation of chloride ions charge passed, in coulombs, after 6 hours of test as

specified in ASTM C 1202 – 97. The model is fit in Poisson probability distribution function with natural log link function. The nature of the model is non-linear and the total binder content (X_1), % of FA (X_2), have direct influence on the response model (Y_4). X_2, and X_3, X_2, and X_4, X_3 and X_4 are interacting with each other and have influence on the response. From the ANOVA analysis, it appears that the probability greater than scaled deviation is less than 0.0001. The model is highly statistically significant with confident level of 99.99 %. All the variables, indicated in the model are also tested individually for chi square statistics. The probability greater than chi square statistics for intercept, all model variables, and their interactions are indicated in Appendix E. The probabilities greater than chi square statistics for all variables are found less than 0.0379 (confidence level more than 96.21%). In some cases it was less than 0.0001 (confidence level more than 99.99 %). All the variables indicated in the model are statistically significant and have great influence on the RCP.

The response surfaces for RCP at 350, 400, and 450 kg/m^3 binder contents with 0.35% of SP content are illustrated in Fig 5.14 to 5.16. At a given binder and a SP content, if the W/B and the % of FA replacement are known, RCP can be predicted from these response surface charts.

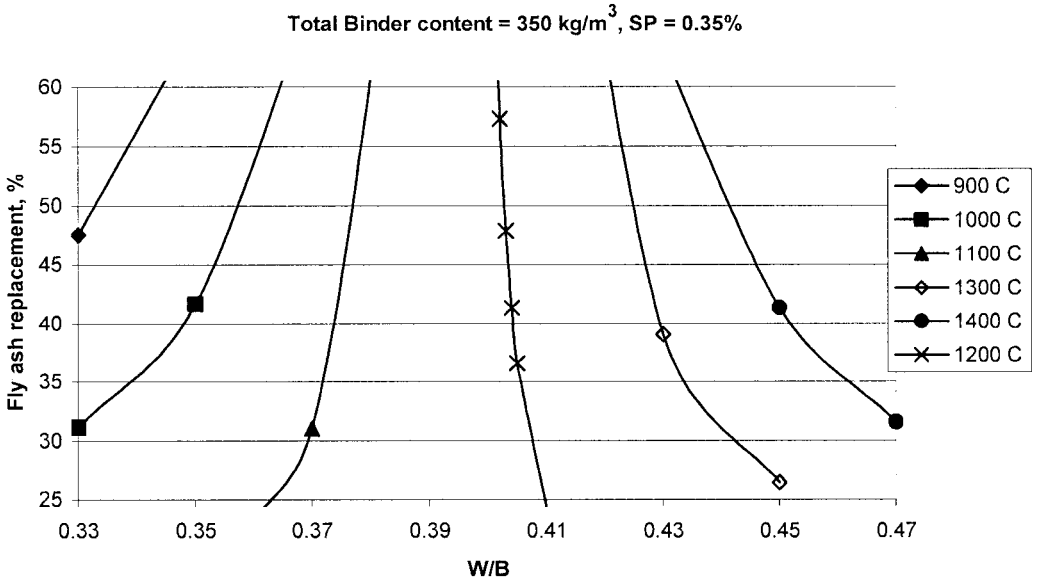

Fig. 5.14: Response surface for variation in RCP at 28-days

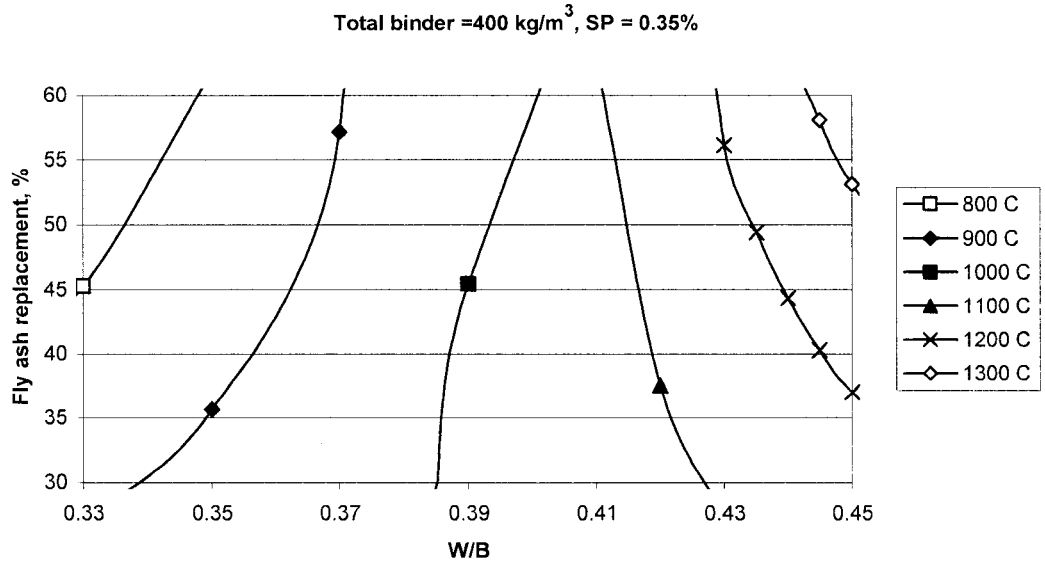

Fig. 5.15: Response surface for variation in RCP at 28-days

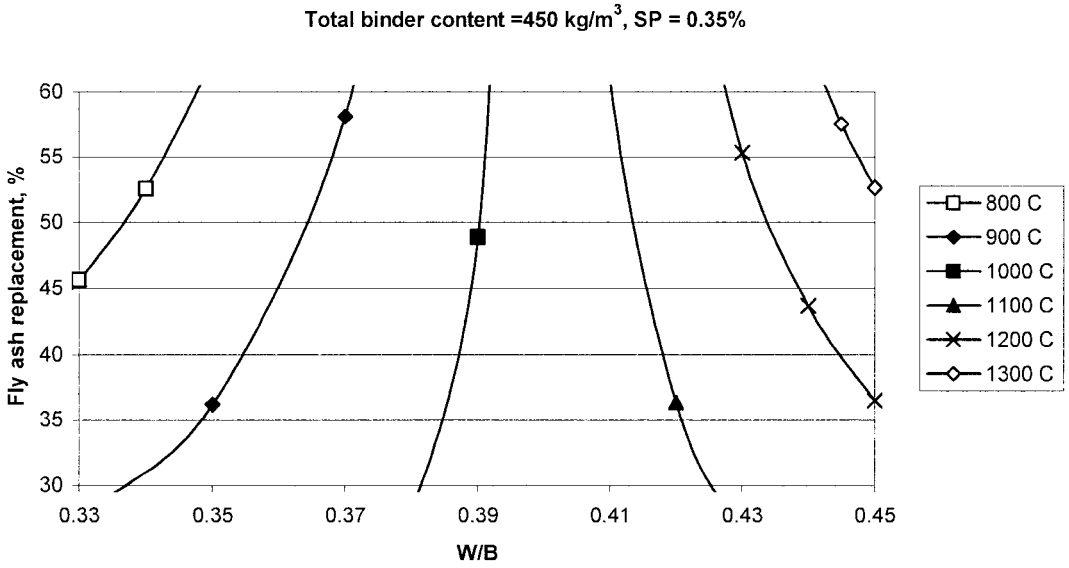

Fig. 5.16: Response surface for variation in RCP at 28-days

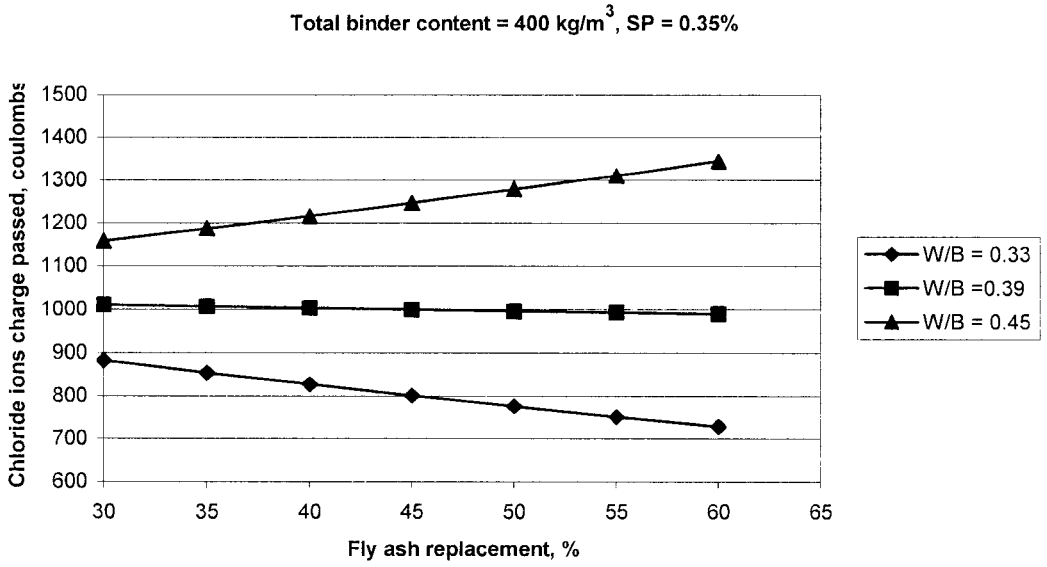

Fig. 5.17: Influence of fly ash replacement on RCP

The influence of FA replacement on RCP is illustrated in Fig. 5.17. It is interesting to note that at a given total binder, and a SP content, RCP decreases with the increase of the

% of FA up to a W/B of 0.4. For a W/B more than 0.4, the RCP is found to increase with the increase of % of FA as shown in Fig. 5.17. The % of FA and W/B have strong interaction between themselves, which affects the response of RCP. This behavior indicates that the W/B significantly affects the pore refinement of FA at early ages (28-day). Hence, for the evaluation of SCC for RCP at 28-days, both variables should be considered.

5.6 Model 5: Material cost

The cost is an important parameter and hence cannot be neglected for the development of any concrete. The material cost model is based on material costs prevailed in eastern Canada market. All figures are in Canadian dollars. The prevailing prices of material considered in the model are as follows:

Cement:	$130 per tonne
Fly ash:	$80 per tonne
Superplasticizer:	$3 per liter
Coarse aggregate:	$16.5 per tonne
Fine aggregate:	$8.25 per tonne

Only material costs are considered and the shipping, placing, or any contingency costs are not included. The proposed cost model is as follows:

Material cost, C $, $Y_5 = 27.2783 + 0.1125\ X_1 - 0.1555\ X_2 + 24.1377\ X_3$

The statistical detail of the material cost model is presented in Appendix F. The model is fit in Normal (Gaussian) probability distribution function with Identity link function. The nature of the model is obviously linear and X_1, X_2, and X_3 variables have influence on the response (cost, Y_5). The variables X_1, and X_3 have positive influence and increase the material cost while X_2 has negative influence and reduces the material cost of concrete. The R^2 value of 0.97 is an indication of the excellent goodness of fit. From the ANOVA analysis, it appears that the probability greater than F statistics (Fisher statistics) is less than 0.0001. The model is highly statistically significant with confident level more than 99.99 %. All the three variables individually also tested for t statistics. The probability greater than t for intercept and all three variable indicated in the model is less than 0.0001 (confidence level more than 99.99%). Hence all the three variables are statistically significant and have great influence on material cost.

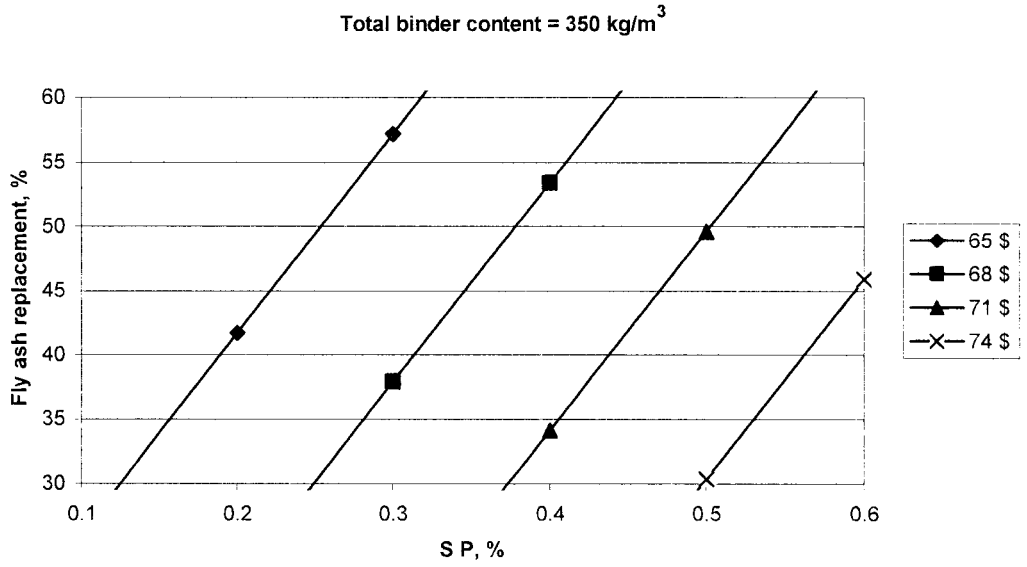

Fig. 5.18: Response surface for variation in material cost.

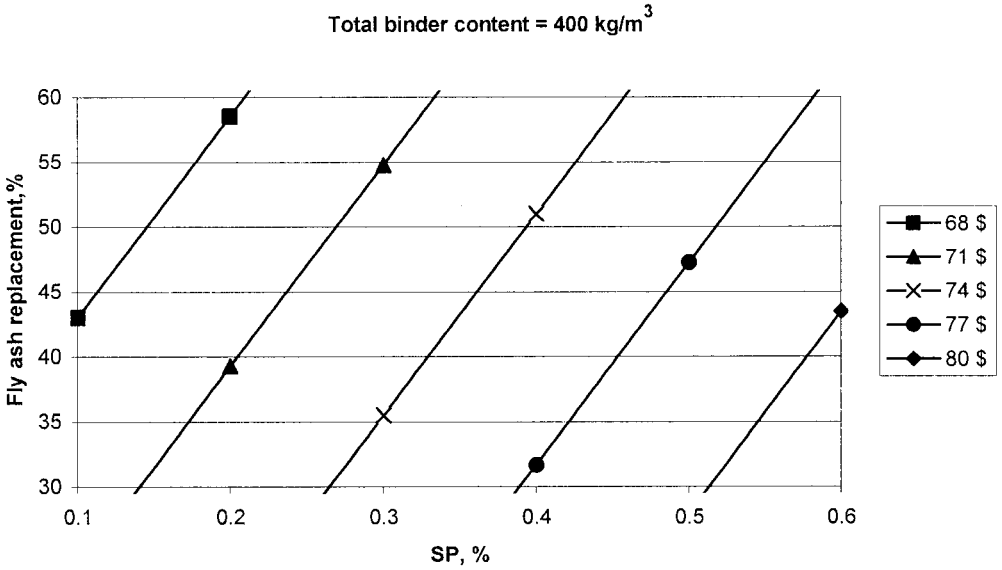

Fig. 5.19 Response surface for variation in material cost.

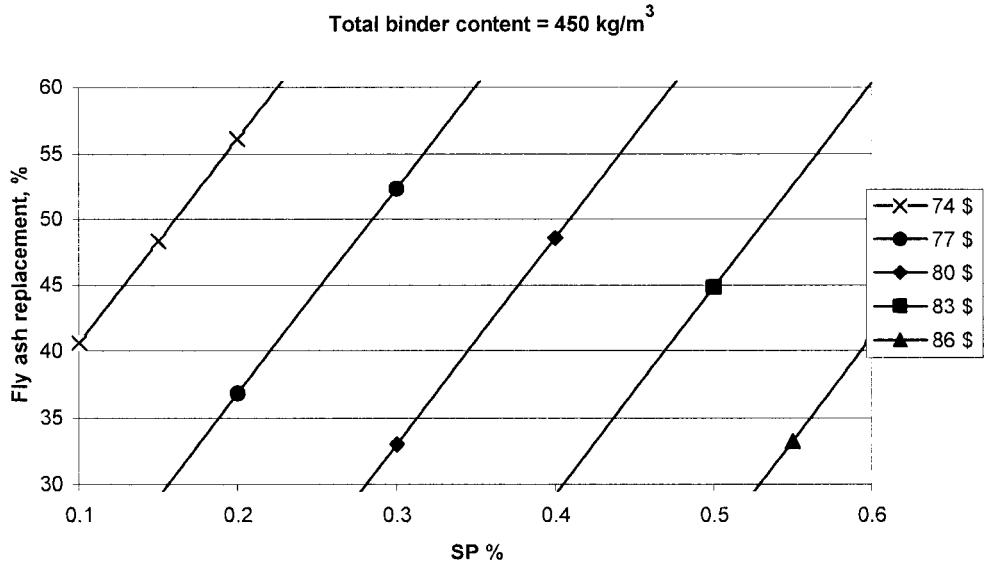

Fig. 5.20: Response surface for variation in material cost.

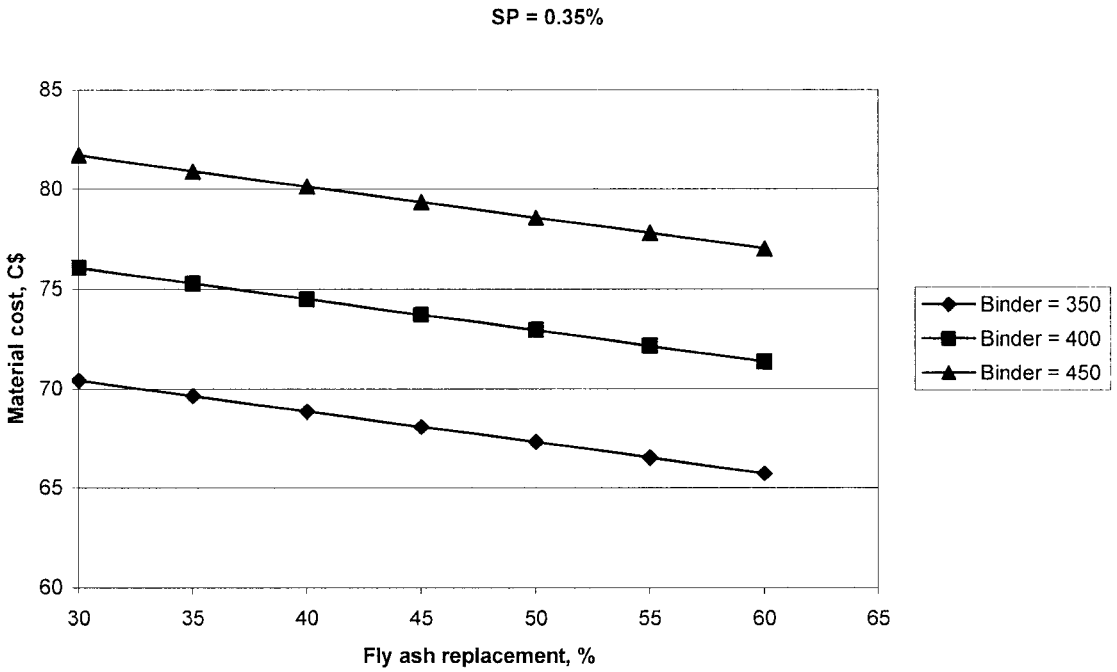

Fig. 5.21: Influence of fly ash replacement on material cost

The influence of FA replacement on material cost for different binder contents is illustrated in Fig. 5.21. Naturally at any binder content, the material cost decreases with the increase of the % of FA replacement as cement is expensive than fly ash. The material cost of SCC can be reduced by \$1.55 per m^3 of SCC on every 10 % increase in FA.

5.7 Optimization and simulations of SCC by using statistical models

Reliable SCC can be developed with high volumes of fly ash by using the proposed models. It is also possible to optimize the cost and the quality of SCC. LINGO 7, optimization software was found very useful to optimize linear and non-linear

mathematical models. If the software is not available, one can use response surface charts discussed in this chapter. The example of optimization of SCC mix for four variables with LINGO 7 software is discussed as follows:

Objective:

A SCC was desired with 650 mm slump flow and a 28-day compressive strength of 45 MPa.

Result:

For an economic point of view, it is advisable to use minimum binder content, and SP dosage as well as an optimum quantity of FA. The SP dosage of 0.3% was selected, which was reasonably low for a slump flow target of 650 mm. The compressive strength of 45 MPa requires a W/B of approximately 0.38 would be appropriate. LINGO 7 was used to optimize the total binder content (X_1), and % FA (X_2) as well as to predict 1-day strength, 28-day strength, RCP, and material cost.

Prediction of X_1 and X_2 (Model 1):

```
Y1=-1793.76+2.0542*X1+5.9456*X2+710.476*X3+2648.08*X4;
Y1=650;
@bnd(350,X1,450);
@bnd(30,X2,60);
X3=0.3;
X4=0.38;
```

Optimization results:

Variable	Value
Y1	650 mm
X1	**450 kg/m^3**
X2	**50 %**
X3	0.30 %
X4	0.38

Prediction of the 1-day compressive strength:

1-day compressive strength can be predicted by using model 2 with four variables optimized from model 1

Y2=1786.34-3.0317*X1-29.8364*X2-2972.19*X3-
3190.45*X4+0.0391*X1*X2+3.7161*X1*X3+5.1744*X1*X4+40.6712*X2*X3+36.976
3*X2*X4+3993.55*X3*X4-0.2706*X1*X2*X3*X4-0.0005*X1^2-363.716*X4^2;

X1=450;
X2=50;
X3=0.3;
X4=0.38;
Y2=12.50 MPa

Prediction of the 28-day compressive strength

28-day compressive strength can be predicted from model 3

Y3=264.0907-0.4297*X1-4.4592*X2-107.2766*X4+0.0106*X1*X2+0.0307*X1*X3;
X1=450;
X2=50;
X3=0.3;
X4=0.38;
Y3=49.65 MPa

Prediction of RCP:

The RCP (charge passed in coulombs) can be predicted by using model 4

ln(Y4)=12.0012-0.0229*X1-0.0436*X2+0.017*X2*X3+0.0947*X2*X4-
1.6182*X3*X4+0.000027*X1^2;
X1=450;
X2=50;
X3=0.3;
X4=0.38;
ln(Y4)= 6.853525
Y4=947 Coulombs

Prediction of the material cost:

The material cost of SCC mix can be estimated from model 5

Y5=27.2783+0.1125*X1-0.1555*X2+24.1377*X3;
X1=450;
X2=50;
X3=0.3;
X4=0.38
Y5 = 77.37 Canadian $

5.8 Validation of the statistical models

Four mixtures were selected randomly to verify the ability of the proposed models to predict the responses (Table 5.1). The slump flow, the 1-day compressive strength, and the 28-day compressive strength were measured and compared with the prediction of the respective models. Table 5.1 shows the quantities of four variables (X_1, X_2, X_3, X_4), measured and model predicted values of slump flow, 1-day compressive strength, and 28-day compressive strength. The tests were carried out with the same materials and under the same testing conditions, except that the batch volumes of mixes were lower (0.02 m^3) than those of previous 21 mixes used for the development of statistical models.

It appears from the results that the predictions of the slump flow, the 1-day compressive strength, and the 28-day compressive strength by respective models are acceptable although significant difference is found between measured and predicted values of the 1-day compressive strength (4.5 MPa.) for T4 mix. This may be due to experimental error.

Table 5.1: Prediction of models

Mix #	Total binder content X1	% of FA X2	% of SP X3	W/B X4	Measured values			Model predicted values		
					Slump flow (mm)	1-day strength (MPa.)	28-day strength (MPa.)	Slump flow (mm)	1-day strength (MPa.)	28-day strength (MPa.)
T1	450	55	0.35	0.35	605	7.7	47	633	9.8	55
T2	350	45	0.35	0.44	535	5.5	39	606	6.1	37
T3	440	30	0.4	0.38	585	14.1	49	578	15.7	46
T4	420	45	0.33	0.39	625	7.5	45	604	12.0	45

5.9 Limitation of models

The proposed statistical models were derived from twenty-one statistically balanced concrete mixtures with CSA Type 10 cement (ASTM Type 1), Sundace FA conforming to ASTM (class F fly ash), a poly-naphthalene sulfonic acid based SP with 40.5% solid content conforming ASTM C 494 type F, 12.5 mm MSA gravel, and natural sand. It is very important to note that derived models are material specific. The absolute responses from the five models can differ, if the properties of materials vary considerably from the materials used to derive the models. However, the models can still be useful for mixture optimization and simulation when presented with different sets of materials. The optimization of cost and quality is also possible with these models even if different sets of materials are used.

Chapter 6 Conclusions and Recommendations

6.1 Conclusions

The following conclusions are drawn from the research study:

1. To standardize the marsh cone test for paste, specific flow time (S_{sp}) is proposed instead of flow time. The specific flow time is the ratio of time required in seconds to fill the standard volumes of container by paste through marsh cone opening to the time required in seconds to fill the same volumes of container by water through the same marsh cone opening.
2. No significant correlation is observed between the plastic viscosity of paste and the slump flow of concrete. The yield stress of paste has reasonably good linear correlation with the slump flow of concrete. The prediction of the flow behavior of the SCC is possible from the rheological parameters of the corresponding paste.
3. A paste having a yield stress of less than 4 Pa. and a specific flow time of less than 2.6 can generate sufficient flow in the corresponding concrete to qualify for SCC.
4. Concrete mixes containing a mortar with a yield stress of less than 6 Pa. and a plastic viscosity of less than 0.6 Pa.s are more likely to qualify for SCC. There are more chances of segregation of concrete mixes containing mortar with a yield stress of less than 1.5 Pa. and a plastic viscosity of less than 0.25 Pa.s.

5. From the ANOVA analysis it is found that the four selected variables: the total binder content, the % of fly ash replacement, the % of superplasticizer, and the water to binder ratio have negative influence on the plastic viscosity of mortar. The % of FA replacement has less negative influence than the other three variables. If higher deformability of concrete is achieved by increasing the % of FA instead of increasing the W/B or S.P, the drop in viscosity would be less and the segregation can be prevented.
6. Filling capacity and the L-box tests are found more appropriate to evaluate the deformability of SCC through congested reinforcing bars. The SCC may have good deformability, if blocking ratio (h_2/h_1) is more than 0.80 and filling capacity between 60 and 95 %.
7. A good correlation is found between the slump flow and the segregation index. Practically no segregation is observed up to a slump flow of 540 mm. The chances of segregation are very high beyond a slump flow of 750 mm.
8. Increasing the % of fly ash replacement and the superplasticizer content leads to delay of initial and final setting times of SCC.
9. No significant difference in drying shrinkage is observed between the different SCC investigated. No significant difference is also observed between SCC with different fly ash percentages.
10. The concrete mixtures in this study are non-air entrained hence they have low resistance to freezing and thawing cycles. No significant difference is found between non-qualified SCC mixes, SCC mixes, and segregated mixes. The non-

air entrained SCC with high volumes of fly ash have exhibited poor resistance to surface scaling.

11. All the four selected variables: the total binder content, the % of fly ash replacement, the % of superplasticizer, and the water-to-binder ratio are statistically significant and have positive influence on the slump flow. At a given binder and a SP content, an increase in the % of FA replacement can increases substantially the slump flow regardless of W/B. An increase in FA replacement by 10% can increase the slump flow by around 60 mm.
12. Fly ash has great capability to reduce the SP demand in achieving a desired slump flow. SP dosages can be estimated and optimized by using the proposed statistical model.
13. At a given total binder and a SP content, an increase in the % of FA replacement substantially reduces the 1-day compressive strength. It is also observed that the 1-day compressive strength reduction is higher at high W/B compared to low W/B.
14. At a given total binder and a SP content, the 28-day compressive strength marginally decreases with the increase of % of FA replacement. Unlike 1-day compressive strength, the decrease in strength is similar for all W/B.
15. At a given total binder and a SP content, the rapid chloride permeability decreased with an increase of % of FA replacement up to W/B of 0.4. For W/B higher than 0.4 the rapid chloride permeability is found to increase with an increase of the % of FA.

16. Reliable SCC can be developed with high volumes of FA by using proposed statistical models with response surface charts or any optimizing software. The proposed models are material specific. The absolute value of the predicted properties would not be the exactly same but it would be close even if different set of materials are used. The models can substantially reduce time, effort, and cost associated with selection of trial batches.
17. Sustainable development in concrete can be achieved by producing SCC with high volumes of FA as it reduces the use of cement, consume the industrial waste, increase the durability, and reduces the noise pollution.

6.2 Recommendations

Following is a list of recommendations for future research on SCC.

1. The rheological parameters for paste such as the plastic viscosity and the yield stress were measured by using Brookfield viscometer. The marsh cone test, which is very easy with handy apparatus, exhibited good correlation with the yield stress of paste. The yield stress of paste is responsible for generating flow in concrete hence it becomes easy to predict the flow behavior of corresponding concrete from the results of the marsh cone test. There is no test found in the literature, which can be correlated with the plastic viscosity of paste. The plastic viscosity is responsible for the segregation of aggregate in concrete. It is recommended to develop an easy and handy test, which can be correlated with the plastic viscosity of paste and the segregation of aggregate in concrete.

2. The rheology of paste and mortar were studied in this research project. The study of rheology of concrete with more advanced and appropriate concrete rheometers is recommended.
3. Segregation is an important characteristic of SCC. It is easy to assess segregation by physical inspection but difficult to measure quantitatively. The segregation index test developed by Fujiwara was used in this study. It is recommended to develop more tests for segregation and settlement of SCC in future.
4. The non-entrained SCC used in the study, exhibited low resistance to freezing and thawing after 300 cycles and poor surface scaling resistance after 50 cycles. The freezing/thawing and surface scaling resistance can be enhanced by entraining air in the concrete and by stabilizing the air void system. It is recommended to study these parameters for air entrained SCC incorporating high volumes of FA. It is also recommended to study the air void stability of SCC.
5. The SCC is developed by using high volumes of class F fly ash. It is recommended to try with other types of FA and other supplementary cementitious materials like blast furnace slag to boost the sustainable development in concrete.

Chapter 7 References

1 N. Bouzoubaa, M. Lachemi, "Self-compacting concrete incorporating high volumes of class F Fly ash, Preliminary results." Cement and Concrete Research 31 (2001), pp. 413 – 420.

2 W. Zhu, J.C. Gibbs, P. Bartos, "Uniformities of in situ properties of self-compacting concrete in full scale structural elements." Cement and Concrete Composites 23 (2001), pp. 57 – 64.

3 H. Okamura, "Self-compacting high performance concrete." Concrete International, 9 (7), July 1997, pp. 50 – 54.

4 Y. Xie, B. Liu, Yin, S. Zhou, "Optimum mix parameters of high-strength self-compacting concrete with ultra pulverized fly ash" Cement and Concrete Research 32 (2002), pp. 477-480.

5 A.W. Saak, H.M. Jeninings, S.P Shah, "New Methodology for designing Self-Compacting Concrete" ACI Materials Journal, 98 (6), November-December 2001, pp. 429-436.

6 C. F. Ferraris, "Measurement of rheological properties of High Performance Concrete: State of the art report" Journal of Research of the National Institute of Standard and Technology. Vol. 104, September- October 1999, pp. 461 – 478.

7 C. F. Ferraris, L. Brower, C. Ozyildirim, J. Daczko, "Workability of Self-Compacting Concrete" The economical solution for durable bridge & transportation structures, International symposium on HPC proceedings. PCI/FHWA/FIB. Septembre 25-27, 2000, Orlando, Florida, pp. 398 – 407.

8 P. Lacombe, D. Beaupre, and N. Pouliot. "Rheology and bonding characteristics of Self-leveling concrete as a repair material." Materials and Structures, Vol. 32, October 1999, pp. 593 – 600.

9 C. F. Ferraris, F. de Larrard, "Testing and modeling of fresh concrete rheology" NISTIR 6094. Building and Fire Research Laboratory, National Institutes of Standards and Technology, Gaithersburg, Maryland 20899, February 1998.

10 C. Tang, T. Yen, C. Chang, and K. Chen, "Optimizing Mixture Proportions for Flowable High-Performance Concrete via Rheology Tests, ACI Materials Journal, 98(6), November-December 2001, pp. 493-502.

11 K. H. Khayat, A. Ghezal, and M. S. Hadriche, "Factorial design models for proportioning self-consolidating concrete" Materials and Structures, Vol. 32, November 1999, pp. 679-686.

12 A. Nanayakkara, K. Ozawa, and K. Maekawa, "Flow and segregation of fresh concrete in tapered pipes", Proceedings, 3rd International symposium on liquid – solid flows, ASME, FED- 75, (1988), pp. 139-144.

13 K. Ozawa, N. Sakata, and H. Okamura, "Evaluation of self-compactibility of fresh concrete using the funnel test", Proceeding of JSCE, 25, June 1995, pp. 59-75.

14 K. H. Khayat and J. Assaad, "Air-Void Stability in Self-Consolidating Concrete" ACI Materials Journal, 99 (4), July-August 2002, pp. 408-416.

15 K.H. Khayat, A. Yahia, and M. Sonebi, "Applications of statistical models for proportioning underwater concrete." ACI Materials Journal, 96 (6) November-December 1999, pp. 634 – 640.

16 P. K. Mehta, P.J.M. Monteiro, " Concrete -- Microstructure, properties, and materials." Indian edition, published by Indian Concrete Institute, Chenai, India, 1997.

17 H. Fujiwara, "Fundamental study on self-compacting property of high-fluidity concrete", Proceeding, Japan Concrete Institutes, 14 (1), June 1992, pp. 27-32.

18 S. Nagataki, H. Fujiwara, "Self-compacting property of highly flowable concrete", V.M. Malhotra edited, ACI, SP 154, June 1995, pp. 301-314.

19 M. Sonebi, P. Batros, W. Zhu, J. Gibbs, A. Tamimi, "Properties of harden concrete" Task 4, final report (2000), Advance concrete masonry center, University of Paisley, Scotland, UK. pp. 6-73. (http:/scc.ce.luth.se)

20 S. Kuroiwa, Y. Matsuoka, M. Hayakawa, and T. Shindoh, "Application of super workable concrete to construction of 20-story building", High performance concrete in severe environments, Ed by Paul Zia, ACI SP-140, 1993, pp. 147-161.

21 B. Persson, "Internal frost resistance and salt frost scaling of self-compacting concrete" Cement and Concrete Research 33 (2003), pp. 373-379.

22 M. J. Simon, E. S. Lagergren, K. A. Synder, "Concrete mixture optimization using statistical mixture design method." Proceeding of PCI/FHWA, International symposium on HPC. New Orleans, October 20-22, 1997, pp. 230 – 244.

23 A. Ghezal and K. Khayat, "Optimizing self-consolidating concrete with lime stone filler by using statistical factorial design methods." ACI Materials Journal, 99 (3), May-June 2002, pp. 264-273.

24 P. K. Mehta, "Pozzolanic and Cementitious byproducts as Mineral Admixtures for Concrete- A Critical Review." ACI International Conference. Edited by V. M. Malhotra, SP 79-1, 1983, pp. 1 – 46.

25 V. M. Malhotra, "CANMET investigation dealing with high-volume fly ash concrete", Advances in concrete technology, second edition, Editor: V. M. Malhotra, Natural Resources Canada, 1994, pp. 445-482.

26 S. Kosmatka, B. Kerkhoff, W. Panarese, N. MacLeod, R. McGrath, "Design and control of concrete mixtures" Seventh Canadian Edition, Cement association of Canada, 2002, pp. 1-355.

27 "2001 Canadian minerals year book", Cement section, O. Vagt – draft, August 2002.

28 G. C. Isaia, "Synergic action of fly ash in ternary mixers of high performance concrete." HPC Proceeding ACI / CANMAT International Conference, Edited by V. M. Malhotra, SP 186-28, 1999, pp. 481-502.

29 Federal Highway Administration, U. S. Department of Transportation, "Fly Ash Facts For Highway Engineers." FHWA-SA-081, August, 1995.

30 L. Robert, Yuan, and E. James, Cook, " Study of class C fly ash concrete." ACI International Conference. Edited by V. M. Malhotra, SP 79-15, 1983, pp. 289 – 306.

31 S. Diamond, "The characterization of fly ashes." Proceedings, Symposium on effect of fly ash incorporation in cement and concrete, Material Research Society, Editor: S. Diamond, 1981, pp. 12-23.

32 B. Mortureux, H. Hornain, E. Gautier, and M. Regourd, "Comparison of the reactivity of different pozzolans." Proceedings, Seventh International Congress on The Chemistry of Cement, Paris, Vol. 3, 1980, pp. 110-115.

33 E. Berry, V. Malhotra, "Fly ash in concrete-A critical review", J. ACI, Proc., 2 (3), 1982, pp. 59-73.

34 E. Berry, V. Malhotra, "Fly ash in concrete." Supplementary cementing materials for concrete, CANMET, Edited by V. M. Malhotra, 1987, pp. 37-229.

35 V. Dodson, "The effect of fly ash on the setting time of concrete – chemical or physical" Proceedings, Symposium on fly ash incorporation in hydrated cement system, Editor: S. Diamond, Materials Research Society, Boston, 1981, pp. 233-243.

36 V.R. Sturrup, R. D. Hooton, and G. Clendenning, "Durability of Fly ash concrete." ACI International Conference, Edited by V. M. Malhotra, SP 79-3, 1983, pp. 71 – 86.

37 C. Goodspeed, S. Vanikar, R. Cook, "High- Performance Concrete (HPC) Define for Highway Structures." High performance concrete committee special report No. 4, Publication No. FHWA-SA-98-082, July 1998.

38 P.-C. Aitcin, "High-Performance Concrete." Published by E & FN SPON, 1998, pp. 121- 263.

39 V. G. Papadakis, " Effect of supplementary cementing materials on concrete resistance against carbonation and chloride ingress." Cement and Concrete Research, 30 (2000), pp. 291 – 299.

40 R.O. Lane, and J. F. Best, "Properties and use of fly ash in Portland cement concrete." Concrete International, 4 (7), July 1982, pp. 81-92.

41 S.R. Schmidt, R.G. Launsby, "Understanding Industrial Designed Experiments" fourth edition, edited by M. J. Kiemele, Air Academic press, Colorado springs, 1994, Chapter 3, pp. 1-48.

42 F. de Larrard, "A Mix Performance Method for High Performance Concrete" High Performance Concrete : From Material to structure, Edited by Yves Malier. Published by E & FN Spon. 2-6 Boundary row, London SE1 8HN. ISBN 0419 17600 4., 1992, Chapter 4, pp. 1-14.

43 P.Mitschka, "Simple conversion of Brookfield R.V.T. readings into viscosity functions" Rheologica Acta 21, (1982), pp. 207-209.

44 K. Wang, S. Maria, K. Gdoutos, S.P. Shah, "Hydration, Rheology, and strength of OPC- Cement kiln dust (CKD)-Slag binder." ACI Materials Journal, 99 (2), March-April 2002, pp. 173-179.

45 O. Petersson, "Workability" SCC, Task 2, final report (1999), Advance concrete masonry center, University of Paisley, Scotland, UK. pp 1-56. (http:/scc.ce.luth.se)

46 K. H. Khayat, A. Ghezal, M.S. Hadriche, "Development of factorial design models for proportioning self-consolidating concrete." V. M. Malhotra edited, Nagataki symposium on vision of concrete: 21st century, June 1998, pp. 173-197.

47 S. Iravani, "Mechanical Properties of High Performance Concrete" ACI Materials Journal 93 (5), September-October 1996, pp. 416-426.

48 M. Pigeon, J. Marchand, and R. Pleau, "Frost Resistant concrete" Construction and Building Material, 10 (5), 1996, pp. 339 – 348.

49 F. Leng, N. Feng, X. Lu, "An experimental study on the properties of chloride ions of fly ash and blast furnace slag concrete." Cement and Concrete Research 30 (2000), pp. 989 – 992.

50 M.F.M. Zain, M. Safiuddin, K.M. Yusof, "A study on the properties of freshly mixed high performance concrete." Cement and Concrete Research 29 (1999), pp. 1427 – 1432.

51 M. Sari, E. Prat, J.F Labastire, "High strength self compacting concrete original solutions associating organic and inorganic admixture." Cement and Concrete Research 29 (1999), pp. 813 – 818.

52 W. Baalbaki, P.C. Aitcin, G. Ballivy, "On predicting modulus of elasticity in high-strength concrete." ACI Materials Journal, 89 (5), September-October 1992, pp. 517-520.

APPENDICES

Appendix A

Statistical Analysis of Plastic viscosity of mortar

Regression Statistics	
Multiple R	0.86
R Square	0.74
Adj. R Square	0.67
Standard Error	0.5513
Observations	21

ANOVA

	DF	*SS*	*MS*	*F*	*Significance F*
Regression	4	13.70	3.43	11.27	0.00015
Residual	16	4.86	0.30		
Total	20	18.57			

	Coefficients	*Standard Error*	*t Stat*	*P-value*
Intercept	0.9658805	0.1221	7.90	6.45E-07
X1	-0.4064173	0.1604	-2.534	0.02211
X2	-0.2777282	0.1529	-1.81	0.0881
X3	-0.4346174	0.1552	-2.80	0.0128
X4	-0.8066536	0.1603	-5.03	0.0001

Statistical analysis of plastic viscosity of mortar

Statistical analysis of Yield stress of mortar

Regression Statistics	
Multiple R	0.86
R Square	0.74
Adj. R Square	0.68
Standard Error	1.78
Observations	21

ANOVA

	DF	*SS*	*MS*	*F*	*Significance F*
Regression	4	147.80	36.95	11.6234	0.0001
Residual	16	50.86	3.18		
Total	20	198.67			

	Coefficients	*Standard Error*	*t Stat*	*P-value*
Intercept	4.9446	0.3949	12.5208	1.109E-09
X1	-1.7924	0.5186	-3.4556	0.0032
X2	-0.7847	0.4945	-1.5868	**0.1321**
X3	-1.6238	0.5018	-3.2355	0.0051
X4	-2.2312	0.5183	-4.3045	0.0005

Statistical analysis of yield stress of mortar

Appendix A Statistical analysis for mortar

Appendix B

The SAS system

Summary of Variables
Y_1 = Slump flow, mm
X_1 = Total binder content, kg/m3
X_2 = Fly ash replacing cement, %
X_3 = S.P percentage w.r.to total binder content, %
X_4 = W/B ratio

Slump flow $Y_1 = X_1, X_2, X_3, X_4$
Response Distribution: Normal
Link Function: Identity

Model Equation
Slump flow Y_1 = -1793 + 2.0542 X_1 + 5.9456 X_2 + 710.476 X_3 + 2648.08 X_4

Summary of Fit			
Mean of Response:	585.71	R-Square:	0.9212
Root MSE:	43.78	Adj R-Sq:	0.9015

Analysis of Variance					
Source	DF	Sum of Squares	Mean Sq.	F stat.	Prob. Greater F
Model	4	358649.557	89662.389	46.78	Less than 0.0001
Error	16	30664.7287	1916.5455		
C Total	20	389314.286			

Parameter Estimates					
Variable	DF	Estimate	Std Error	t stat	Prob. Greater Than t stat.
Intercept	1	-1793.7557	239.198	-7.5	Less than 0.0001
X1	1	2.0542	0.4009	5.12	0.0001
X2	1	5.9456	1.3363	4.45	0.0004
X3	1	710.4758	80.1785	8.86	Less than 0.0001
X4	1	2648.0827	349.5872	7.57	Less than 0.0001

Appendix B. Statistical details for model 1

Appendix C

SAS System

Summary of Variables	
Y_2 =	1 Day strength, MPa
X_1 =	Total binder content, kg/m3
X_2 =	Fly ash replacing cement, %
X_3 =	S.P percentage w.r.to total binder content, %
X_4 =	W/B ratio

1 D strength Y_2 = X_1, X_2, X_3, X_4, X1X2, X1X3, X1X4, X2X3, X2X4, X3X4, X1X2X3X4, $X1^2$, $X4^2$	
Response Distribution:	Normal
Link Function:	Identity

Model Equation
1 D strength Y_2 = 1786.34 - 3.0317X1 - 29.8364X2 - 2972.19X3 -3190.45X4 + 0.0391X1X2 +3.7161X1X3 + 5.1744X1X4 + 40.6712X2X3 + 36.9763X2X4 + 3993.55X3X4 - 0.2706X1X2X3X4 - 0.0005$X1^2$ - 363.7157$X4^2$

Summary of Fit			
Mean of Response:	11.78	R-Square:	0.9870
Root MSE:	0.5970	Adj R-Sq:	0.9651

Analysis of Variance					
Source	DF	Sum of Squares	Mean Sq.	F stat.	Prob. Greater than F stat.
Model	13	201.8506	15.527	43.57	Less than 0.0001
Error	7	2.4948	0.3564		
C Total	20	204.3454			

Parameter Estimates					
Variable	DF	Estimate	Std Error	t stat	Prob. Greater than t stat.
Intercept	1	1786.3369	506.8091	3.51	0.0098
X1	1	-3.0317	0.8914	-3.4	0.0114
X2	1	-29.8364	8.2262	-3.63	0.0084
X3	1	-2972.1888	779.8308	-3.81	0.0066
X4	1	-3190.4484	985.3975	-3.24	0.0143
X1X2	1	0.0391	0.0101	3.86	0.0062
X1X3	1	3.7161	0.959	3.87	0.0061
X1X4	1	5.1744	1.4605	3.54	0.0094
X2X3	1	40.6712	10.9859	3.7	0.0076
X2X4	1	36.9763	11.1978	3.3	0.0131
X3X4	1	3993.5513	1068.7928	3.74	0.0073
X1X2X3X4	1	-0.2706	0.0734	-3.69	0.0078
$X1^2$	1	-0.0005	0.0002	-2.58	0.0365
$X4^2$	1	-363.7157	127.1946	-2.86	0.0244

Appendix C Statistical details for model 2

Appendix D

The SAS system

Summary of Variables	
Y_3 =	28 D strength, MPa.
X_1 =	Total binder content, kg/m3
X_2 =	Fly ash replacing cement, %
X_3 =	S.P percentage w.r.to total binder content, %
X_4 =	W/B ratio

28 Day strength $Y_3 = X_1, X_2, X_4, X_1X_2, X_1X_3$	
Response Distribution:	Normal
Link Function:	Identity

Model Equation
28 D strength $Y_3 = 264.091 - 0.4297X_1 - 4.4592X_2 - 107.277X_4 + 0.0106X_1X_2 + 0.0307X_1X_3$

Summary of Fit			
Mean of Response:	44.7362	R-Square:	0.7593
Root MSE:	3.2439	Adj R-Sq:	0.6791

Analysis of Variance					
Source	DF	Sum of Squares	Mean Sq.	F stat.	Prob. Greater than F stat
Model	5	497.9512	99.5902	9.46	0.0003
Error	15	157.8445	10.523		
C Total	20	655.7957			

Parameter Estimates					
Variable	DF	Estimate	Std Error	t stat	Prob. Greater than t stat.
Intercept	1	264.0907	87.4264	3.02	0.0086
X1	1	-0.4297	0.2353	-1.83	0.0878
X2	1	-4.4592	2.0994	-2.12	0.0507
X4	1	-107.2766	32.0834	-3.34	0.0044
X1X2	1	0.0106	0.0053	2.01	0.0622
X1X3	1	0.0307	0.0149	2.07	0.0566

Appendix D. Statistical details for model 3

Appendix E

The SAS system

Summary of Variables	
Y_4 =	Rapid chloride permeability, Coulombs
X_1 =	Total binder content, kg/m3
X_2 =	Fly ash replacing cement, %
X_3 =	S.P percentage w.r.to total binder content, %
X_4 =	W/B ratio

Rapid chloride permeability $Y_4 = X_1, X_2, X_2X_3, X_2X_4, X_3X_4, X_1^2$	
Response Distribution:	Poison
Link Function:	Log

Model Equation
RCP, $Log(Y_4) = 12.0012 - 0.0229X_1 - 0.0436X_2 + 0.017X_2X_3 + 0.0947X_2X_4 - 1.6182X_3X_4 + 0.0000269X_1^2$

Summary of Fit			
Mean of Response:	1001.3810	Deviance:	209.1753
Scale:	1.000	Daviance/DF:	14.9411
Pearson chiSq	214.5897	Pearson chisq/DF	15.3278

Analysis of Deviance					
Source	DF	Deviance	Dev/DF	Scaled Dev	Prob. Greater than Scaled dev.
Model	6	319.3343	53.2224	319.3343	Less than 0.0001
Error	14	209.1753	14.9411	209.1753	
C Total	20	528.5096			

Parameter Estimates					
Variable	DF	Estimate	Std Error	ChiSq	Prob. Greater than ChiSq stat.
Intercept	1	12.0012	1.4588	67.6822	Less than 0.0001
X1	1	-0.0229	0.0073	9.9363	0.0016
X2	1	-0.0436	0.0056	61.2223	Less than 0.0001
X2X3	1	0.017	0.0069	6.0869	0.0136
X2X4	1	0.0947	0.0086	120.2509	Less than 0.0001
X3X4	1	-1.6182	0.7795	4.3092	0.0379
$X1^2$	1	0.0000269	9.11E-05	8.7252	0.0031

Appendix E. Statistical details for model 4

Appendix F

The SAS system

Summary of Variables
Y_5 = Material cost, C$
X_1 = Total binder content, kg/m3
X_2 = Fly ash replacing cement, %
X_3 = S.P percentage w.r.to total binder content, %
X_4 = W/B ratio

Material cost $Y_5 = X_1, X_2, X_3$	
Response Distribution:	Normal
Link Function:	Identity

Model Equation
Material cost, C$, Y_5 = 27.2783 + 0.1125 X_1 -0.1555 X_2 + 24.1377 X_3

Summary of Fit			
Mean of Response:	73.7457	R-Square:	0.9658
Root MSE:	0.8648	Adj R-Sq:	0.9597

Analysis of Variance					
Source	DF	Sum of Squares	Mean Sq.	F stat.	Prob. Greater than F stat.
Model	3	358.7677	119.5892	159.92	Less than 0.0001
Error	17	12.7128	0.7478		
C Total	20	371.4805			

Parameter Estimates					
Variable	DF	Estimate	Std Error	t stat	Prob. Greater than t stat.
Intercept	1	27.2783	3.3945	8.04	Less than 0.0001
X1	1	0.1125	0.0078	14.37	Less than 0.0001
X2	1	-0.1555	0.0261	-5.96	Less than 0.0001
X3	1	24.1377	1.5658	15.42	Less than 0.0001

Appendix F. Statistical details for model 5